DEVELOPMENT OF PYRUVATE DEHYDROGENASE VARIANTS AS A METABOLIC ENGINEERING STRATEGY

by

WILLIAM CHRISTOPHER MOXLEY

(Under the Direction of Mark A. Eiteman)

ABSTRACT

Microbial production of biochemicals from renewable sources is a cost-effective alternative to chemical synthesis production methods using petroleum-based feedstocks. The efficiency of microbial production processes is often enhanced by altering metabolism using metabolic engineering concepts and strategies. In this work, a strategy is developed to enhance the production of pyruvate-derived biochemicals by modifying pyruvate dehydrogenase, a key enzyme in pyruvate metabolism. The first study provides proof-of-concept for this strategy by generating pyruvate dehydrogenase variants that influence metabolic flux at the pyruvate node in central metabolism. The second study demonstrates that pyruvate dehydrogenase variants enhance the production of acetoin, a pyruvate-derived biochemical. The final study broadens the substrate range for production of pyruvate or pyruvate-derived biochemicals by engineering *Escherichia coli* strains able to efficiently produce pyruvate from sucrose.

INDEX WORDS: *Escherichia coli*, pyruvate, acetoin, sucrose, pyruvate dehydrogenase, AceE, fermentation, batch, chemostat

DEVELOPMENT OF PYRUVATE DEHYDROGENASE VARIANTS AS A METABOLIC ENGINEERING STRATEGY

by

WILLIAM CHRISTOPHER MOXLEY

B.S., University of Georgia, 2016

A Dissertation Submitted to the Graduate Faculty of The University of Georgia in Partial Fulfillment of the Requirements for the Degree

DOCTOR OF PHILOSOPHY

ATHENS, GEORGIA

2022

DEVELOPMENT OF PYRUVATE DEHYDROGENASE VARIANTS AS A METABOLIC ENGINEERING STRATEGY

by

WILLIAM CHRISTOPHER MOXLEY

Major Professor:	Mark A. Eiteman
Committee:	Diana M. Downs
	William N. Lanzilotta
	William B. Whitman

Electronic Version Approved:

Ron Walcott
Vice Provost for Graduate Education and Dean of the Graduate School
The University of Georgia
December 2022

DEDICATION

Dedicated to my wife, Silke, and family who supported me throughout my graduate studies.

TABLE OF CONTENTS

Page

CHAPTER 1

INTRODUCTION AND LITERATURE REVIEW

Pyruvic acid (pyruvate), also known as 2-oxopropionic acid, is an important carboxylic acid that functions as a key metabolite in nearly all living organisms. Pyruvate is the simplest form of the alpha-keto acids; it is a three-carbon compound with a carboxylic acid and a ketone group. Although its importance as a metabolic intermediate is ubiquitous, it is also industrially produced as a commodity chemical through chemical and biological synthesis methods (Li et al., 2001). Pyruvate is sold as a food additive, nutritional supplement, and common laboratory chemical (European Food Safety Authority (EFSA), 2009; Hermann et al., 2004; Kalman et al., 1999; Koh-Banerjee et al., 2005). Most notably, pyruvate serves as a metabolic precursor to many higher value products such as L-DOPA, isoprenoids, amino acids, isobutanol, acetoin, and 2,3-butanediol (Blombach et al., 2007; Blombach and Eikmanns, 2011; Chatzivasileiou et al., 2019; Park et al., 1998; Smith et al., 2006; Xiao and Lu, 2014; Yang et al., 2017).

Pyruvate production via chemical synthesis is achieved by the dehydration and decarboxylation of tartaric acid (Howard and Fraser, 1932). The process requires high temperatures which is often cited as a driver for increased production costs (Ingle et al., 2015; Li et al., 2001). Biological production offers a potentially cost-effective alternative method. Metabolic engineering strategies applied to produce pyruvate and pyruvate-derived chemicals often share a common goal: divert pyruvate flux away from central metabolism and to the

formation of a product. In this research, we develop an additional tool to aid metabolic engineering efforts in manipulating pyruvate flux in *Escherichia coli*.

MICROBIAL-DERIVED PRODUCTS FROM PYRUVATE

Pyruvate is an important metabolite in biological-based chemical production processes because it serves as a precursor to higher value compounds. The commercialization of bioprocesses to produce some pyruvate-derived chemicals has seen success, while some processes are still in development. The following section introduces examples of industrially relevant products derived from pyruvate, which are at various stages of commercialization.

1.1.1 Lactic acid. One of the most widely produced pyruvate-derived chemicals is lactic acid, with an annual production of 1,220 kilotons in 2016 (Singhvi et al., 2018). Though lactic acid can be produced through chemical or microbial routes, the specificity of producing D- or L-lactic acid at high purity is one of the characteristics that makes microbial fermentation a more desirable route (Eiteman and Ramalingam, 2015). Most notably, lactic acid is used to produce poly(lactic acid), a popular bioplastic and the most widely used material for 3D printing (Tümer and Erbil, 2021; Wehrenberg, 1981). Lactic acid producing bacteria (LAB), such as *Lactobacillus delbrueckii*, are commonly used for lactic acid production with typical host selection parameters being the specificity of D- or L-lactic acid and the desired feedstock (Abedi and Hashemi, 2020). Pyruvate produced microbially from the catabolism of sugars is converted, in one step, to lactic acid either by L-lactate dehydrogenase (EC 1.1.1.27) or D-lactate dehydrogenase (EC 1.1.1.28). Yields from various renewable sugar streams exceed 0.90 g/g with titers as high as ~160 g/L (Abedi and Hashemi, 2020).

1.1.2 Valine. L-valine is a pyruvate-derived amino acid that is produced by fermentation with a global annual production of ~550 tons and is used as a component of animal feed and cosmetics (Denina et al., 2010; Wendisch, 2020). *E. coli* and *Corynebacterium glutamicum* are commonly used for L-valine production (EFSA Panel on Additives and Products or Substances used in Animal Feed (FEEDAP), 2020, 2015). L-valine is synthesized from pyruvate through the branched chain amino acid pathway, which is also responsible for L-isoleucine and L-leucine biosynthesis. The L-valine pathway consists of four enzymes: acetolactate synthase (EC 2.2.1.6), ketol-acid reductoisomerase (EC 1.1.1.86), dihydroxy-acid dehydratase (EC 4.2.1.9), and valine transaminase (EC 2.6.1.42) (Umbarger, 1996). Complex feedback inhibition regulating the branched chain amino acid pathway and the availability of pyruvate are common targets for engineering L-valine producing strains (Denina et al., 2010; Gao et al., 2021). L-valine titers exceeding 100 g/L and yields above 0.50 g/g have been achieved (Gao et al., 2021).

1.2.3 (2,3)-butanediol. (2,3)-butanediol (2,3-BDO) is an industrially relevant compound that can be used as a fuel additive, intermediate for pharmaceuticals, and a component in cosmetics (Tinôco et al., 2021). It is a chiral molecule and has three different configurations: (2R,3R), (2R,3S), and (2S,3S). Although 2,3-BDO is not widely produced through fermentation, efforts to commercialize industrial production are led by LanzaTech and GS Caltex Corporation (Tinôco et al., 2021). Like L-valine, the first step of the 2,3-BDO biosynthesis pathway is the condensation of two pyruvate molecules by acetolactate synthase (EC 2.2.1.6) to yield acetolactate. Acetolactate is then decarboxylated by acetolactate decarboxylase (EC 4.1.1.5) to yield R-acetoin, which is subsequently reduced to 2,3-BDO by either meso-2,3-butanediol

dehydrogenase (EC 1.1.1.B20) or 2R,3R-butanediol dehydrogenase (EC 1.1.1.4) to yield their respective enantiomer. Alternatively, acetolactate can spontaneously convert to diacetyl which is subsequently converted to R-acetoin by diacetyl reductase (EC 1.1.1.304), allowing the formation of 2S,3S-BDO through 2S,3S-butanediol dehydrogenase (EC 1.1.1.76). Some microorganisms naturally produce 2,3-BDO as a fermentation product, such as *Klebsiella oxytoca* and *Serratia marcescens* (Ji et al., 2011). Although titers as high as 150 g/L with yields close to 100% of the theoretical maximum have been achieved, product recovery and process development have been identified as critical areas of improvement to make commercial production successful (Ji et al., 2011; Tinôco et al., 2021).

1.2 PYRUVATE NODE IN CENTRAL METABOLISM

Native pyruvate consuming pathways facilitate oxidative and fermentative metabolism through the generation metabolic intermediates, NADH or NAD^+, and mixed-acid end products. This section describes enzymes of interest in relation to *E. coli* central metabolism.

1.2.1 Pyruvate dehydrogenase complex. The pyruvate dehydrogenase complex (PDHc) converts pyruvate to acetyl-CoA, consuming the majority of pyruvate in central metabolism (Zhao et al., 2004). PDHc mediates a key conversion in aerobic central metabolism, as it is considered the terminus of glycolysis and links glycolysis to the TCA cycle. PDHc is one of the largest multi-enzyme complexes known, consisting of 12 AceE (E1, EC 1.2.4.1) dimers, 24 AceF (E2, EC 2.3.1.12) monomers, and 6 LpdA (E3, EC 1.8.1.4) dimers with a total molecular weight of 4.57 MDa (Figure 1.1a; Arjunan et al., 2002). The E1 component uses thiamine diphosphate and Mg(II) as cofactors, the E2 component contains covalently-bound lipoyl groups

as cofactors, and the E3 component uses FAD as a cofactor (Arjunan et al., 2002). The rate-limiting step, the decarboxylation of pyruvate, is catalyzed by the E1 component which has a k_{cat} of 38 s^{-1} and a K_m for pyruvate of 260 µM (Kale et al., 2007). PDHc is negatively regulated at the protein level through competitive inhibition by acetyl-CoA and NADH (Hansen and Henning, 1966; Schmincke-Ott and Bisswanger, 1981; Shen and Atkinson, 1970).

The genes coding for the three subunits of PDHc are *aceE* encoding AceE (E1), *aceF* encoding AceF (E2), and *lpdA* (E3) encoding LpdA (E3; Figure 1.1a). They are organized in an operon that is negatively regulated by a repressor protein PdhR, encoded by *pdhR*, which binds and represses expression of the *pdhR-aceEF-lpdA* readthrough transcript (Olvera et al., 2009; Quail et al., 1994; Quail and Guest, 1995; Spencer and Guest, 1985). Although *pdhRp* acts as the major promoter for PDHc expression, alternate promoters upstream of *aceE* can drive expression of the *aceEF-lpdA* transcript (Olvera et al., 2009; Quail and Guest, 1995; Spencer and Guest, 1985). In the absence of pyruvate, PdhR binds and represses the expression of PDHc from the *pdhRp* promoter while expression is derepressed in the presence of pyruvate.

1.2.2 Pyruvate-formate lyase. The anaerobic conversion of pyruvate to acetyl-CoA and formate is catalyzed by PflB (pyruvate-formate lyase; EC 2.3.1.54), encoded by *pflB*. Under anaerobic conditions, PDHc is allosterically inhibited by NADH and transcriptionally repressed by ArcAB. Conversely, *pflB* transcription is promoted by ArcAB, along with the anaerobic-associated regulator FNR (Sawers and Suppmann, 1992). At the protein level, PflB requires activation by the iron-sulfur protein PflA [pyruvate-formate lyase activating enzyme; EC 1.97.1.4], which creates an oxygen-sensitive glycyl radical in the active site of PflB required for activity (Knappe et al., 1984; Wagner et al., 1992; Zhang et al., 2001). PflB has a k_{cat} of 11 s^{-1} and a K_m for

pyruvate of 2 mM, about one order of magnitude higher than the K_m of PDHc (Knappe et al., 1974; Knappe and Blaschkowski, 1975).

1.2.3 Pyruvate oxidase. Pyruvate oxidase (PoxB, EC 1.2.5.1), encoded by *poxB*, catalyzes the oxidative decarboxylation of pyruvate to acetate. Its function supports metabolic efficiency at high growth rates under aerobic conditions, contributing to "overflow metabolism" hallmarked by the transient excretion and reuptake of acetate (Abdel-Hamid et al., 2001; Vemuri et al., 2006, 2005). PoxB localizes to the peripheral inner membrane, through an amphipathic C-terminal domain, and uses TPP, FAD, and Mg^{2+} as cofactors while using ubiquinone as an electron acceptor (Chang and Cronan, 1984; Grabau and Cronan, 1986; Mather et al., 1982). PoxB is activated by lipid binding, and the active form of PoxB has a k_{cat} of ~200 – 400 s^{-1} and a K_m for pyruvate of ~20 mM (Bertagnolli and Hager, 1991; Chang and Cronan, 2000).

1.2.4 Lactate dehydrogenase. Lactate dehydrogenase (LdhA, EC 1.1.1.28), encoded by *ldhA*, catalyzes the NAD-linked dehydrogenation of pyruvate to D-lactate (Bunch et al., 1997; Tarmy and Kaplan, 1968). LdhA functions to maintain redox balance under conditions of excess NADH. Though LdhA is associated with anaerobic metabolism, it is expressed at a basal level during aerobic growth and can function to produce lactate in conditions of excess pyruvate (Bunch et al., 1997; Zelić et al., 2003). LdhA is allosterically activated by pyruvate and has a k_{cat} of ~410 s^{-1} and a K_m for pyruvate of ~7.2 mM (Furukawa et al., 2014; Tarmy and Kaplan, 1968).

1.2.5 Phosphoenolpyruvate synthetase. Phosphoenolpyruvate synthetase (PpsA, EC 2.7.9.2), encoded by *ppsA*, catalyzes the conversion of pyruvate to phosphoenolpyruvate to support

gluconeogenesis and growth on pyruvate as a carbon source (Brice and Kornberg, 1967; Cooper and Kornberg, 1967). PpsA is subject to activation/inactivation, though it is protected from inactivation in the presence of pyruvate (Burnell, 2010). Activated PpsA has a K_m of ~83 µM for pyruvate (Berman and Cohn, 1970).

1.3 STRATEGIES TO INCREASE PRODUCTION OF PYRUVATE-DERIVED PRODUCTS

Production of pyruvate-derived chemicals inherently leads to a competition between a pathway to a product and the utilization of pyruvate for growth, energy, and cell maintenance. This section describes existing strategies based on process design and metabolic engineering to balance this competition and optimize product formation.

1.3.1 Process design strategies

One of the first methods to manipulate microorganisms to overproduce pyruvate and pyruvate-derived chemicals is through modulating nutrients and/or oxygenation. The use of thiamine and lipoic acid auxotrophic microorganisms were among the first examples of this strategy (Maleki et al., 2017; Yokota and Takao, 1989). As thiamine and lipoic acid are required for PDHc, among other central metabolic enzymes, limiting the supply of these cofactors can reduce PDHc activity and allow for pyruvate accumulation. For example, a multivitamin-auxotrophic strain of the yeast *Yarrowia lipolytica* accumulated 61.3 g/L pyruvate through optimizing the levels of thiamine supplied in the medium (Morgunov et al., 2004). An inverse correlation between pyruvate accumulation and thiamine levels were observed, with a decrease in PDHc activity at lower thiamine concentrations.

Manipulation of the redox balance through controlling dissolved oxygen concentrations in the culture is an additional route. Microaerobic environments, in which the dissolved oxygen concentration is controlled at about 5% of air saturation, enable elevated NADH levels as the low oxygen concentration limits the capacity of the electron transport chain to oxidize NADH. Limiting oxygen, in combination with inactivation of fermentative pyruvate-consuming pathways, allows indirect control of PDHc flux by increasing the NADH concentration, which inhibits PDHc activity. Using this method, *E. coli* achieved a maximum titer of 65.2 g/L pyruvate (Causey et al., 2004).

1.3.2 Metabolic engineering strategies

Metabolic engineering and synthetic biology have emerged as promising tools for fine-tuning metabolism to meet the cellular demands of growth while also producing chemicals at high rates and titers. The most widely used strategy to direct metabolic flux toward a product is the inactivation or deletion of nonessential pathways that compete for common precursors. In the context of pyruvate production in *E. coli*, *ldhA* and *poxB* are common targets for gene deletion as they are nonessential and prevent pyruvate flux toward the undesirable byproducts lactate and acetate (Moxley and Eiteman, 2021; Zelić et al., 2003; Zhu et al., 2008). Likewise, genes that allow for the consumption of pyruvate as a carbon source are often deleted. For instance, deletion of *ppsA* can prevent pyruvate assimilation and increase pyruvate yield (Maleki et al., 2018; Moxley and Eiteman, 2021; Zhu et al., 2008). Another example is deletion of *aceE* and/or *aceF*, encoding subunits of the PDHc (Maleki et al., 2018; Tomar et al., 2003; Zhu et al., 2008). Inactivation of the PDHc is important for producing pyruvate or pyruvate-derived products as it converts a majority of pyruvate in central metabolism to acetyl-CoA under aerobic conditions

(Zhao et al., 2004). Unlike *ldhA*, *poxB*, and *ppsA*, however, PDHc is essential for growth of *E. coli* on glucose, and its inactivation requires the supplementation of an additional carbon source, such as acetate, to supply acetyl-CoA for cell growth (Langley and Guest, 1977).

Supplementation of an additional carbon source, as imposed by PDHc inactivation, is undesirable as it represents an additional cost for commercial processes, which are often developed to use cheap feedstocks (Burgard et al., 2016). Because complete inactivation of PDHc necessitates an additional carbon source, approaches to decrease but not abolish carbon flux through PDHc have more recently been studied. One example is through the promoter engineering, where the native promoter of *aceE* is replaced with a weaker promoter. This strategy has been applied to decrease the expression of AceE in *Corynebacterium glutamicum* (Buchholz et al., 2013). However, when applied to *E. coli*, this approach becomes more complicated due to the transcriptional regulation imposed on *aceE* that is absent in other organisms such as *C. glutamicum* (Quail and Guest, 1995; Schreiner et al., 2005; Spencer and Guest, 1985). To achieve a decrease in *aceE* expression in *E. coli*, more sophisticated metabolic engineering strategies have been applied. One example is the use of RNA silencing through expression of antisense RNA to block translation of a target mRNA transcript, effectively decreasing the concentration of the corresponding protein in the cell (Nakashima and Tamura, 2009). When applied to *aceE*, the resulting strain showed a decrease of ~70% in translated *aceE* mRNA, which correlated to a >99% decrease in AceE activity (Nakashima et al., 2014). Interestingly, the strain was not auxotrophic for acetate, suggesting that <1% of AceE activity is sufficient for growth on glucose and highlighting the fast and competitive kinetic parameters of the PDHc. Similarly, Clustered Regularly Interspaced Short Palindromic Repeats (CRISPR) technology has been applied to decrease the expression of *aceE* (Ziegler et al., 2021). In this

strategy, a catalytically inactive Cas9 (dCas9) is used together with a guide RNA to target promoter regions of target genes to inhibit RNA polymerase binding and transcription. Two guide RNA sequences targeting *pdhRp* and *aceEp* have been used to decrease PDHc activity and accumulate ~11.3 g/L pyruvate from glucose (Ziegler et al., 2021).

1.4 APPLICATIONS OF ENZYME ENGINEERING

Protein engineering is a useful metabolic engineering tool that allows enzymes to be optimized for a desired application. One of the most common uses for protein engineering is to increase the efficiency of a pathway by alleviating the limiting step(s). One fundamental example of this comes from the successful commercialization of microbial production of 1,3-propanediol by Genencor and DuPont (Nakamura and Whited, 2003). Here, a novel glycerol dehydratase resistant to inhibition by 1,3-propanediol was generated by combining portions of heterologous dehydratase genes to generate a fusion protein. Similarly, decreasing inhibition by NADH of central metabolic enzymes through targeted substitutions was critical in the commercialization of bio-based 1,4-butanediol by Genomatica (Yim et al., 2011). Improved glycolytic and TCA cycle flux under microaerobic environments was achieved by use of the NADH-resistant variant enzymes LpdA[D354K], a component of the pyruvate and 2-oxoglutarate dehydrogenase complexes, and GltA[R163L], citrate synthase (Kim et al., 2008; Pereira et al., 1994).

Protein engineering is also applied to increase activity of heterologous enzymes expressed in *E. coli*. For example, CimA [citramalate synthase;EC:2.3.3.21], an enzyme of the citramalate pathway native to *Methanococcus jannaschi,* was engineering for the production of 1-propanol and 1-butanol in *E. coli* with the resulting CimA variant increasing production of both alcohols by at least 9-fold (Atsumi and Liao, 2008). To accomplish this, error-prone PCR

was used to construct a library of *cimA* variants, which were subject to multiple rounds of growth-based selection and DNA shuffling. Random mutagenesis coupled to a selection method is a powerful tool to generate novel enzymes with substitutions that would be impossible to conceive otherwise. Alternatively, structure-guided protein engineering is a useful tool that does not require a selection method to isolate novel enzymes with the desired characteristics. For example, a variant of xylose reductase (EC 1.1. 1.307) was engineered to preferentially use NADH over NADPH as a cofactor to improve ethanol production in *Saccharomyces cerevisiae* (Watanabe et al., 2007). Here, existing crystal structures and previous literature were used to rationally design substitutions to influence NADH binding.

Increasing flux through a pathway is a common goal of protein engineering, which involves engineering enzymes of pathways toward the desired product. In this way, the competition between central metabolism and product formation is addressed by improving the pathway to the product. Alternatively, protein engineering can be applied to enzymes of native metabolism which compete for precursors common to both product and biomass formation. In this case, an enzyme of central metabolism, which often exhibit fast and competitive kinetics (Bar-Even et al., 2011), can be engineered with reduced activity to allow an enzyme in a production pathway to better compete for the same substrate. Using this rationale, production of pyruvate-derived biochemicals could be improved through engineering variants of the pyruvate dehydrogenase that increase the availability of pyruvate as a precursor for a competing pathway.

1.5 DISSERTATION OUTLINE

This dissertation is divided into 4 sections. Chapter 2 is a proof-of-concept study where rational protein design was applied to the EI component of the PDHc (AceE, EC 1.2.4.1) with

the overall goal of decreasing carbon flux through PDHc. Three of the 16 tested variant *aceE* alleles allowed for varying levels of pyruvate accumulation and reduced growth rates in the initial shake flask screen where byproduct pathways to lactate (*ldhA*) and acetate (*poxB*) were deleted. Assessment of pyruvate accumulating strains in 1 L controlled batch culture indicated an additional deletion in phosphoenolpyruvate synthetase (*ppsA*) was necessary to prevent assimilation of accumulated pyruvate. An inverse correlation between growth rate and pyruvate accumulation was observed and highlights the competition for pyruvate between cell growth and product formation. Nitrogen-limited chemostat cultures further substantiated the diversion of carbon away from growth as a strain containing a variant *aceE* allele consumed glucose 65% faster while increasing *aceE* expression 2.6-fold to match the growth rate of the wild-type control strain. Though a strain with severely reduced PDHc flux still requires acetate to support biomass formation at a practical rate, the benefit was realized in an increased volumetric productivity compared to the Δ*aceE* control strain. Three *aceE* variant alleles, conferring different carbon flux distributions at the pyruvate node, were identified in this work that can be used as metabolic engineering tools to increase the production of pyruvate-derived chemicals.

Chapter 3 furthers the development of *aceE* variants by generating additional variants by random mutagenesis and investigating the suite of *aceE* variants to the production of acetoin as a model pyruvate-derived product. Two additional *aceE* alleles were identified from random mutagenesis and screening that confer pyruvate accumulation at decreased a growth rate. When mutated *aceE* alleles were integrated into the chromosome of *E. coli* W Δ*poxB* Δ*ldhA* Δ*ppsA*, the five resulting strains displayed different pyruvate yields and growth rates, suggesting that each *aceE* variant confers unique pyruvate metabolism and carbon flux distributions at the pyruvate node. When applied to the production of acetoin in 1.25 L controlled batch culture, the best

acetoin production strain did not correlate with the best pyruvate producing strain, suggesting there may be an optimal distribution depending on the target product and pathway used. The use of *aceE* variants enabled high level production of acetoin, where the first enzyme (ALS, EC 2.2.1.6) in the production pathway competes poorly with the wild-type PDHc.

Chapter 4 explores the accumulation of pyruvate using sucrose as a carbon source to broaden the substrate range used to produce pyruvate or pyruvate-derived chemicals. Sucrose is comparable to glucose as a low-cost carbon source for industrial fermentation processes, but sucrose metabolism in *E. coli* is less understood. Pyruvate producing strains of *E. coli* W, an isolate naturally capable of metabolizing sucrose, displayed pyruvate yields and productivities comparable to when glucose is used as a carbon source. The work represents the first efforts to engineer microorganisms to produce pyruvate from sucrose.

Chapter 5 summarizes the three previous chapters, draws conclusions and proposes an area for the future development of *aceE* variants as a metabolic engineering strategy. Of particular interest is the adaptation of *aceE* variants to an industrial process that requires fast biomass formation followed by growth-limited product formation.

1.6 REFERENCES

Abdel-Hamid, A.M., Attwood, M.M., Guest, J.R., 2001. Pyruvate oxidase contributes to the aerobic growth efficiency of *Escherichia coli*. Microbiology 147, 1483–1498. https://doi.org/10.1099/00221287-147-6-1483

Abedi, E., Hashemi, S.M.B., 2020. Lactic acid production – producing microorganisms and substrates sources-state of art. Heliyon 6, e04974. https://doi.org/10.1016/j.heliyon.2020.e04974

Arjunan, P., Nemeria, N., Brunskill, A., Chandrasekhar, K., Sax, M., Yan, Y., Jordan, F., Guest, J.R., Furey, W., 2002. Structure of the Pyruvate Dehydrogenase Multienzyme Complex

E1 Component from *Escherichia coli* at 1.85 Å Resolution. Biochemistry 41, 5213–5221. https://doi.org/10.1021/bi0118557

Atsumi, S., Liao, J.C., 2008. Directed evolution of *Methanococcus jannaschii* citramalate synthase for biosynthesis of 1-propanol and 1-butanol by *Escherichia coli*. Appl Environ Microbiol 74, 7802–7808.

Bar-Even, A., Noor, E., Savir, Y., Liebermeister, W., Davidi, D., Tawfik, D.S., Milo, R., 2011. The moderately efficient enzyme: Evolutionary and physicochemical trends shaping enzyme parameters. Biochemistry 50, 4402–4410. https://doi.org/10.1021/BI2002289/SUPPL_FILE/BI2002289_SI_004.XLS

Berman, K.M., Cohn, M., 1970. Phosphoenolpyruvate Synthetase of *Escherichia coli* Purification, Some Properties, and the Role of Divalent Metal Ions. J Biol Chem 245, 5309–5318. https://doi.org/10.1016/S0021-9258(18)62756-5

Bertagnolli, B.L., Hager, L.P., 1991. Activation of *Escherichia coli* pyruvate oxidase enhances the oxidation of hydroxyethylthiamin pyrophosphate. J Biol Chem 266, 10168–10173. https://doi.org/10.1016/S0021-9258(18)99205-7

Blombach, B., Eikmanns, B.J., 2011. Current knowledge on isobutanol production with *Escherichia coli, Bacillus subtilis* and *Corynebacterium glutamicum*. Bioeng Bugs 2, 346–50. https://doi.org/10.4161/bbug.2.6.17845

Blombach, B., Schreiner, M.E., Holátko, J., Bartek, T., Oldiges, M., Eikmanns, B.J., 2007. L-Valine production with pyruvate dehydrogenase complex-deficient *Corynebacterium glutamicum*. Appl Environ Microbiol 73, 2079–2084. https://doi.org/10.1128/AEM.02826-06

Brice, C.B., Kornberg, H.L., 1967. Location of a gene specifying phosphopyruvate synthase activity on the genome of *Escherichia coli* K12. Proc R Soc Lond B Biol Sci 168, 281–292.

Buchholz, J., Schwentner, A., Brunnenkan, B., Gabris, C., Grimm, S., Gerstmeir, R., Takors, R., Eikmanns, B.J., Blombach, B., 2013. Platform Engineering of *Corynebacterium glutamicum* with Reduced Pyruvate Dehydrogenase Complex Activity for Improved Production of L-Lysine, L-Valine, and 2-Ketoisovalerate. Appl Environ Microbiol 79, 5566–75. https://doi.org/10.1128/AEM.01741-13

Bunch, P.K., Mat-Jan, F., Lee, N., Clark, D.P., 1997. The *IdhA* gene encoding the fermentative lactate dehydrogenase of *Escherichia coli*. Microbiology 143, 187–195. https://doi.org/10.1099/00221287-143-1-187

Burgard, A., Burk, M.J., Osterhout, R., van Dien, S., Yim, H., 2016. Development of a commercial scale process for production of 1,4-butanediol from sugar. Curr Opin Biotechnol 42, 118–125. https://doi.org/10.1016/J.COPBIO.2016.04.016

Burnell, J.N., 2010. Cloning and characterization of *Escherichia coli* DUF299: a bifunctional ADP-dependent kinase--Pi-dependent pyrophosphorylase from bacteria. BMC Biochem 11, 1–8. https://doi.org/10.1186/1471-2091-11-1

Causey, T.B., Shanmugam, K.T., Yomano, L.P., Ingram, L.O., 2004. Engineering *Escherichia coli* for efficient conversion of glucose to pyruvate. Proc Natl Acad Sci U S A 101, 2235–40. https://doi.org/10.1073/PNAS.0308171100

Chang, Y.-Y., Cronan, J.E., 2000. Conversion of *Escherichia coli* pyruvate oxidase to an "α-ketobutyrate oxidase." Biochemical Journal 352, 717–724.

Chang, Y.Y., Cronan, J.E., 1984. An *Escherichia coli* mutant deficient in pyruvate oxidase activity due to altered phospholipid activation of the enzyme. Proc Natl Acad Sci U S A 81, 4348–4352. https://doi.org/10.1073/PNAS.81.14.4348

Chatzivasileiou, A.O., Ward, V., Edgar, S.M.B., Stephanopoulos, G., 2019. Two-step pathway for isoprenoid synthesis. Proc Natl Acad Sci U S A 116, 506–511. https://doi.org/10.1073/PNAS.1812935116

Cooper, R.A., Kornberg, H.L., 1967. The direct synthesis of phospho*enol*pyruvate from pyruvate by *Escherichia coli*. Proc R Soc Lond B Biol Sci 168, 263–280.

Denina, I., Paegle, L., Prouza, M., Holátko, J., Pátek, M., Nenvera, J., Ruklisha, M., 2010. Factors enhancing L-valine production by the growth-limited L-isoleucine auxotrophic strain *Corynebacterium glutamicum* Δ*ilvA* Δ*panB ilvN*M13 (pECKA*ilvBNC*). J Ind Microbiol Biotechnol 37, 689–699. https://doi.org/10.1007/s10295-010-0712-y

EFSA Panel on Additives and Products or Substances used in Animal Feed (FEEDAP), 2020. Safety and efficacy of l-valine produced by fermentation using *Corynebacterium glutamicum* CGMCC 7.358 as a feed additive for all animal species. EFSA Journal 18. https://doi.org/10.2903/j.efsa.2020.6286

EFSA Panel on Additives and Products or Substances used in Animal Feed (FEEDAP), 2015. Scientific Opinion on the safety and efficacy of L-valine produced by *Escherichia coli* NITE SD 00066 for all animal species. EFSA Journal 13. https://doi.org/10.2903/j.efsa.2015.3965

Eiteman, M.A., Ramalingam, S., 2015. Microbial production of lactic acid. Biotechnol Lett 37, 955–972. https://doi.org/10.1007/s10529-015-1769-5

European Food Safety Authority (EFSA), 2009. Calcium acetate, calcium pyruvate, calcium succinate, magnesium pyruvate magnesium succinate and potassium malate added for nutritional purposes to food supplements. EFSA Journal 1088, 1–25. https://doi.org/10.2903/j.efsa.2009.1088

Furukawa, N., Miyanaga, A., Togawa, M., Nakajima, M., Taguchi, H., 2014. Diverse allosteric and catalytic functions of tetrameric d-lactate dehydrogenases from three Gram-negative bacteria. AMB Express 4, 1–12. https://doi.org/10.1186/S13568-014-0076-1

Gao, H., Tuyishime, P., Zhang, X., Yang, T., Xu, M., Rao, Z., 2021. Engineering of microbial cells for L-valine production: challenges and opportunities. Microb Cell Fact 20, 1–6. https://doi.org/10.1186/s12934-021-01665-5

Grabau, C., Cronan, J.E., 1986. In vivo function of *Escherichia coli* pyruvate oxidase specifically requires a functional lipid binding site. Biochemistry 25, 3748–3751. https://doi.org/10.1021/BI00361A003

Hansen, R.G., Henning, U., 1966. Regulation of pyruvate dehydrogenase activity in *Escherichia coli* K12. Biochim Biophys Acta 122, 355–358. https://doi.org/10.1016/0926-6593(66)90076-2

Hermann, H.P., Arp, J., Pieske, B., Kögler, H., Baron, S., Janssen, P.M.L., Hasenfuss, G., 2004. Improved systolic and diastolic myocardial function with intracoronary pyruvate in patients with congestive heart failure. Eur J Heart Fail 6, 213–218. https://doi.org/10.1016/J.EJHEART.2003.10.001

Howard, J.W., Fraser, W.A., 1932. Preparation of pyruvic acid. Org. Synth. Coll. 1, 475–480.

Ingle, U., Rajagopalan, S., Padmanabhan, S., 2015. Isolation and scale-up of sodium pyruvate from fermentation broth using a repulsive extraction and crystallization method. Journal of Chemical Technology and Biotechnology 90, 2240–2248. https://doi.org/10.1002/jctb.4539

Ji, X.J., Huang, H., Ouyang, P.K., 2011. Microbial 2,3-butanediol production: A state-of-the-art review. Biotechnol Adv 29, 351–364. https://doi.org/10.1016/j.biotechadv.2011.01.007

Kale, S., Arjunan, P., Furey, W., Jordan, F., 2007. A dynamic loop at the active center of the *Escherichia coli* pyruvate dehydrogenase complex E1 component modulates substrate utilization and chemical communication with the E2 component. J Biol Chem 282, 28106–16. https://doi.org/10.1074/jbc.M704326200

Kalman, D., Colker, C.M., Wilets, I., Roufs, J.B., Antonio, J., 1999. The effects of pyruvate supplementation on body composition in overweight individuals. Nutrition 15, 337–340. https://doi.org/10.1016/S0899-9007(99)00034-9

Kim, Y., Ingram, L.O., Shanmugam, K.T., 2008. Dihydrolipoamide Dehydrogenase Mutation Alters the NADH Sensitivity of Pyruvate Dehydrogenase Complex of *Escherichia coli* K-12. J Bacteriol 190, 3851–3858. https://doi.org/10.1128/JB.00104-08

Knappe, J., Blaschkowski, H.P., 1975. Pyruvate formate-lyase from *Escherichia coli* and its activation system. Methods Enzymol 41, 508–518. https://doi.org/10.1016/S0076-6879(75)41107-7

Knappe, J., Blaschkowski, H.P., Gröbner, P., Schmttt, T., 1974. Pyruvate formate-lyase of *Escherichia coli*: the acetyl-enzyme intermediate. Eur J Biochem 50, 253–263. https://doi.org/10.1111/J.1432-1033.1974.TB03894.X

Knappe, J., Neugebauer, F.A., Blaschkowski, H.P., Ganzler, M., 1984. Post-translational activation introduces a free radical into pyruvate formate-lyase. Proc Natl Acad Sci U S A 81, 1332–1335. https://doi.org/10.1073/PNAS.81.5.1332

Koh-Banerjee, P.K., Ferreira, M.P., Greenwood, M., Bowden, R.G., Cowan, P.N., Almada, A.L., Kreider, R.B., 2005. Effects of calcium pyruvate supplementation during training on body composition, exercise capacity, and metabolic responses to exercise. Nutrition 21, 312–319. https://doi.org/10.1016/J.NUT.2004.06.026

Langley, D., Guest, J.R., 1977. Biochemical genetics of the α keto acid dehydrogenase complexes of *Escherichia coli* K12: isolation and biochemical properties of deletion mutants. J Gen Microbiol 99, 263–276. https://doi.org/10.1099/00221287-99-2-263

Li, Y., Chen, J., Lun, S.Y., 2001. Biotechnological production of pyruvic acid. Appl Microbiol Biotechnol 57, 451–459. https://doi.org/10.1007/s002530100804

Maleki, N., Eiteman, M., Maleki, N., Eiteman, M.A., 2017. Recent Progress in the Microbial Production of Pyruvic Acid. Fermentation 3, 8. https://doi.org/10.3390/fermentation3010008

Maleki, N., Safari, M., Eiteman, M.A., 2018. Conversion of glucose-xylose mixtures to pyruvate using a consortium of metabolically engineered *Escherichia coli*. Eng Life Sci 18, 40–47. https://doi.org/10.1002/elsc.201700109

Mather, M., Schopfer, L.M., Massey, V., Gennis, R.B., 1982. Studies of the Flavin Adenine Dinucleotide Binding Region in *Escherichia coli* Pyruvate Oxidase*. J Biol Chem 257, 12887–12892. https://doi.org/10.1016/S0021-9258(18)33598-1

Morgunov, I.G., Kamzolova, S. v., Perevoznikova, O.A., Shishkanova, N. v., Finogenova, T. v., 2004. Pyruvic acid production by a thiamine auxotroph of *Yarrowia lipolytica*. Process Biochemistry 39, 1469–1474. https://doi.org/10.1016/S0032-9592(03)00259-0

Moxley, W.C., Eiteman, M.A., 2021. Pyruvate Production by *Escherichia coli* by Use of Pyruvate Dehydrogenase Variants. Appl Environ Microbiol 87, e00487-21. https://doi.org/10.1128/AEM.00487-21

Nakamura, C.E., Whited, G.M., 2003. Metabolic engineering for the microbial production of 1, 3-propanediol. Curr Opin Biotechnol 14, 454–459.

Nakashima, N., Ohno, S., Yoshikawa, K., Shimizu, H., Tamura, T., 2014. A Vector Library for Silencing Central Carbon Metabolism Genes with Antisense RNAs in *Escherichia coli*. Appl Environ Microbiol 80, 564–573. https://doi.org/10.1128/AEM.02376-13

Nakashima, N., Tamura, T., 2009. Conditional gene silencing of multiple genes with antisense RNAs and generation of a mutator strain of *Escherichia coli*. Nucleic Acids Res 37, e103. https://doi.org/10.1093/nar/gkp498

Olvera, L., Mendoza-Vargas, A., Flores, N., Olvera, M., Sigala, J.C., Gosset, G., Morett, E., Bolívar, F., 2009. Transcription Analysis of Central Metabolism Genes in *Escherichia coli*. Possible Roles of σ38 in Their Expression, as a Response to Carbon Limitation. PLoS One 4, e7466. https://doi.org/10.1371/JOURNAL.PONE.0007466

Park, H.-S., Lee, J.-Y., Kim, H.-S., 1998. Production of L-DOPA(3,4-Dihydroxyphenyl-L-alanine) from Benzene by Using A Hybrid Pathway. Biotechnol Bioeng 58, 339–343. https://doi.org/10.1002/(SICI)1097-0290(19980420)58:2/3

Pereira, D.S., Donald, L.J., Hosfield, D.J., Duckworth, H.W., 1994. Active site mutants of *Escherichia coli* citrate synthase. Effects of mutations on catalytic and allosteric properties. Journal of Biological Chemistry 269, 412–417.

Quail, M.A., Guest, J.R., 1995. Purification, characterization and mode of action of PdhR, the transcriptional repressor of the *pdhR–aceEF–lpd* operon of *Escherichia coli*. Mol Microbiol 15, 519–529. https://doi.org/10.1111/J.1365-2958.1995.TB02265.X

Quail, M.A., Haydon, D.J., Guest, J.R., 1994. The *pdhR-aceEF-lpd* operon of *Escherichia coli* expresses the pyruvate dehydrogenase complex. Mol Microbiol 12, 95–104. https://doi.org/10.1111/J.1365-2958.1994.TB00998.X

Sawers, G., Suppmann, B., 1992. Anaerobic induction of pyruvate formate-lyase gene expression is mediated by the ArcA and FNR proteins. J Bacteriol 174, 3474–3478. https://doi.org/10.1128/JB.174.11.3474-3478.1992

Schmincke-Ott, E., Bisswanger, H., 1981. Dihydrolipoamide Dehydrogenase Component of the Pyruvate Dehydrogenase Complex from *Escherichia coli*. Eur J Biochem 114, 413–420. https://doi.org/10.1111/J.1432-1033.1981.TB05162.X

Schreiner, M.E., Fiur, D., Holátko, J., Pátek, M., Eikmanns, B.J., 2005. E1 Enzyme of the Pyruvate Dehydrogenase Complex in *Corynebacterium glutamicum*: Molecular Analysis of the Gene and Phylogenetic Aspects. J Bacteriol 187, 6005–6018. https://doi.org/10.1128/JB.187.17.6005-6018.2005

Shen, L.C., Atkinson, D.E., 1970. Regulation of pyruvate dehydrogenase from *Escherichia coli*: interactions of adenylate energy charge and other regulatory parameters. J Biol Chem 245, 5974–5978. https://doi.org/10.1016/S0021-9258(18)62650-X

Singhvi, M., Zendo, T., Sonomoto, K., 2018. Free lactic acid production under acidic conditions by lactic acid bacteria strains: challenges and future prospects. Appl Microbiol Biotechnol 102, 5911–5924. https://doi.org/10.1007/s00253-018-9092-4

Smith, G.M., Lee, S.A., Reilly, K.C., Eiteman, M.A., Altman, E., 2006. Fed-batch two-phase production of alanine by a metabolically engineered *Escherichia coli*. Biotechnol Lett 28, 1695–1700. https://doi.org/10.1007/S10529-006-9142-3

Spencer, M.E., Guest, J.R., 1985. Transcription analysis of the *sucAB, aceEF* and *lpd* genes of *Escherichia coli*. Mol Gen Genet 200, 145–154. https://doi.org/10.1007/BF00383328

Tarmy, E.M., Kaplan, N.O., 1968. Kinetics of *Escherichia coli* B D-Lactate Dehydrogenase and Evidence for Pyruvate-controlled Change in Conformation*. J Biol Chem 243, 2587–2596. https://doi.org/10.1016/S0021-9258(18)93414-9

Tinôco, D., Borschiver, S., Coutinho, P.L., Freire, D.M.G., 2021. Technological development of the bio-based 2,3-butanediol process. Biofuels, Bioproducts and Biorefining 15, 357–376. https://doi.org/10.1002/bbb.2173

Tomar, A., Eiteman, M.A., Altman, E., 2003. The effect of acetate pathway mutations on the production of pyruvate in *Escherichia coli*. Appl Microbiol Biotechnol 62, 76–82. https://doi.org/10.1007/s00253-003-1234-6

Tümer, E.H., Erbil, H.Y., 2021. Extrusion-based 3d printing applications of pla composites: A review. Coatings 11, 390. https://doi.org/10.3390/coatings11040390

Umbarger, H.E., 1996. Biosynthesis of the branched-chain amino acids, in: *Escherichia Coli* and *Salmonella*: Cellular and Molecular Biology, 2nd Ed. ASM Press, Washington, DC. pp. 442–457.

Vemuri, G.N., Altman, E., Sangurdekar, D.P., Khodursky, A.B., Eiteman, M.A., 2006. Overflow Metabolism in *Escherichia coli* during Steady-State Growth: Transcriptional Regulation and Effect of the Redox Ratio. Appl Environ Microbiol 72, 3653–3661. https://doi.org/10.1128/AEM.72.5.3653-3661.2006

Vemuri, G.N., Minning, T.A., Altman, E., Eiteman, M.A., 2005. Physiological response of central metabolism in *Escherichia coli* to deletion of pyruvate oxidase and introduction of heterologous pyruvate carboxylase. Biotechnol Bioeng 90, 64–76. https://doi.org/10.1002/BIT.20418

Wagner, A.F.V., Frey, M., Neugebauer, F.A., Schafer, W., Knappe, J., 1992. The free radical in pyruvate formate-lyase is located on glycine-734. Proc Natl Acad Sci U S A 89, 996–1000. https://doi.org/10.1073/PNAS.89.3.996

Watanabe, S., Saleh, A.A., Pack, S.P., Annaluru, N., Kodaki, T., Makino, K., 2007. Ethanol production from xylose by recombinant *Saccharomyces cerevisiae* expressing protein-engineered NADH-preferring xylose reductase from *Pichia stipitis*. Microbiology 153, 3044–3054.

Wehrenberg, R.H., 1981. Lactic acid polymers: strong, degradable thermoplastics. Materials engineering 94.

Wendisch, V.F., 2020. Metabolic engineering advances and prospects for amino acid production. Metab Eng 58, 17–34. https://doi.org/10.1016/j.ymben.2019.03.008

Xiao, Z., Lu, J.R., 2014. Strategies for enhancing fermentative production of acetoin: A review. Biotechnol Adv 32, 492–503. https://doi.org/10.1016/j.biotechadv.2014.01.002

Yang, T., Rao, Z., Zhang, X., Xu, M., Xu, Z., Yang, S.-T., 2017. Metabolic engineering strategies for acetoin and 2,3-butanediol production: advances and prospects. Crit Rev Biotechnol 37, 990–1005. https://doi.org/10.1080/07388551.2017.1299680

Yim, H., Haselbeck, R., Niu, W., Pujol-Baxley, C., Burgard, A., Boldt, J., Khandurina, J., Trawick, J.D., Osterhout, R.E., Stephen, R., Estadilla, J., Teisan, S., Schreyer, H.B., Andrae, S., Yang, T.H., Lee, S.Y., Burk, M.J., van Dien, S., 2011. Metabolic engineering of *Escherichia coli* for direct production of 1,4-butanediol. Nat Chem Biol 7, 445–452. https://doi.org/10.1038/nchembio.580

Yokota, A., Takao, S., 1989. Pyruvic acid production by lipoic acid auxotrophs of *Enterobacter aerogenes*. Agric Biol Chem 53, 705–711.

Zelić, B., Gerharz, T., Bott, M., Vasić-Rački, Đ., Wandrey, C., Takors, R., 2003. Fed-Batch Process for Pyruvate Production by Recombinant *Escherichia coli* YYC202 Strain. Eng Life Sci 3, 299–305. https://doi.org/10.1002/ELSC.200301756

Zhang, W., Wong, K.K., Magliozzo, R.S., Kozarich, J.W., 2001. Inactivation of pyruvate formate-lyase by dioxygen: defining the mechanistic interplay of glycine 734 and cysteine 419 by rapid freeze-quench EPR. Biochemistry 40, 4123–4130. https://doi.org/10.1021/BI002589K

Zhao, J., Baba, T., Mori, H., Shimizu, K., 2004. Effect of *zwf* gene knockout on the metabolism of *Escherichia coli* grown on glucose or acetate. Metab Eng 6, 164–174. https://doi.org/10.1016/J.YMBEN.2004.02.004

Zhu, Y., Eiteman, M.A., Altman, R., Altman, E., 2008. High Glycolytic Flux Improves Pyruvate Production by a Metabolically Engineered *Escherichia coli* Strain. Appl Environ Microbiol 74, 6649–6655. https://doi.org/10.1128/AEM.01610-08

Ziegler, M., Hägele, L., Gäbele, T., Takors, R., 2021. CRISPRi enables fast growth followed by stable aerobic pyruvate formation in *Escherichia coli* without auxotrophy. Eng Life Sci 22, 70–84. https://doi.org/10.1002/ELSC.202100021

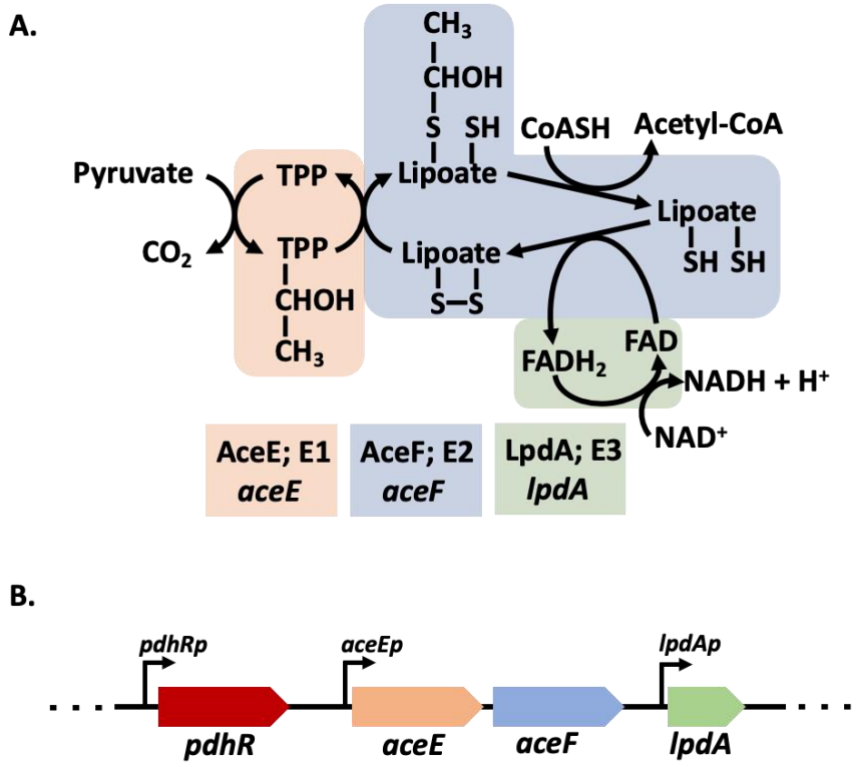

Figure 1.1 – (A) Reaction scheme of pyruvate decarboxylation and acetyl-CoA formation catalyzed by the pyruvate dehydrogenase complex. The three components are: pyruvate dehydrogenase (orange), dihydrolipoamide acetyltransferase (blue), and dihydrolipoamide dehydrogenase (green). (B) The chromosomal organization of the *pdhR-aceEF-lpdA* operon.

CHAPTER 2

PYRUVATE PRODUCTION BY ESCHERICHIA COLI BY USE OF PYRUVATE DEHYDROGENASE VARIANTS

Moxley, W.C. and Eiteman, M.A. 2021 *Applied and Environmental Microbiology* 87:e00487-21.

Reprinted with permission of publisher.

2.1 ABSTRACT

Altering metabolic flux at a key branchpoint in metabolism has commonly been accomplished through gene knockouts or by modulating gene expression. An alternative approach to direct metabolic flux preferentially toward a product is decreasing the activity of a key enzyme through protein engineering. In *Escherichia coli*, pyruvate can accumulate from glucose when carbon flux through the pyruvate dehydrogenase complex is suppressed. Based on this principle, 16 chromosomally expressed AceE variants were constructed in *E. coli* C and compared for growth rate and pyruvate accumulation using glucose as the sole carbon source. To prevent conversion of pyruvate to other products, the strains also contained deletions in two nonessential pathways: lactate dehydrogenase (*ldhA*) and pyruvate oxidase (*poxB*). The effect of deleting phosphoenolpyruvate synthase (*ppsA*) on pyruvate assimilation was also examined. The best pyruvate-accumulating strains were examined in controlled batch and continuous processes. In a nitrogen-limited chemostat process at steady-state growth rates of 0.15 – 0.28 h^{-1}, an engineered strain expressing the AceE[H106V] variant accumulated pyruvate at a yield of 0.59-0.66 g pyruvate/g glucose with a specific productivity of 0.78 – 0.92 g pyruvate/g cells·h. These results provide proof-of-concept that pyruvate dehydrogenase complex variants can effectively shift carbon flux away from central carbon metabolism to allow pyruvate accumulation. This approach can potentially be applied to other key enzymes in metabolism to direct carbon toward a biochemical product.

IMPORTANCE

Microbial production of biochemicals from renewable resources has become an efficient and cost-effective alternative to traditional chemical synthesis methods. Metabolic engineering

tools are important for optimizing a process to perform at an economically feasible level. This study describes an additional tool to modify central metabolism and direct metabolic flux to a product. We have shown that variants of the pyruvate dehydrogenase complex can direct metabolic flux away from cell growth to increase pyruvate production in *Escherichia coli.* This approach could be paired with existing strategies to optimize metabolism and create industrially relevant and economically feasible processes.

2.2 INTRODUCTION

A well-optimized microorganism and process are important for microbial conversion of inexpensive substrates like glucose to biochemicals at high yields and productivities. Directing metabolic flux from central metabolism to a biochemical product inherently involves a competition between native metabolism (i.e., cell growth) and the typically synthetic pathway toward that product. Commonly, the focus for improving the process lies in the pathway from central metabolism leading to that biochemical (the "product pathway"), for example, by increasing the activity of enzymes in that pathway (Koffas et al., 2003) or by elevating the expression of the introduced genes (Alper et al., 2005; Aristidou et al., 1994).

One common approach to reduce the competition between the product pathway and native enzymes is to knockout genes of nonessential pathways that compete for precursor metabolites. For example, *Escherichia coli* with deletions in genes to native fermentation and acetate assimilation pathways allow acetate to accumulate as the main fermentation product (Causey et al., 2003). Similarly, *E. coli* with an inactive phosphoenolpyruvate (PEP)-consuming glucose phosphotransferase system directs more PEP toward the aromatic pathway due to increased PEP availability (Flores et al., 1996; Martínez et al., 2015). In some cases, gene

knockouts result in auxotrophy, necessitating medium supplementation. For example, L-glutamate and L-leucine are required for growth of citramalate-producing *E. coli* strains having deletions in *leuCD* and *gltA* (Wu and Eiteman, 2016). Similarly, shikimate formation using *E. coli aroK aroL* creates an aromatic amino acid requirement (Knop et al., 2001).

A gene knockout typically represents the complete elimination of a flux. Modulating the activity of an enzyme is potentially more beneficial than completely shutting off a pathway. One approach to modulating flux is to use strains auxotrophic for specific enzyme cofactors or affectors, which then are limited in the medium to control flux through a pathway. For example, thiamine or lipoic acid auxotrophs can accumulate pyruvate (Yokota et al., 1994; Yokota and Takao, 1989; Yonehara and Miyata, 1994). The auxotroph grown in a thiamine- or lipoic acid-limiting medium reduces the specific activity of the pyruvate dehydrogenase complex (PDHc), leading to increased pyruvate accumulation. Similarly, manganese limitation increases citric acid accumulation by *Aspergillus niger* (Kubicek and Röhr, 1977; Papagianni, 2007).

Another sophisticated method for controlling the enzyme activity during a process is through promoter engineering, which involves either a static or dynamic control of the expression level of key enzymes. The most common approach for promoter engineering is increasing the expression of enzymes in the product pathway (Colón et al., 1995; Ikeda and Katsumata, 1992; Koffas et al., 2003). Alternatively, the expression of a competing enzyme in native metabolism can be diminished by introducing a weaker promoter. For example, *Corynebacterium glutamicum* produces more L-valine by down-modulating a gene in a competing pathway (*ilvA*) while up-modulating two genes in the L-valine synthesis pathway (*ilvD* and *ilvE*)(Holátko et al., 2009). Promoter engineering affects specific enzyme activity by decreasing the concentration of the native enzyme and does not alter the kinetic parameters of

that enzyme (i.e., k_{cat} and K_m). Promoter engineering can have unpredictable effects on existing metabolic networks (Kim and Copley, 2012) and may require the maintenance of plasmid DNA (Bhattacharya and Dubey, 1995; Dong et al., 1995).

The central metabolite pyruvate is produced by microbial processes (Maleki et al., 2017) and is also a metabolic precursor for several biochemicals such as isobutanol and 2,3-butanediol (Atsumi et al., 2008). Metabolic engineering strategies used to accumulate pyruvate commonly include inactivating pyruvate-consuming pathways. In *E. coli*, for example, by-product pathways that convert pyruvate to acetate and lactate are blocked respectively by inactivating *poxB* and *ldhA* (Tomar et al., 2003; Zelić et al., 2003). Under aerobic conditions, the majority of pyruvate is converted into acetyl CoA by the PDHc (Zhao et al., 2004), therefore controlling metabolic flux toward acetyl CoA is important for accumulation of pyruvate and products derived from pyruvate.

The PDHc is a large multi-unit complex of three different enzymes. The first dehydrogenase, the E1 component (or AceE) coded by *aceE*, converts pyruvate to CO_2 and transfers the remaining hydroxyethyl group onto an enzyme-bound thiamine diphosphate (ThDP) and subsequently to a lipoate moiety of the adjacent E2 component coded by *aceF*. The E2 component transfers acetyl to CoA forming acetyl CoA, while the remaining dihydrolipoate is reoxidized by the E3 component coded by *lpdA* forming NADH. One strategy to accumulate pyruvate is by the deletion of any one of these three PDHc enzyme components (Tomar et al., 2003; Zelić et al., 2003). However, PDHc-deficient *E. coli* strains cannot synthesize acetyl CoA from pyruvate under aerobic conditions and require a secondary carbon source such as acetate (Langley and Guest, 1978). Additional nutrient requirements increase operating costs of the process; therefore, an appealing alternative is instead to decrease the activity of the complex. In

addition to thiamine or lipoic acid auxotrophy to control activity of the complex, another strategy for pyruvate accumulation is oxygen limitation to encourage elevated concentrations of NADH, which inhibits the E3 component (Bisswanger, 1974; Schmincke‐Ott and Bisswanger, 1981). Promoter engineering can also decrease the PDHc activity by decreasing the expression of one of the subunits of the complex. For example, the native *aceE* promoter in *Corynebacterium glutamicum* was replaced by weaker promoter variants to produce a range of growth rates and PDHc activities (Buchholz et al., 2013). Subsequent overexpression of L-valine biosynthetic genes *ilvBNCE* resulted in all variants accumulating more L-valine than the strain with the native promoter.

An alternate approach to direct metabolic flux preferentially toward a product pathway is to decrease the intrinsic activity of the competing native enzyme at that metabolic branchpoint. Changing the intrinsic activity could be accomplished by altering key residues which affect substrate binding (i.e., K_m) or turnover (i.e., k_{cat}). Alteration of substrate affinity in a highly active native enzyme would allow the product pathway to be more competitive. This approach could potentially be combined with promoter engineering or other methods to allow greater flexibility to optimize carbon flux to a desired product. Since the E1 component of PDHc is the rate-limiting step, the AceE protein is an appropriate target for reducing flux between pyruvate and acetyl CoA.

The goal of this proof-of-concept study is to create variants of PDHc which reduce the native carbon flux to acetyl CoA and shift flux to pyruvate. We hypothesize that PDHc variants of *E. coli* having reduced activity would accumulate pyruvate from glucose during aerobic growth. In order to prevent conversion of pyruvate to other products, the strains also contained

deletions in two nonessential pathways: lactate dehydrogenase (*ldhA*) and pyruvate oxidase (*poxB*).

2.3 MATERIAL AND METHODS

Strains and genetic modifications. Strains used in this study are shown in Table 1. The *ppsA* gene knockout in *E. coli* C (ATCC 8739) was constructed by methods previously described (Datsenko and Wanner, 2000). The *aceE*, *ldhA*, and *poxB* gene knockout strains were acquired from the Keio (FRT)Kan collection (Baba et al., 2006). Gene knockouts were transduced into recipient strains by P1 phage transduction. Knockouts were selected on Lysogeny Broth (LB) or TYA (Chang and Cronan, 1982) plates supplemented with kanamycin. Forward primers external to the target gene and reverse primers within the kanamycin resistance cassette were used to confirm proper chromosomal integration. The kan^R marker was removed by expression of FLP recombinase from pCP20 (Datsenko and Wanner, 2000). Gene knockouts and removal of the markers were verified by PCR. To construct MEC813, a chloramphenicol-*sacB* (cam-*sacB*) cassette and 500 bp of homology flanking *aceE* was amplified from pCM03 and integrated into the *aceE* locus of MEC785 expressing the lambda red system from pKD46. Flanking regions surrounding *aceE* were sequence verified.

A scarless approach was used to integrate point-mutated *aceE* variants (Yang et al., 2014). pKSI-1 harboring a point-mutated *aceE* was used as donor DNA. If integration was unsuccessful using the method above, the point-mutated *aceE* variant and 500 bp of flanking homology were amplified from the respective plasmid and used to transform electrocompetent MEC813 expressing the lambda red system from pKD46 (Datsenko and Wanner, 2000). Counter-selection against *sacB* was used to select mutants that lost the cam-*sacB* cassette by

plating transformants on medium containing sucrose (Thomason et al., 2014). Colonies were confirmed by colony PCR, and point-mutated *aceE* genes were amplified from the chromosome, gel purified, and sequenced to confirm mutations.

Plasmid construction. Plasmids used in this study are listed in Table 2, and primers used in this study are listed in Table 3. pKSI-1 (Addgene plasmid # 51725; http://n2t.net/addgene:51725 ; RRID:Addgene_51725) and pREDTKI (Addgene plasmid # 51628 ; http://n2t.net/addgene:51628 ; RRID:Addgene_51628) were gifts from Sheng Yang (Yang et al., 2014). Plasmids were constructed using NEBuilder HiFi Assembly (New England Biolabs, Ipswich, MA, USA) or *Escherichia coli* DH5α-mediated assembly (Kostylev et al., 2015). Phusion High-Fidelity Polymerase (New England Biolabs, Ipswich, MA, USA) or PrimeStar Max High-Fidelity Polymerase (Takara Bio, Mountain View, CA, USA) was used to amplify DNA for cloning and genome integration. Quick-DNA Miniprep and Zyppy Plasmid Miniprep Kits were used to purify genomic and plasmid DNA (Zymo Research, Irvine, CA, USA). DNA Clean and Concentrator and Zymoclean Gel DNA Recovery Kits were used to purify PCR fragments (Zymo Research, Irvine, CA, USA). Restriction enzymes were purchased from New England Biolabs. Plasmids were confirmed by restriction digest and sequencing (ACGT, Inc., Wheeling, IL, USA).

To construct pCM01, a cam-*sacB* cassette was amplified from pEL04 (Lee et al., 2001) and cloned into the MCS of pKSI-I (Yang et al., 2014). To construct pCM02, *aceE* with 500 bp of flanking DNA on both sides was cloned into the multiple cloning site (MCS) of pKSI-1. The cam-*sacB* cassette was amplified from pCM01 with I-SceI restriction sites incorporated into both primers, and cloned into pCM02, replacing bases 4 – 2,596 of the coding sequence of *aceE*, to

generate pCM03. All plasmids harboring a single point-mutated *aceE* variant were generated from pCM02 using mutagenic primers that incorporated mutations into homologous regions used for DNA assembly. To create pCM21, which harbors two point mutations, pCM04 was used as a template to incorporate the mutation E401A. Codon usage frequency of *E. coli* was considered in the design of point mutations.

Media and Growth Conditions. During plasmid and strain construction, cultures were grown on LB while all *aceE* deletion mutants were grown in TYA medium. As needed, the following antibiotics were included in medium (final concentrations): ampicillin (100 µg/mL), kanamycin (40 µg/mL), and chloramphenicol (20 µg/mL). For counter-selection against *sacB*, the medium was supplemented with 250 g/L sucrose, and NaCl was excluded.

The defined basal medium to which carbon/energy sources were added contained (per L): 3.5 g NH_4Cl, 0.29 g KH_2PO_4, 0.50 $K_2HPO_4 \cdot 3H_2O$, 2.0 g K_2SO_4, 0.45 g $MgSO_4 \cdot 7H_2O$, 0.25 mg $ZnSO_4 \cdot 7H_2O$, 0.125 mg $CuCl_2 \cdot 2H_2O$, 1.25 mg $MnSO_4 \cdot H_2O$, 0.875 mg $CoCl_2 \cdot 6H_2O$, 0.06 mg H_3BO_3, 0.25 mg $Na_2MoO_4 \cdot 2H_2O$, 5.5 mg $FeSO_4 \cdot 7H_2O$, 20 mg $Na_2EDTA \cdot 2H_2O$, 20 mg citric acid, 20 mg thiamine·HCl, and 20.9 g 3-[*N*-morpholino]propanesulfonic acid (100 mM). Thiamine was filtered sterilized, while other medium components were autoclaved in compatible mixtures, combined and then adjusted to a pH of 7.1 with 20% (w/v) NaOH.

Shake flask experiments. A single colony from an LB plate was used to inoculate 3 mL TYA. After 6-10 h of growth, this culture was used to inoculate 3 mL of basal medium with 5 g/L D-(+)-glucose to an initial optical density at 600 nm (OD) of 0.05. After 12-15 h of growth, this culture was used to inoculate three 250 mL baffled shake flasks containing 50 mL of basal

medium with 5 g/L glucose to an OD of 0.02. All cultures were grown aerobically at 37°C on a rotary shaker at 225 rpm. Flasks were sampled 6-8 times for measurement of growth rate and extracellular metabolite concentrations.

Batch and repeated batch processes. A single colony from an LB plate was used to inoculate 3 mL TYA. After 6-10 h of growth, this culture was used to inoculate a 250 mL shake flask containing 50 mL of basal medium with 5 g/L glucose or 5 g/L glucose plus 2.34 g/L $Na(CH_3COO)\cdot 3H_2O$ (1 g/L acetate) to an OD of 0.02. When the shake flask culture reached an OD of 2, the entire 50 mL contents were used to inoculate a 2.5 L bioreactor (Bioflo 2000, New Brunswick Scientific Co., New Brunswick, NJ, USA) containing 950 mL basal medium with 15 g/L glucose. Duplicate batch processes were performed.

A repeated batch process started as a 1.0 L batch process described above containing 15 g/L glucose and 2 g/L acetate. When glucose was just depleted, a 17 mL solution containing glucose was added to increase its concentration nominally to 15 g/L. Batch and repeated batch studies were conducted with a constant agitation of 400 rpm and at 37°C. Air and/or oxygen-supplemented air was sparged at 1.0 L/min to maintain a dissolved oxygen concentration above 40% of saturation. The pH was controlled at 7.0 using 25% (w/v) KOH/5% NH_4OH and 20% (w/v) H_2SO_4. Antifoam C (Sigma) was used as necessary to control foaming.

Continuous process

Nitrogen-limited steady-state processes were conducted as chemostats and started as a 0.5 L batch process containing basal medium with 15 g/L glucose and the following modifications: NH_4Cl concentration was reduced from 3.5 g/L to 1 g/L and 3-[*N*-morpholino]propanesulfonic acid concentration was reduced from 20.9 g/L to 10.5 g/L (50 mM). Each strain was initially

cultured in TYA and then inoculated into a 150 mL baffled shake flask containing 25 mL of modified basal medium with 15 g/L glucose. When the shake flask culture reached an OD of 2, the entire 25 mL contents were used to inoculate a 1.0 L bioreactor (Bioflo 310, New Brunswick Scientific Co., New Brunswick, NJ, USA) containing 475 mL modified basal medium with 15 g/L glucose. After growth to an OD of 4, the chemostat was initiated at a nominal dilution rate of 0.15 h^{-1}, 0.20 h^{-1}, or 0.28 h^{-1}. The influent medium contained modified basal medium with 15 g/L glucose, and pH was adjusted to 8 to facilitate the control of pH within the bioreactor (at 7.0). The process operated at 37°C using 400 rpm agitation. Air and/or oxygen-supplemented air was sparged at 0.5 L/min to maintain a dissolved oxygen concentration above 40% of saturation. The pH was controlled at 7.0 with 30% w/v KOH, and antifoam C (Sigma) was used as necessary to control foaming.

Analytical methods. The optical density at 600 nm (OD) (UV-650 spectrophotometer, Beckman Instruments, San Jose, CA, USA) was used to monitor cell growth. For dry cell weight measurement, three 20.0 mL samples were centrifuged (3300 × g, 10 min), the pellets washed by vortex mixing with 20 mL DI water and then centrifuged again. After washing three times, the cell pellets were dried at 60°C for 24 h and weighed. Samples were routinely frozen at -20°C for further analysis, and thawed samples were centrifuged (4°C, 10000 × g for 10 min), and filtered (0.45 µm nylon, Acrodisc, Pall Corporation, Port Washington, NY). Liquid chromatography was used to quantify pyruvate, glucose and organic products using RI detection (Eiteman and Chastain, 1997). Ammonium was quantified by the Laboratory for Environmental Analysis (University of Georgia, Athens, GA, USA) using the phenate method (Solórzano, 1969).

RT-qPCR. Total RNA was prepared from chemostat samples (10^9 cells) at each dilution rate using Monarch Total RNA Miniprep Kit (New England Biolabs, Ipswich, MA, USA). RNA was used as a template for PCR to confirm that no genomic DNA was remaining. One-Step quantitative reverse transcriptase PCR (RT-qPCR) was performed using Luna Universal One-Step RT-qPCR Kit (New England Biolabs, Ipswich, MA, USA) on a StepOne Plus instrument (Applied Biosystems, Foster City, CA). Primer pairs for *aceE* and the housekeeping gene *rpoD* were confirmed to have similar efficiencies. Triplicate 20 µL reactions containing 4 ng total RNA were analyzed. No-template and no-RT controls were included. The $2^{-\Delta\Delta C_T}$ method was used to calculate fold change in expression from C_T values generated by the StepOne Plus software (Livak and Schmittgen, 2001).

2.4 Results

Variant strain screening. The principal goal of this proof-of-concept study was to generate point mutations in the E1 component of PDHc coded by *aceE* to decrease the activity of this enzyme and thereby reduce the flux from pyruvate to acetyl-CoA. Certain mutations, such as those critical in mediating the reaction or those integral to structure, would likely inactivate PDHc, eliminate the flux, and prevent growth of the strain on glucose as the sole carbon source. Our hypothesis was that other less severe mutations would permit growth but accumulate pyruvate, the substrate for that enzyme. To prevent the conversion of pyruvate to the typical by-products lactate and acetate, the *ldhA* and *poxB* genes were deleted in all strains (Tomar et al., 2003; Zelić et al., 2003).

The E1 subunit of the PDHc in *E. coli* consists of an AceE homodimer containing two symmetrical active site clefts that are formed at the interface of the two monomers. These active

site domains catalyze the ThDP-dependent decarboxylation of pyruvate to an intermediate, 2α-hydroxyethylidene-ThDP, and subsequently acetylates lipoate moieties of the E2 subunit (Bisswanger, 1974; Kluger, 1987; Stephens et al., 1983). Previous studies and protein structure were used to propose target residues in AceE involved in active site formation and pyruvate binding that might reduce activity without eliminating it (Arjunan et al., 2002; Kale et al., 2007; Nemeria et al., 2001). In particular, we targeted 1) the residues lining the active site cleft, and 2) the inner active site loop, one of two dynamic loops that gate the active site and interact with the E2 subunit (Kale et al., 2007). In the active site cleft lining, three histidine residues and one tyrosine residue were targeted for mutagenesis: H106, H142, and H640 are proximal to the reactive C2 atom of the thiazolium ring of ThDP where they are predicted to orient pyruvate in the active site, while Y177 is predicted to interact with ThDP intermediates (Arjunan et al., 2002). The inner mobile loop is comprised of residues 401 – 413 flanked on the N-terminal side by three glycine residues (Kale et al., 2007). In this region, G395, E401, K403, and K410 were targeted for mutagenesis. E401 and K403 stabilize the loop by forming hydrogen bonds with G395 and other adjacent residues, while K410 assists in ThDP entry into the active site cleft. These 8 residues were mutated to generate 16 AceE variants (15 single-point mutations, 1 double-point mutation) incorporated into the *E. coli* chromosome.

In order to determine whether each selected AceE mutation altered central metabolism, the single-point mutation variants were examined in triplicate in shake flasks for specific growth rate and pyruvate yield (Figure 2.1). Of the 15 strains with single-point mutations, 13 showed growth on glucose as the sole carbon source. MEC861 (AceE[E401D]) and MEC919 (AceE[H640V]) did not grow after 24 h. MEC860 (AceE[H106M]) and MEC826 (AceE[H106V]) were the only variants that accumulated pyruvate at yields of 0.19 ± 0.03 g/g

(MEC860) and 0.48 ± 0.02 g/g (MEC826). The accumulation of pyruvate correlated with a decrease in growth rate. Compared to MEC825 expressing the wild-type AceE (1.00 ± 0.04 h^{-1}), the H106M variant attained a growth rate of 0.66 ± 0.03 h^{-1}, while the H106V variant attained a growth rate of 0.34 ± 0.03 h^{-1}. All other variants attained growth rates above 0.86 h^{-1}. We also constructed strain MEC956 containing two mutations (AceE[H106M;E401A]). MEC956 attained a growth rate of 0.04 h^{-1}, 96% slower than MEC825, and a 0.86 g/g pyruvate yield in shake flasks. MEC826 (AceE[H106V]) attained the highest pyruvate yield at a reasonable growth rate and was chosen for further studies.

Effect of *ppsA* inactivation in pyruvate-accumulating strains. PEP synthase encoded by *ppsA* converts pyruvate into PEP and is essential when pyruvate is used as the sole carbon source (Brice and Kornberg, 1967; Niersbach et al., 1992). When MEC826 was grown in shake flask, pyruvate was slowly consumed after glucose was depleted (data not shown). This result suggested that these variants have a route to assimilate pyruvate, and we suspected PEP synthase was the cause. To minimize pyruvate utilization, and potentially increase its yield, *ppsA* was inactivated in MEC826 to yield MEC905 (C *aceE*::*aceE*$^{[H106V]}$ *ldhA poxB ppsA*). We also constructed MEC961 (C *aceE*::*aceE ldhA poxB ppsA*) expressing the wild-type AceE. These two strains were grown in triplicate in shake flasks as before to determine specific growth rate and pyruvate yield. MEC961 grew at a specific growth rate of 1.04 ± 0.00 h^{-1} and did not accumulate pyruvate, identical to results observed with MEC825. In contrast, MEC905 attained a specific growth rate of 0.32 ± 0.01 h^{-1} and accumulated pyruvate at a yield of 0.52 ± 0.02 g/g. Compared to the strain with *ppsA* (MEC826), MEC905 exhibited a small decrease in growth rate and increase in pyruvate yield.

Controlled batch processes. Our initial comparison of AceE variants was conducted in shake flasks in which oxygenation and pH were not well-controlled. We therefore compared growth and pyruvate formation using MEC825, MEC826, MEC905, or MEC961 in controlled 1.0 L bioreactors using 15 g/L glucose as the sole carbon source (Figure 2.2). All four strains contain knockouts in *ldhA* and *poxB*. MEC825 and MEC961 express the wild-type AceE, while MEC826 and MEC905 express the variant AceE[H106V]. The strains differ in having an intact *ppsA* gene (MEC825 and MEC826) or a *ppsA* deletion (MEC905 and MEC961). Both MEC825 (Figure 2.2a) and MEC961 (Figure 2.2b) depleted the glucose in less than 7 h and attained a growth rates of 0.93 – 0.99 h^{-1}. Neither strain accumulated pyruvate. MEC826 achieved a pyruvate yield of 0.29 ± 0.05 g/g (Figure 2.2c), while MEC905 achieved a yield of 0.43 ± 0.01 g/g (Figure 2.2d). These two strains expressing the AceE[H106V] variant showed no significant difference in growth rate (0.39 ± 0.01 h^{-1}). MEC826 metabolized pyruvate within two hours after glucose was depleted, whereas MEC905 metabolized pyruvate slowly after glucose depletion, demonstrating that pyruvate assimilation due to the activity of PEP synthase is significant.

Steady-state process. During batch growth all nutrients are in excess for essentially the entire process. In contrast, a steady-state process conducted as a chemostat permits the selection of one growth-limiting nutrient. Because the accumulation of pyruvate and other carbon products is often enhanced by carbon-excess conditions (Zhu et al., 2008), we examined pyruvate accumulation using MEC905 and MEC961 at nominal growth rates of 0.15, 0.20, and 0.28 h^{-1} under nitrogen limitation (Figure 2.3, Table S2.1). Nitrogen limitation was confirmed (as opposed to oxygen limitation) by 1) maintaining the DO above 30% saturation, 2) the absence of

anaerobic products in the effluent such as formate, 3) the presence of glucose in the effluent, and 4) the absence of nitrogen in the effluent. Additionally, we examined *aceE* expression levels in each strain at the target dilution rates. These strains both contain *ldhA, poxB,* and *ppsA* knockouts, but MEC905 expresses the AceE[H106V] variant and MEC961 expresses wild-type AceE. After five residence times to achieve steady-state at each of the three dilution rates, MEC905 accumulated pyruvate at an average yield of 0.62 ± 0.04 g/g with an average specific productivity of 0.84 ± 0.07 g/gh. At each dilution rate MEC961 accumulated insignificant pyruvate (average yield of only 0.01 ± 0.00 g/g). In contrast, MEC905 did not accumulate acetate, while MEC961 accumulated acetate at an average yield of 0.11 ± 0.01 g/g and specific productivity of 0.09 ± 0.02 g/gh. At each dilution rate the specific glucose consumption rate of MEC905 (average 1.37 ± 0.19 g/gh) was much greater than that of MEC961 (0.83 ± 0.10 g/gh). Between the two strains at three dilution rates, *aceE* was upregulated 2.61 ± 0.54 fold in MEC905 compared to MEC961 (Table S2.2).

Pyruvate production by H106M/E401A variant strains. Of the AceE variants examined, MEC956 was the only strain that contained two point mutations (AceE[H106M;E401A]). This strain grew very poorly using glucose as the sole carbon source (0.04 h^{-1}), but it attained a pyruvate yield exceeding 0.80 g/g in shake flasks, higher than previously reported (Causey et al., 2004). This result suggests a two-phase process in which the strain is grown initially on complex carbon sources or on a carbon source biochemically downstream of PDHc to supply acetyl CoA (Tomar et al., 2003; Zelić et al., 2003). To prevent pyruvate assimilation by MEC956, *ppsA* was inactivated to generate MEC994 (C *aceE*::*aceE*$^{[H106M;E401A]}$ *ldhA poxB ppsA*). The performance

of MEC994 was compared to MEC992 (C *aceE ldhA poxB ppsA*) which contains an *aceE* knockout.

MEC992 and MEC994 were each grown under controlled batch conditions at 1.0 L scale initially containing 15 g/L glucose and 2 g/L acetate, with 15 g glucose added once after the glucose was depleted. As expected, growth of MEC992 ceased after acetate depletion, while MEC994 sustained a slow growth rate (Figure 2.4). After acetate depletion, MEC992 accumulated pyruvate at a yield of 0.77 g/g and volumetric productivity of 1.25 g/Lh, and converted the added glucose to pyruvate at a yield of 0.78 g/g and volumetric productivity of 1.28 g/Lh (Figure 2.4a). By the end of the process, MEC992 generated 18.8 g/L in 19.5 h for an overall yield of 0.73 g/g and productivity of 0.96 g/Lh (includes growth). In comparison, MEC994 converted the initial glucose to pyruvate at 0.73 g/g yield with a volumetric productivity of 1.32 g/Lh, and converted the added glucose at 0.74 g/g yield with a volumetric productivity of 1.70 g/Lh (Figure 2.4b). At the end of the process, MEC994 accumulated 17.1 g/L pyruvate in 16.6 h for an overall yield of 0.68 g/g and productivity of 1.03 g/Lh. Thus, under twice-repeated batch conditions the *aceE* deletion strain MEC992 provided a slightly greater yield but a lower productivity. Importantly, pyruvate productivity for MEC994 increased by 29% between the first and second period of glucose consumption, while the pyruvate productivity was essentially unchanged for MEC992. This result suggests that slow growth during pyruvate formation could better maintain pyruvate production during a prolonged process with glucose as the sole carbon source.

During all batch and continuous processes, no significant unknown peaks were observed and additional by-products (e.g., succinate, ethanol, citrate, glyoxylate, formate, etc.) were less than 0.1 g/L.

2.5 DISCUSSION

In this proof-of-concept study, point mutations in AceE were engineered into the chromosome of *E. coli,* and the strains were screened for their ability to accumulate pyruvate. The goal was to use a structure-based approach to engineer AceE variants having reduced activity, such that pyruvate conversion to acetyl CoA by PDHc was greatly diminished but not eliminated. By considering the pyruvate binding domain of AceE and previous structural studies, we mutated residues involved in active site formation and substrate binding (Arjunan et al., 2002; Kale et al., 2007; Nemeria et al., 2001).

The H106 mutations were the only mutation site which allowed pyruvate accumulation (H106M and H106V), and resulted in a >15% decrease in growth rates. These mutations are most likely inhibiting pyruvate reacting with the thiazolium ring of ThDP and/or decreasing the stability of reaction intermediates. Although the most likely explanation for pyruvate accumulation and reduced growth rate is that these mutations affect the kinetic properties of the enzyme, we cannot rule out reduced protein stability or altered regulation. Eight of the nine variants with substitutions in mobile loop residues (G395, E401, K403, and K410) had a comparatively minor impact on growth rate and did not accumulate pyruvate in shake flask culture. These results suggest that the mobile loop in these variants was marginally impaired and did not impact PDHc activity sufficiently to accumulate pyruvate. Interestingly, a few variants that were previously reported to have very low *in vitro* activity did not lead to pyruvate accumulation. For example, Y177F, E401A, and K403A have been previously shown to reduce PDHc activities by 93%, 90%, and 88%, respectively (Kale et al., 2007; Nemeria et al., 2001), yet strains chromosomally expressing these mutations displayed only a 5-15% decrease in

growth rate on glucose with no pyruvate accumulation (Figure 2.1). Thus, even a considerable decrease in enzyme activity does not predict pyruvate accumulation. These results can be explained by the differences between *in vitro* and *in vivo* environments and the fact that *in vitro* assays do not replicate the intracellular environment (Davidia et al., 2016; García-Contreras et al., 2012). Additionally, a relationship was observed between a strain's specific growth rate and pyruvate yield: the lower the growth rate, the greater the pyruvate yield. A threshold growth rate appears to exist for pyruvate accumulation: E401A and K403N (growth rate of 0.86 – 0.89 h^{-1}, about 15% lower than MEC825) did not accumulate pyruvate while H106M (0.66 h^{-1}) did.

Two variants examined (E401D, H640V) were not able to grow on glucose as a sole carbon source, indicating these substitutions were too deleterious to allow sufficient PDHc activity required for growth. E401 likely contributes to loop stability by hydrogen bonding with proximal glycine residues, and a charge reversal substitution (E401K) has been shown to impair mobile loop function (Kale et al., 2007). The E401D substitution likely disrupts stabilizing hydrogen bonds similar to the E401K substitution, as the side chain carboxyl of E401D is oriented away from the original position where undesirable hydrogen bonds can decrease loop stability. In comparison, the fact that E401A only reduced growth rate slightly (Figure 2.1) demonstrates that the specific substitution is critical to the enzyme. H640 is located in the active site cleft and likely is involved in the reaction between pyruvate and ThDP to stabilize the reaction intermediates (Arjunan et al., 2002). Since the H640V variant could not utilize glucose as a carbon source, this mutation may inhibit the formation and stability of intermediates.

MEC956 contained one mutation in the active site (H106M) and one mutation in the mobile loop (E401A). This strain attained the highest pyruvate yield in shake flask culture but grew very slowly, much slower than MEC860 (H106M alone), despite the observation that

MEC827 (E401A alone) resulted in only a modest decline in growth rate with no pyruvate generation. Clearly, the combination of mutations causes a synergistic effect on enzyme activity.

Since growing MEC956 on glucose as the sole carbon source would be impractical due to its slow growth rate, a two-phase process was used where acetate was supplied in the initial phase to support biomass formation. Using this process, MEC994 (C *aceE*::*aceE*$^{[H106M;E401A]}$ *poxB ldhA ppsA*) was effective in generating pyruvate after acetate was consumed. When compared to MEC992 (C *aceE poxB ldhA ppsA*), the diminished activity of AceE[H106M;E401A] allowed MEC994 to grow on glucose, leading to a slight decrease in pyruvate yield but an increase in volumetric productivity. The AceE[H106M;E401A] variant is a similar alternative to inactivating *aceE* to increase and prolong the productivity of pyruvate-producing strains.

The observed inverse correlation between growth rate and pyruvate accumulation emphasizes the competition between cell growth and product formation. In pyruvate-accumulating strains, the decreased activity of PDHc reduced the rate of acetyl CoA formation, and carbon flux was diverted from central metabolism to pyruvate accumulation. This balance is further evident when comparing MEC905 (AceE[H106V]) and MEC961 (wild-type AceE) under nitrogen-limited steady-state conditions. On a per cell basis and considering the three different dilution rates, MEC905 consumed glucose 65% faster and sustained 2.6-fold greater *aceE* expression levels than MEC961 in order to maintain the target growth rates and presumably equivalent acetyl CoA formation rates needed for biomass formation.

By-product pathways to lactate and acetate were effectively blocked by the deletion of the *ldhA* and *poxB* genes (Tomar et al., 2003; Zelić et al., 2003), and neither lactate nor acetate (nor other typical by-products) was observed in cultures during growth of any variant in shake

flasks or batch processes. Pyruvate consumption was observed when glucose was depleted, an effect that was largely eliminated by the *ppsA* deletion. The *ppsA* deletion therefore resulted in much greater pyruvate yield with limited effect on growth rate.

Of the 12 precursors generated in central metabolism during aerobic growth of wild-type *E. coli* on glucose, pyruvate ranks second on a molar basis in the quantity withdrawn for biomass, with over 86% of the carbon entering pyruvate from PEP exiting through PDHc (Zhao et al., 2004). The kinetic parameters of *E. coli* AceE, the rate-limiting component of the complex, for pyruvate are k_{cat} of 38 s^{-1} and K_m of 260 μM (Kale et al., 2007). Any other enzyme overexpressed in an attempt to generate a product derived from pyruvate must directly compete with AceE. For example, acetolactate synthase (ALS) leading to the formation of isobutanol and valine has kinetic parameters of k_{cat} of 121 s^{-1} and K_m of 13,600 μM, although the Q487S point mutation on ALS alters those parameters to k_{cat} of 11 s^{-1} and K_m of 1,100 μM (Atsumi et al., 2009). The intracellular pyruvate concentration under aerobic conditions when *E. coli* grows maximally is about 5,000 μM (Rahman et al., 2006; Vemuri et al., 2006). Assuming this pyruvate concentration, AceE would operate near capacity (i.e., considering Michaelis-Menten kinetics – $38 \times 5000/(260 + 5000) = 36$ s^{-1}), while the seemingly faster wild-type ALS would be at 25% capacity (30 s^{-1}). Considering the case where the same quantity of these two enzymes are present without additional affectors, ALS flux is predicted to be 20% lower than the flux through PDHc despite having a k_{cat} which is 3.2-fold greater. These simplified calculations serve to emphasize that enzyme activity is based both on the enzyme turnover (k_{cat}) and substrate binding (K_m), and that a high K_m limits the effectiveness of the enzyme, which itself depends on growth conditions. Unsurprisingly, enzymes like AceE found in central metabolism tend to have low

values for K_m, which stands as a hurdle for a pathway toward any biochemical which must compete with these enzymes.

Continuing this example comparing AceE and ALS, merely expressing more ALS unfortunately becomes self-limiting since the presence of more ALS would tend to reduce pyruvate levels as has been observed with other enzymes (Yang et al., 2001), allowing AceE with its much lower K_m to become even more competitive. As an illustration, when wild-type *E. coli* is growing at 0.1 h^{-1} the intracellular pyruvate has diminished to 1,500 μM (Vemuri et al., 2006), a level at which AceE is operating at 32 s^{-1} (85% capacity) while at this concentration wild-type ALS would be operating only at 12 s^{-1} (10%), necessitating 2.7-fold expression more than PDHc to allow pyruvate to partition equally between the two enzymes. Decreased expression of PDHc, for example, by using weak promoters to drive expression of *aceE* (Buchholz et al., 2013), can effectively decrease V_{max}, but does not affect the intrinsic kinetic properties of AceE (k_{cat} and K_m). Modification of native enzymes at key junctures in metabolism offers an additional degree of flexibility in pathway engineering.

In summary, reducing the activity of PDHc through point mutations is a means to accumulate pyruvate during *E. coli* growth on glucose as the sole carbon source. Reduced PDHc activity simultaneously leads to a reduction in growth rate. This metabolic engineering strategy offers an additional approach in the toolbox to redirect carbon toward biochemical products.

ACKNOWLEDGMENTS

The authors thank Sarah Lee for technical support for this project. The authors also acknowledge financial support of the U.S. National Science Foundation (CBET-1802533), the U.S. Department of Agriculture, National Institute of Food and Agriculture (2017-06510), and

the Southeastern Regional Sun Grant Center at the University of Tennessee through a grant provided by the U.S. Department of Agriculture (2014-38502-22598).

2.6 REFERENCES

Alper, H., Fischer, C., Nevoigt, E., Stephanopoulos, G., 2005. Tuning genetic control through promoter engineering. Proc Natl Acad Sci U S A 102, 12678–12683. https://doi.org/10.1073/pnas.0504604102

Aristidou, A.A., San, K. -Y, Bennett, G.N., 1994. Modification of central metabolic pathway in *Escherichia coli* to reduce acetate accumulation by heterologous expression of the *Bacillus subtilis* acetolactate synthase gene. Biotechnol Bioeng 44, 944–951. https://doi.org/10.1002/bit.260440810

Arjunan, P., Nemeria, N., Brunskill, A., Chandrasekhar, K., Sax, M., Yan, Y., Jordan, F., Guest, J.R., Furey, W., 2002. Structure of the Pyruvate Dehydrogenase Multienzyme Complex E1 Component from *Escherichia coli* at 1.85 Å Resolution. Biochemistry 41, 5213–5221. https://doi.org/10.1021/bi0118557

Atsumi, S., Hanai, T., Liao, J.C., 2008. Non-fermentative pathways for synthesis of branched-chain higher alcohols as biofuels. Nature 451. https://doi.org/10.1038/nature06450

Atsumi, S., Li, Z., Liao, J.C., 2009. Acetolactate synthase from *Bacillus subtilis* serves as a 2-ketoisovalerate decarboxylase for isobutanol biosynthesis in *Escherichia coli*. Appl Environ Microbiol 75, 6306–6311. https://doi.org/10.1128/AEM.01160-09

Baba, T., Ara, T., Hasegawa, M., Takai, Y., Okumura, Y., Baba, M., Datsenko, K.A., Tomita, M., Wanner, B.L., Mori, H., 2006. Construction of *Escherichia coli* K-12 in-frame, single-gene knockout mutants: The Keio collection. Mol Syst Biol 2, 2006.0008. https://doi.org/10.1038/msb4100050

Bhattacharya, S.K., Dubey, A.K., 1995. Metabolic burden as reflected by maintenance coefficient of recombinant *Escherichia coli* overexpressing target gene. Biotechnol Lett 17, 1155–1160. https://doi.org/10.1007/BF00128377

Bisswanger, H., 1974. Regulatory Properties of the Pyruvate-Dehydrogenase Complex from *Escherichia coli* Thiamine Pyrophosphate as an Effector. Eur J Biochem 48, 377–387. https://doi.org/10.1111/j.1432-1033.1974.tb03779.x

Brice, C.B., Kornberg, H.L., 1967. Location of a gene specifying phosphopyruvate synthase activity on the genome of *Escherichia coli* K12. Proc R Soc Lond B Biol Sci 168, 281–292.

Buchholz, J., Schwentner, A., Brunnenkan, B., Gabris, C., Grimm, S., Gerstmeir, R., Takors, R., Eikmanns, B.J., Blombach, B., 2013. Platform Engineering of *Corynebacterium glutamicum* with Reduced Pyruvate Dehydrogenase Complex Activity for Improved Production of L-Lysine, L-Valine, and 2-Ketoisovalerate. Appl Environ Microbiol 79, 5566–75. https://doi.org/10.1128/AEM.01741-13

Causey, T.B., Shanmugam, K.T., Yomano, L.P., Ingram, L.O., 2004. Engineering *Escherichia coli* for efficient conversion of glucose to pyruvate. Proc Natl Acad Sci U S A 101, 2235–40. https://doi.org/10.1073/PNAS.0308171100

Causey, T.B., Zhou, S., Shanmugam, K.T., Ingram, L.O., 2003. Engineering the metabolism of *Escherichia coli* W3110 for the conversion of sugar to redox-neutral and oxidized products: Homoacetate production. Proc Natl Acad Sci U S A 100, 825–832. https://doi.org/10.1073/pnas.0337684100

Chang, Y.Y., Cronan, J.E., 1982. Mapping nonselectable genes of *Escherichia coli* by using transposon Tn10: Location of a gene affecting pyruvate oxidase. J Bacteriol 151, 1279–1289. https://doi.org/10.1128/jb.151.3.1279-1289.1982

Colón, G.E., Nguyen, T.T., Jetten, M.S.M., Sinskey, A.J., Stephanopoulos, G., 1995. Production of isoleucine by overexpression of *ilvA* in a *Corynebacterium lactofermentum* threonine producer. Appl Microbiol Biotechnol 43, 482–488. https://doi.org/10.1007/BF00218453

Datsenko, K.A., Wanner, B.L., 2000. One-step inactivation of chromosomal genes in *Escherichia coli* K-12 using PCR products. Proc Natl Acad Sci U S A 97, 6640–6645. https://doi.org/10.1073/pnas.120163297

Davidia, D., Noorb, E., Liebermeisterc, W., Bar-Evend, A., Flamholze, A., Tummlerf, K., Barenholza, U., Goldenfelda, M., Shlomig, T., Miloa, R., 2016. Global characterization of *in vivo* enzyme catalytic rates and their correspondence to *in vitro* k_{cat} measurements. Proc Natl Acad Sci U S A 113, 3401–3406. https://doi.org/10.1073/pnas.1514240113

Dong, H., Nilsson, L., Kurland, C.G., 1995. Gratuitous overexpression of genes in *Escherichia coli* leads to growth inhibition and ribosome destruction. J Bacteriol 177, 1497–1504. https://doi.org/10.1128/jb.177.6.1497-1504.1995

Eiteman, M.A., Chastain, M.J., 1997. Optimization of the ion-exchange analysis of organic acids from fermentation. Anal Chim Acta 338, 69–75. https://doi.org/10.1016/S0003-2670(96)00426-6

Flores, N., Xiao, J., Berry, A., Bolivar, F., Valle, F., 1996. Pathway engineering for the production of aromatic compounds in *Escherichia coli*. Nat Biotechnol 14, 620–623. https://doi.org/10.1038/nbt0596-620

García-Contreras, R., Vos, P., Westerhoff, H. v., Boogerd, F.C., 2012. Why *in vivo* may not equal *in vitro* - New effectors revealed by measurement of enzymatic activities under the

same *in vivo*-like assay conditions. FEBS Journal 279, 4145–4159. https://doi.org/10.1111/febs.12007

Holátko, J., Elišáková, V., Prouza, M., Sobotka, M., Nešvera, J., Pátek, M., 2009. Metabolic engineering of the L-valine biosynthesis pathway in *Corynebacterium glutamicum* using promoter activity modulation. J Biotechnol 139, 203–210. https://doi.org/10.1016/j.jbiotec.2008.12.005

Ikeda, M., Katsumata, R., 1992. Metabolic engineering to produce tyrosine or phenylalanine in a tryptophan-producing *Corynebacterium glutamicum* strain. Appl Environ Microbiol 58, 781–785. https://doi.org/10.1128/aem.58.3.781-785.1992

Kale, S., Arjunan, P., Furey, W., Jordan, F., 2007. A dynamic loop at the active center of the *Escherichia coli* pyruvate dehydrogenase complex E1 component modulates substrate utilization and chemical communication with the E2 component. J Biol Chem 282, 28106–16. https://doi.org/10.1074/jbc.M704326200

Kim, J., Copley, S.D., 2012. Inhibitory cross-talk upon introduction of a new metabolic pathway into an existing metabolic network. Proc Natl Acad Sci U S A 109, E2856–E2864. https://doi.org/10.1073/pnas.1208509109

Kluger, R., 1987. Thiamin Diphosphate: A Mechanistic Update on Enzymic and Nonenzymic Catalysis of Decarboxylation. Chem Rev 87, 863–876. https://doi.org/10.1021/cr00081a001

Knop, D.R., Draths, K.M., Chandran, S.S., Barker, J.L., von Daeniken, R., Weber, W., Frost, J.W., 2001. Hydroaromatic equilibration during biosynthesis of shikimic acid. J Am Chem Soc 123, 10173–10182. https://doi.org/10.1021/ja0109444

Koffas, M.A.G., Jung, G.Y., Stephanopoulos, G., 2003. Engineering metabolism and product formation in *Corynebacterium glutamicum* by coordinated gene overexpression. Metab Eng 5, 32–41. https://doi.org/10.1016/S1096-7176(03)00002-8

Kostylev, M., Otwell, A.E., Richardson, R.E., Suzuki, Y., 2015. Cloning should be simple: *Escherichia coli* DH5α-mediated assembly of multiple DNA fragments with short end homologies. PLoS One 10, e0137466. https://doi.org/10.1371/journal.pone.0137466

Kubicek, C.P., Röhr, M., 1977. Influence of manganese on enzyme synthesis and citric acid accumulation in *Aspergillus niger*. European Journal of Applied Microbiology 4, 167–175. https://doi.org/10.1007/BF01390476

Langley, D., Guest, J.R., 1978. Biochemical genetics of the alpha-keto acid dehydrogenase complexes of *Escherichia coli* K12: genetic characterization and regulatory properties of deletion mutants. J Gen Microbiol 106, 103–117. https://doi.org/10.1099/00221287-106-1-103

Lee, E.-C., Yu, D., Martinez de Velasco, J., Tessarollo, L., Swing, D.A., Court, D.L., Jenkins, N.A., Copeland, N.G., 2001. A Highly Efficient *Escherichia coli*-Based Chromosome Engineering System Adapted for Recombinogenic Targeting and Subcloning of BAC DNA. Genomics 73, 56–65. https://doi.org/10.1006/GENO.2000.6451

Livak, K.J., Schmittgen, T.D., 2001. Analysis of relative gene expression data using real-time quantitative PCR and the 2-ΔΔCT method. Methods 25, 402–408. https://doi.org/10.1006/meth.2001.1262

Maleki, N., Eiteman, M., Maleki, N., Eiteman, M.A., 2017. Recent Progress in the Microbial Production of Pyruvic Acid. Fermentation 3, 8. https://doi.org/10.3390/fermentation3010008

Martínez, J.A., Bolívar, F., Escalante, A., 2015. Shikimic acid production in *Escherichia coli*: From classical metabolic engineering strategies to omics applied to improve its production. Front Bioeng Biotechnol 23, 145. https://doi.org/10.3389/fbioe.2015.00145

Nemeria, N., Yan, Y., Zhang, Z., Brown, A.M., Arjunan, P., Furey, W., Guest, J.R., Jordan, F., 2001. Inhibition of the *Escherichia coli* pyruvate dehydrogenase complex E1 subunit and its tyrosine 177 variants by thiamin 2-thiazolone and thiamin 2-thiothiazolone diphosphates. Evidence for reversible tight-binding inhibition. J Biol Chem 276, 45969–78. https://doi.org/10.1074/jbc.M104116200

Niersbach, M., Kreuzaler, F., Geerse, R.H., Postma, P.W., Hirsch, H.J., 1992. Cloning and nucleotide sequence of the *Escherichia coli* K-12 *ppsA* gene, encoding PEP synthase. Mol Gen Genet 231, 332–336. https://doi.org/10.1007/BF00279808

Papagianni, M., 2007. Advances in citric acid fermentation by *Aspergillus niger*: Biochemical aspects, membrane transport and modeling. Biotechnol Adv 25, 244–263. https://doi.org/10.1016/j.biotechadv.2007.01.002

Rahman, M., Hasan, M.R., Oba, T., Shimizu, K., 2006. Effect of *rpoS* gene knockout on the metabolism of *Escherichia coli* during exponential growth phase and early stationary phase based on gene expressions, enzyme activities and intracellular metabolite concentrations. Biotechnol Bioeng 94, 585–595. https://doi.org/10.1002/bit.20858

Schmincke-Ott, E., Bisswanger, H., 1981. Dihydrolipoamide Dehydrogenase Component of the Pyruvate Dehydrogenase Complex from *Escherichia coli* K12: Comparative Characterization of the Free and the Complex-Bound Component. Eur J Biochem 114, 413–420. https://doi.org/10.1111/j.1432-1033.1981.tb05162.x

Solórzano, L., 1969. Determination of ammonia in natural waters by the phenolhypochlorite method. Limnol Oceanogr 14, 799–801.

Stephens, P.E., Darlison, M.G., LEwis, H.M., Guest, J.R., 1983. The Pyruvate Dehydrogenase Complex of *Escherichia coli* K12: Nucleotide Sequence Encoding the Dihydrolipoamide

Acetyltransferase Component. Eur J Biochem 133, 481–489. https://doi.org/10.1111/j.1432-1033.1983.tb07490.x

Thomason, L.C., Sawitzke, J.A., Li, X., Costantino, N., Court, D.L., 2014. Recombineering: Genetic engineering in bacteria using homologous recombination. Curr Protoc Mol Biol 106, 1–16. https://doi.org/10.1002/0471142727.mb0116s106

Tomar, A., Eiteman, M.A., Altman, E., 2003. The effect of acetate pathway mutations on the production of pyruvate in *Escherichia coli*. Appl Microbiol Biotechnol 62, 76–82. https://doi.org/10.1007/s00253-003-1234-6

Vemuri, G.N., Altman, E., Sangurdekar, D.P., Khodursky, A.B., Eiteman, M.A., 2006. Overflow Metabolism in *Escherichia coli* during Steady-State Growth: Transcriptional Regulation and Effect of the Redox Ratio. Appl Environ Microbiol 72, 3653–3661. https://doi.org/10.1128/AEM.72.5.3653-3661.2006

Wu, X., Eiteman, M.A., 2016. Production of citramalate by metabolically engineered *Escherichia coli*. Biotechnol Bioeng 113, 2670–2675. https://doi.org/10.1002/bit.26035

Yang, J., Sun, B., Huang, H., Jiang, Y., Diao, L., Chen, B., Xu, C., Wang, X., Liu, J., Jiang, W., Yang, S., 2014. High-efficiency scarless genetic modification in *Escherichia coli* by using lambda red recombination and I-SceI cleavage. Appl Environ Microbiol 80, 3826–34. https://doi.org/10.1128/AEM.00313-14

Yang, Y.T., Bennett, G.N., San, K.Y., 2001. The effects of feed and intracellular pyruvate levels on the redistribution of metabolic fluxes in *Escherichia coli*. Metab Eng 3, 115–123. https://doi.org/10.1006/mben.2000.0166

Yokota, A., Shimizu, H., Terasawa, Y., Takaoka, N., Tomita, F., 1994. Pyruvic acid production by a lipoic acid auxotroph of *Escherichia coli* W1485. Appl Microbiol Biotechnol 41, 638–646. https://doi.org/10.1007/BF00167278

Yokota, A., Takao, S., 1989. Pyruvic acid production by lipoic acid auxotrophs of *Enterobacter aerogenes*. Agric Biol Chem 53, 705–711.

Yonehara, T., Miyata, R., 1994. Fermentative production of pyruvate from glucose by *Torulopsis glabrata*. J Ferment Bioeng 78, 155–159. https://doi.org/10.1016/0922-338X(94)90255-0

Zelić, B., Gerharz, T., Bott, M., Vasić-Rački, Đ., Wandrey, C., Takors, R., 2003. Fed-Batch Process for Pyruvate Production by Recombinant *Escherichia coli* YYC202 Strain. Eng Life Sci 3, 299–305. https://doi.org/10.1002/ELSC.200301756

Zhao, J., Baba, T., Mori, H., Shimizu, K., 2004. Effect of *zwf* gene knockout on the metabolism of *Escherichia coli* grown on glucose or acetate. Metab Eng 6, 164–174. https://doi.org/10.1016/J.YMBEN.2004.02.004

Zhu, Y., Eiteman, M.A., Altman, R., Altman, E., 2008. High Glycolytic Flux Improves Pyruvate Production by a Metabolically Engineered *Escherichia coli* Strain. Appl Environ Microbiol 74, 6649–6655. https://doi.org/10.1128/AEM.01610-08

Table 2.1 - Strains used in this study.

Strain	Relevant characteristics	Reference
ATCC 8739	*Escherichia coli* C	Wild-type
MEC785	ATCC 8739 *aceE732*::(FRT) *ldhA744*::(FRT) *poxB772*::(FRT)	This study
MEC813	MEC785 *aceE*::cam-*sacB 869,658-872,250* (flanked by I-SceI sites)	This study
MEC817	MEC813 *aceE*::*aceE*$^{[H106N]}$	This study
MEC825	MEC813 *aceE*::*ace*	This study
MEC826	MEC813 *aceE*::*aceE*$^{[H106V]}$	This study
MEC827	MEC813 *aceE*::*aceE*$^{[E401A]}$	This study
MEC860	MEC813 *aceE*::*aceE*$^{[H106M]}$	This study
MEC861	MEC813 *aceE*::*aceE*$^{[E401D]}$	This study
MEC862	MEC813 *aceE*::*aceE*$^{[K403A]}$	This study
MEC863	MEC813 *aceE*::*aceE*$^{[K403N]}$	This study
MEC864	MEC813 *aceE*::*aceE*$^{[K403Q]}$	This study
MEC865	MEC813 *aceE*::*aceE*$^{[K410M]}$	This study
MEC866	MEC813 *aceE*::*aceE*$^{[K410N]}$	This study
MEC867	MEC813 *aceE*::*aceE*$^{[K410Q]}$	This study
MEC868	MEC813 *aceE*::*aceE*$^{[G395A]}$	This study
MEC905	MEC826 *ppsA*::(FRT)	This study
MEC918	MEC813 *aceE*::*aceE*$^{[H142V]}$	This study
MEC919	MEC813 *aceE*::*aceE*$^{[H640V]}$	This study
MEC955	MEC813 *aceE*::*aceE*$^{[Y177F]}$	This study
MEC956	MEC813 *aceE*::*aceE*$^{[H106M;E401A]}$	This study
MEC961	MEC825 *ppsA*::(FRT)	This study
MEC992	MEC785 *ppsA*::(FRT)	This study
MEC994	MEC956 *ppsA*::(FRT)	This study

Table 2.2 - Plasmids used in this study.

Name	Relevant characteristics	Description	Source
pKD4	Amp^R, Kan^R; R6K ori	Source of Kan^R cassette	Datsenko and Wanner, 2000
pKD46	Amp^R; pSC101 ori (ts); *araBAD* promoter for λ Red genes	λ Red helper plasmid	Datsenko and Wanner, 2000
pCP20	Amp^R, Cam^R; pSC101 ori (ts)	Expression of FLP	Datsenko and Wanner, 2000
pEL04	Cam^R; pSC101 ori (ts)	Source of cam^R:sacB cassette	Lee et al., 2001
pREDTKI	Kan^R; pSC101 ori (ts); *araBAD* promoter for λ Red genes; *trc* promoter for I-SceI	Bifunctional λ Red and I-SceI helper plasmid	Yang et al., 2014
pKSI-I	Amp^R; pUC ori	pBluescript II KS(-) with I-SceI–MCS–I-SceI cassette	Yang et al., 2014
pCM01	Amp^R; pUC ori	pKSI-I + cam^R:*sacB*	This study
pCM02	Amp^R; pUC ori	pKSI-1 + *aceE*	This study
pCM03	Amp^R; pUC ori	pKSI-I + *aceE*::cam^R:*sacB*	This study
pCM04	Amp^R; pUC ori	pKSI-I + *aceE*[H106M[	This study
pCM05	Amp^R; pUC ori	pKSI-I + *aceE*[H106N]	This study
pCM06	Amp^R; pUC ori	pKSI-I + *aceE*[H106V]	This study
pCM07	Amp^R; pUC ori	pKSI-I + *aceE*[E401A]	This study
pCM08	Amp^R; pUC ori	pKSI-I + *aceE*[E401D]	This study
pCM09	Amp^R; pUC ori	pKSI-I + *aceE*[K403A]	This study
pCM10	Amp^R; pUC ori	pKSI-I + *aceE*[K403N]	This study
pCM11	Amp^R; pUC ori	pKSI-I + *aceE*[K403Q]	This study
pCM12	Amp^R; pUC ori	pKSI-I + *aceE*[K410M]	This study
pCM13	Amp^R; pUC ori	pKSI-I + *aceE*[K410N]	This study
pCM14	Amp^R; pUC ori	pKSI-I + *aceE*[K410Q]	This study
pCM16	Amp^R; pUC ori	pKSI-I + *aceE*[G395A]	This study
pCM17	Amp^R; pUC ori	pKSI-I + *aceE*[H142V]	This study
pCM18	Amp^R; pUC ori	pKSI-I + *aceE*[H640V]	This study
pCM19	Amp^R; pUC ori	pKSI-I + *aceE*[Y177F]	This study
pCM21	Amp^R; pUC ori	pKSI-I + *aceE*[H106M;E401A]	This study

Table 2.3 - Primers used in this study.

Name	Description	Sequence 5'-3'
MEP166	ldhA_F	TTAAGCATTCAATACGGGTATTGTG
MEP167	ldhA_R	GTCATTACTTACACATCCCGCCATC
MEP168	aceE_F	TGAGCGTTCTCTGCGTCGTCTGGAG
MEP169	aceE_R	ATCGCCAACAGAGACTTTGATCTC
MEP288	poxB_F	CCGGTTGTCGCTGCCTGC
MEP289	poxB_R	TTCAAACAGATAGTTATGCGCGGCC
MEP290	ppsA_F	CGCACAGAAGCGTAGAACGTTATG
MEP291	ppsA_R	CGTTTAGGTGAACGATCATGCGC
MEP398	KSI-HA-ace-F	GACAAGGCTTCTATGGAAGCTGCAGGAATTCGATATCAAG
MEP399	KSI-HA-ace-R	GAGTACGGCGTTTGATTCCGATCCACTAGTTCTAGAGCG
MEP400	ace-HA-KSI-F	GCTCTAGAACTAGTGGATCGGAATCAAACGCCGTACTC
MEP401	ace-HA-KSI-R	TTGATATCGAATTCCTGCAGCTTCCATAGAAGCCTTGTCG
MEP402	cam-HA-KSI-F	CGCTCTAGAACTAGTGGATCTGTGACGGAAGATCACTTC
MEP403	cam-HA-KSI-R	CTTGATATCGAATTCCTGCAGATCAAAGGGAAAACTGTCC
MEP404	KSI-HA-cam-F	GACAGTTTTCCCTTTGATCTGCAGGAATTCGATATCAAG
MEP405	KSI-HA-cam-R	GAAGTGATCTTCCGTCACAGATCCACTAGTTCTAGAGCG
MEP418	ace-seq-1	GAAATATCTGGAACACCGTGG
MEP419	ace-seq-2	CCAAAGGCAAAGCGACAG
MEP420	ace-seq-3	CTTACTATAAAGAAGACGAGAAAGGTC
MEP421	aceE-HA-SCE-R	CACATAGGGATAACAGGGTAATCATGGGTTATTCCTTATC
MEP422	aceE-HA-SCE-F	GGACAGTAGGGATAACAGGGTAATAAGTGGTTGCTGACGC
MEP423	cam-HA-SCE-R	CCACTTATTACCCTGTTATCCCTACTGTCCATATGCACAG
MEP424	cam-HA-SCE-F	CCCATGATTACCCTGTTATCCCTATGTGACGGAAGATCAC
MEP428	aceE-H106M-F	AACTGGGCGGCATGATGGCGTCCTT
MEP429	aceE-H106M-R	AAGGACGCCATCATGCCGCCCAGTT
MEP430	aceE-H106V-F	AACTGGGCGGCGTGATGGCGTCCTT
MEP431	aceE-H106V-R	AAGGACGCCATCACGCCGCCCAGTT
MEP432	aceE-H106N-F	AACTGGGCGGCAACATGGCGTCCTT
MEP433	aceE-H106N-R	AAGGACGCCATGTTGCCGCCCAGTT
MEP434	aceE-E401A-F	GGCATGGGCGACGCGGCTGCAGGTAAAAACATCGCGCACC

Name	Description	Sequence 5'-3'
MEP435	aceE-E401A-R	GGTGCGCGATGTTTTTACCTGCAGCCGCGTCGCCCATGCC
MEP440	aceE-E401D-F	GGCATGGGCGACGCGGCTGATGGTAAAAACATCGCGCACC
MEP441	aceE-E401D-R	GGTGCGCGATGTTTTTACCATCAGCCGCGTCGCCCATGCC
MEP442	aceE-K403A-F	GGCATGGGCGACGCGGCTGAAGGTGCAAACATCGCGCACC
MEP443	aceE-K403A-R	GGTGCGCGATGTTTGCACCTTCAGCCGCGTCGCCCATGCC
MEP444	aceE-K403N-F	GGCATGGGCGACGCGGCTGAAGGTAACAACATCGCGCACC
MEP445	aceE-K403N-R	GGTGCGCGATGTTGTTACCTTCAGCCGCGTCGCCCATGCC
MEP446	aceE-K403Q-F	GGCATGGGCGACGCGGCTGAAGGTCAGAACATCGCGCACC
MEP447	aceE-K403Q-R	GGTGCGCGATGTTCTGACCTTCAGCCGCGTCGCCCATGCC
MEP448	aceE-K410N-F	CATCGCGCACCAGGTTAACAAAATGAACATGGACG
MEP449	aceE-K410N-R	CGTCCATGTTCATTTTGTTAACCTGGTGCGCGATG
MEP450	aceE-K410Q-F	CATCGCGCACCAGGTTCAGAAAATGAACATGGACG
MEP451	aceE-K410Q-R	CGTCCATGTTCATTTTCTGAACCTGGTGCGCGATG
MEP452	aceE-K410M-F	CATCGCGCACCAGGTTATGAAAATGAACATGGACG
MEP453	aceE-K410M-R	CGTCCATGTTCATTTTCATAACCTGGTGCGCGATG
MEP454	aceE-G395A-F	GCTCATACCATTAAAGGTTACGCGATGGGCGACGCGGCTG
MEP455	aceE-G395A-R	CAGCCGCGTCGCCCATCGCGTAACCTTTAATGGTATGAGC
MEP602	aceE-H640V-F	AACGGCGAAGGTCTGCAGGTAGAAGATGGTCACAGCCAC
MEP603	aceE-H640V-R	GTGGCTGTGACCATCTTCTACCTGCAGACCTTCGCCGTT
MEP604	aceE-H142V-F	TACTTCCAGGGCGTAATCTCCCCG
MEP605	aceE-H142V-R	CGGGGAGATTACGCCCTGGAAGTA
MEP655	aceE-Y177F-F	GCAATGGCCTCTCTTCCTTCCCGCACCCGAAACTGATGC
MEP656	aceE-Y177F-R	GCATCAGTTTCGGGTGCGGGAAGGAAGAGAGGCCATTGC
MEP852	aceE-RT-F	GTATTGGCGATCTGTGCTGG
MEP853	aceE-RT-R	CTGTGACCATCTTCGTGCTG
MEP856	rpoD-RT-F	TGATGCTGGCTGAAAACACC
MEP857	rpoD-RT-R	AGTTCAACGGTGCCCATTTC

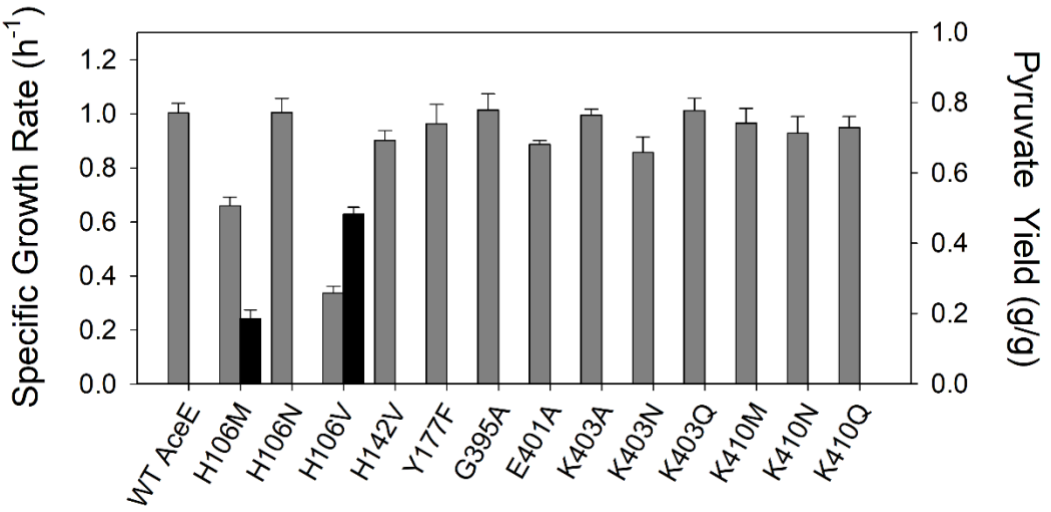

Figure 2.1 - Comparison of *E. coli ldhA poxB* AceE variants grown in shake flasks with 5 g/L glucose: specific growth rate (h^{-1}, gray bars) and pyruvate yield (g/g, black bars). WT AceE indicates wild-type AceE. Error bars indicate standard deviation from three replicates.

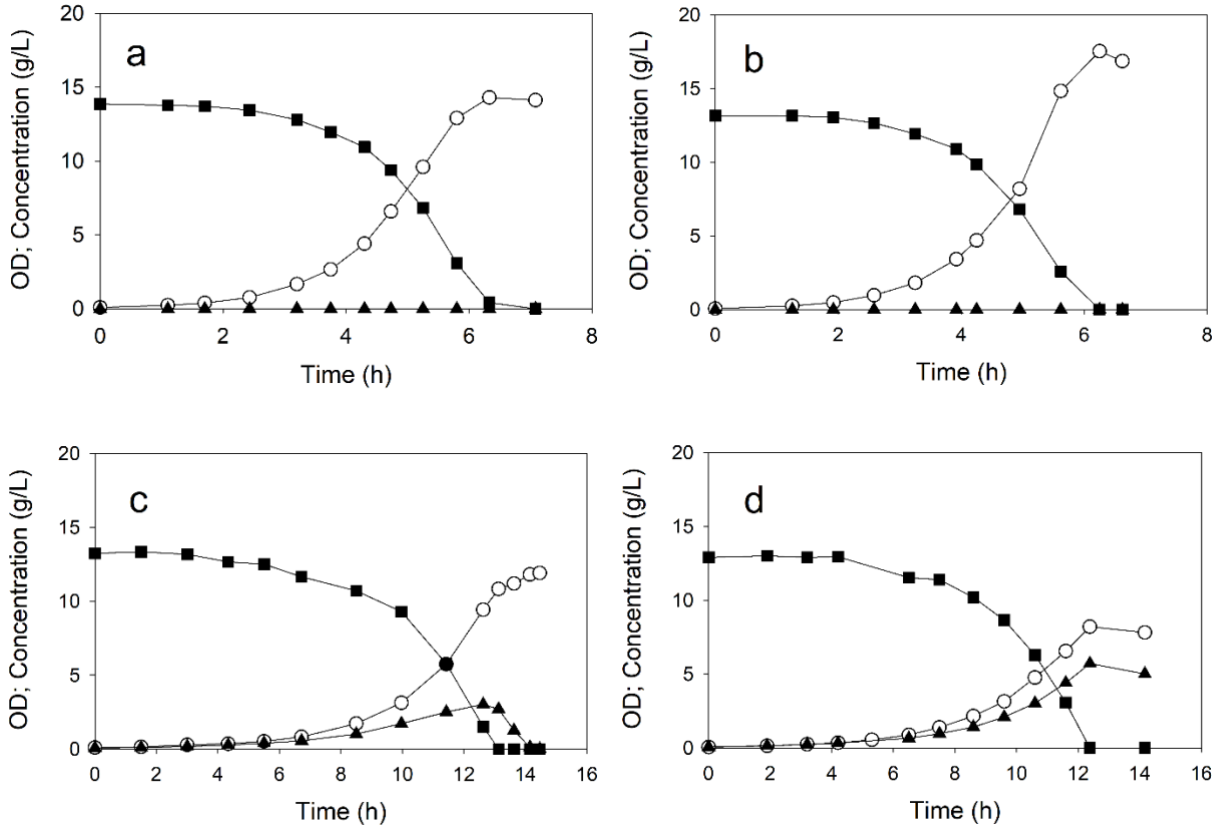

Figure 2.2 - Controlled 1.0 liter batch growth of *E. coli* AceE variants with 15 g/L glucose. a) MEC825 (C *ldhA poxB aceE*::*aceE*); b) MEC961 (C *ldhA poxB aceE*::*aceE ppsA*); c) MEC826 (C *ldhA poxB aceE*::*aceE*$^{[H106V]}$); d) MEC905 (C *ldhA poxB aceE*::*aceE*$^{[H106V]}$ *ppsA*). Glucose (■), pyruvate (▲), OD (○).

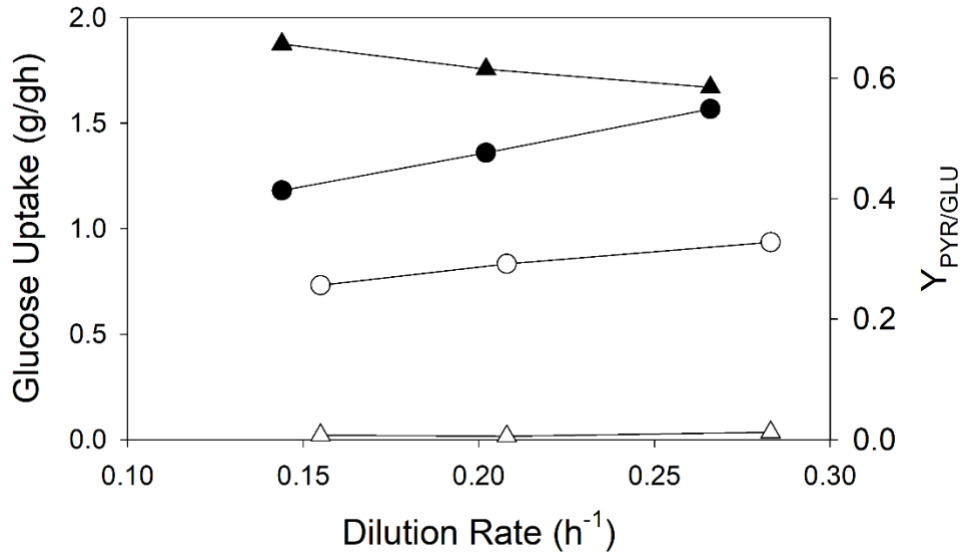

Figure 2.3 - Comparison of glucose uptake rate (g/gh, ▲, △) and pyruvate yield (g/g, ●, ○) of MEC905 (C *ldhA poxB aceE*::*aceE*$^{[H106V]}$ *ppsA*, filled symbols) and MEC961(C *ldhA poxB aceE*::*aceE ppsA*, unfilled symbols) during steady-state growth at the indicated dilution rates (h^{-1}).

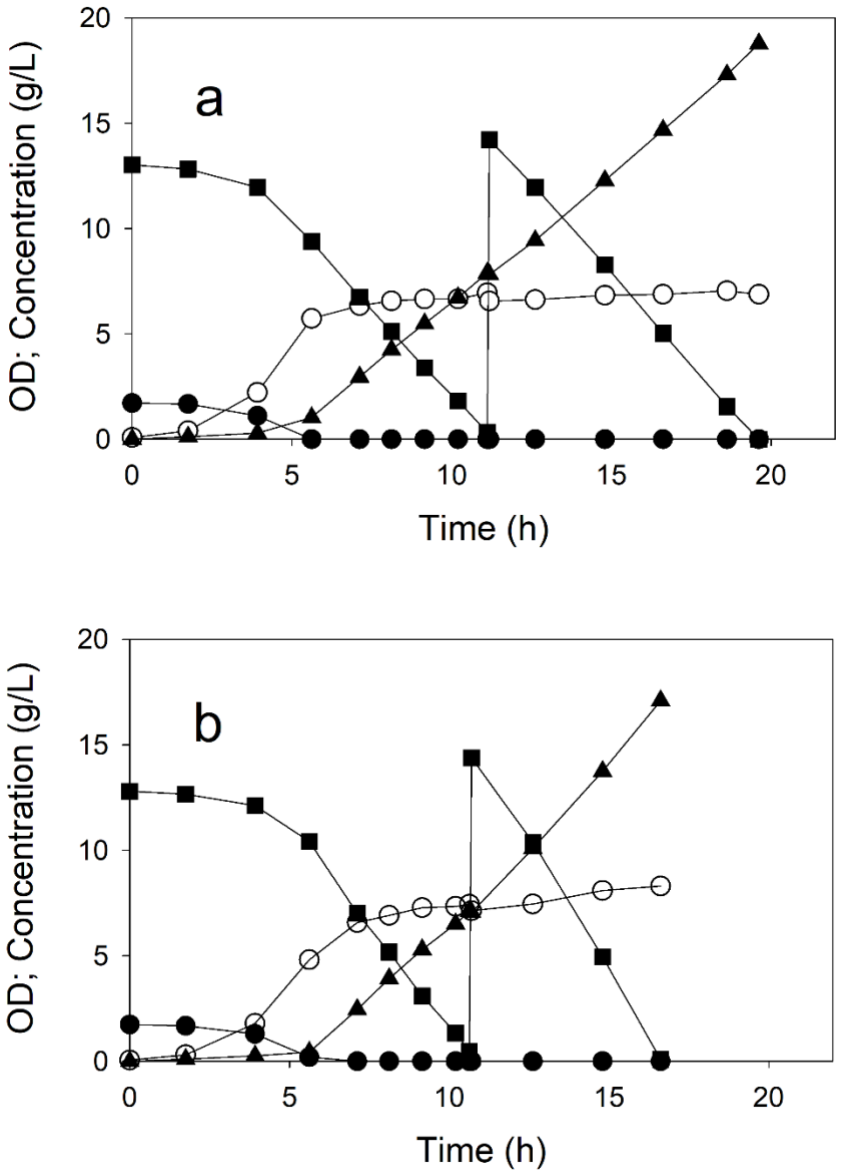

Figure 2.4 - Growth and pyruvate formation in a controlled 1.0 liter repeated-batch process with 15 g/L glucose and 2 g/L acetate. A 17 mL solution containing 15 g of glucose (and no acetate) was added when the initial glucose was depleted. a) MEC992 (C *ldhA poxB aceE ppsA*); b) MEC994 (C *ldhA poxB aceE*::*aceE*$^{[H106M;E401A]}$ *ppsA*). Glucose (■), pyruvate (▲), acetate (●), OD (○).

CHAPTER 3

IMPROVING THE GENERATION OF PYRUVATE-DERIVED ACETOIN BY ESCHERICHIA COLI ACEE VARIANTS CODING PYRUVATE DEHYDROGENASE

Moxley, W.C., Brown, R.E., Eiteman, M.A. Resubmitted to *Engineering in Life Sciences*. 11/23/22. R.E. Brown constructed the 44_ediss plasmid from the 445_ediss plasmid as donated by S. Pflugl (Tech. Univ. Wien). R.E. Brown worked extensively with the C strain and its derivatives. W.C. Moxley ultimately demonstrated that the W background permits significantly greater plasmid stability than the C strain, constructed the analogous knockouts in the W strain, repeated several shake flask fermentations using that strain, developed the bioreactor processes used for accumulation of acetoin, and wrote the manuscript.

3.1 ABSTRACT

Several chromosomally expressed AceE variants were constructed in *E. coli* Δ*ldhA* Δ*poxB* Δ*ppsA* and compared using glucose as the sole carbon source. These variants were examined in shake flask cultures for growth rate, pyruvate accumulation, and acetoin production via heterologous expression of the *budA* and *budB* genes from *Enterobacter cloacae* ssp. *dissolvens*. The best acetoin-producing strains were subsequently studied in controlled batch culture at the one-liter scale. PDH variant strains attained up to 4-fold greater acetoin than the strain expressing the wild-type PDH. In a repeated batch process, the H106V PDH variant strain attained over 43 g/L of pyruvate-derived products, acetoin (38.5 g/L) and 2R,3R-butanediol (5.0 g/L), corresponding to an effective concentration of 59 g/L considering the dilution. The acetoin yield from glucose was 0.29 g/g with a volumetric productivity of 0.9 g/L·h (0.34 g/g and 1.0 g/L·h total products). The results demonstrate a new tool in pathway engineering, the modification of a key metabolic enzyme to improve the formation of a product via a kinetically slow, introduced pathway. Direct modification of the pathway enzyme offers an alternative to promoter engineering in cases where the promoter is involved in a complex regulatory network.

3.2 INTRODUCTION

Innovative metabolic engineering tools and strategies are essential for building efficient microorganisms to produce biochemicals. Generally, to enhance the formation of a specific product, the pathway to that biochemical is targeted, for example, optimizing enzymes (Atsumi and Liao, 2008; Marcheschi et al., 2012; Zhang et al., 2010) or plasmid constructs (Flores et al., 1996; Koffas et al., 2003; Yakandawala et al., 2008). The central goal of these approaches is to modify the expression, regulation, or catalytic activity of enzymes to increase metabolic carbon

flux through the pathway leading to the product. Unfortunately, any heterologous pathway competes with native metabolism supporting cell growth. A key branchpoint inevitably exists between native enzymes and the first enzyme in the pathway leading to the product. For example, products derived from pyruvate such as 2,3-butanediol (Ji et al., 2011), acetoin (Xiao and Lu, 2014), and isobutanol (Lan and Liao, 2013), must directly compete with several native pathways which could include pyruvate dehydrogenase (Reed and Willms, 1966), pyruvate oxidase (Williams and Hager, 1966), pyruvate decarboxylase (Gounaris et al., 1975), pyruvate carboxylase (Utter and Keech, 1963), and lactate dehydrogenase (Tarmy and Kaplan, 1968).

Many strategies exist to eliminate or reduce competing pathways. For enzymes which are not required for growth, gene knockouts have become routine (Causey et al., 2003; Dittrich et al., 2005). More recently, studies have sought to reduce the activity of native pathways by modifying the promoter region of a key enzyme. For example, the native *aceE* promoter was replaced with a modified *vanABK* promoter yielding a strain of *Corynebacterium glutamicum* in which *aceE* expression was controlled by the presence of a *vanABKp*-sensitive effector molecule (Siebert et al., 2021). Similarly, CRISPR interference decreases the expression of the pyruvate dehydrogenase complex (PDH) by targeting the promoter regions of *pdhR* and *aceE*, resulting in pyruvate accumulation by *Escherichia coli* (Ziegler et al., 2021).

Alternatively, the intrinsic activity of a competing enzyme may be altered by making substitutions in key residues on that protein in order to reduce but not eliminate flux through the required native pathway (Tovilla-Coutiño et al., 2020). Using this approach, protein variants of AceE, the E1 component of PDH, led to the accumulation of pyruvate in *E. coli* (Moxley and Eiteman, 2021). The use of PDH variants as a metabolic engineering tool could also potentially increase the production of pyruvate-derived biochemicals.

Acetoin, a metabolic precursor to 2,3-butanediol, is derived from pyruvate (Figure 3.1) by the enzymes acetolactate synthase (ALS; Schloss et al., 1985) and acetolactate decarboxylase (ALDC; Løken and Størmer, 1970). Acetoin is a pale-yellow liquid with a yogurt odor and butter taste which is commercially used as a flavor or fragrance in foods, cigarettes, cosmetics, and biological pest controls (Kandasamy et al., 2016; Xiao and Lu, 2014). Acetoin is the simplest acyloin, a compound with a hydroxy group adjacent to a ketone, an important structure useful for the chemical synthesis of various products (Xiao and Lu, 2014). Although acetoin is produced via chemical synthesis from fossil feedstocks, interest in microbially produced acetoin is growing, as consumer demand for natural products increases in the cosmetics and food industries (Xiao and Lu, 2014).

Many bacteria and yeast naturally produce acetoin as part of the butanediol fermentation pathway. *E. coli* lacks the complete butanediol fermentation pathway, but generates intermediate acetolactate during valine biosynthesis. One strategy for microbial acetoin production in native butanediol producers is to limit the conversion of acetoin to 2,3-butanediol. For example, overexpression of a water-forming NADH oxidase in *Serratia marcescens*, a native 2,3-butanediol producer, achieved an acetoin titer of 75.2 g/L with a 52% reduction of 2,3-butanediol titer (Sun et al., 2012). This approach to increase acetoin titer has also been successfully applied to other native producers including *Bacillus subtilis* and *Klebsiella pneumoniae* (Ji et al., 2013; Zhang et al., 2014). While there are many native acetoin and 2,3-butanediol producers, non-native hosts, such as *E. coli*, have also been engineered to produce these compounds. The general strategy to engineer acetoin producing *E. coli* strains is to express heterologous genes encoding ALS and ALDC from native acetoin or butanediol producing microorganisms. For example, *E. coli* expressing *alsS* (encoding ALS) from *B. subtilis* and *alsD* (encoding ALDC) from

Aeromonas hydrophila achieved an acetoin titer of 21 g/L (Oliver et al., 2013). Often paired with heterologous gene expression is the inactivation of by-product pathways. For example, knockouts in *ldhA, pta, ackA, butA,* and *nagA* decreased by-product formation and increased acetoin titer five-fold to 14 g/L in engineered *C. glutamicum* strains (Mao et al., 2017).

In *E. coli* and many other bacteria, pyruvate is primarily metabolized to acetyl-CoA by PDH under aerobic conditions. Thus, ALS directly competes for the substrate pyruvate with AceE, the pyruvate-binding subunit of PDH. Strategies aimed at reducing this competition include deleting *aceE* to direct pyruvate flux toward ALS. For example, 0.87 g/L of acetoin was produced when genes for ALS and ALDC were expressed in an *E. coli* strain containing a deletion in *aceEF* (Nielsen et al., 2010). While a deletion of *aceE* can increase the availability of pyruvate for acetoin production, under aerobic conditions this strategy requires the supplementation of an additional carbon source such as acetate (Langley and Guest, 1978; Tomar et al., 2003). Rather than eliminate the activity of AceE, an alternative strategy would be to reduce the activity of AceE by modification of the amino acid sequence of the enzyme itself. This strategy does not preclude other approaches, such as knockouts in genes coding for competing pathways not required for growth.

The aim of this study was to examine AceE variants as a tool to increase the production of the pyruvate-derived biochemical acetoin. We hypothesize that reducing the flux through PDH will enable increased acetoin production during growth on defined medium with glucose as the sole carbon source. Alleles encoding AceE variants were engineered into *E. coli* W containing deletions in pyruvate oxidase (*poxB*), lactate dehydrogenase (*ldhA*), and phosphoenolpyruvate (PEP) synthetase (*ppsA*). An acetoin pathway containing ALS (*budB*) and

ALDC (*budA*) from *Enterobacter cloacae* ssp. *dissolvens* was expressed in each strain to test the impact of AceE variants on acetoin yield.

3.3 MATERIALS AND METHODS

Media. Cultures were routinely grown on Lysogeny Broth (LB) during plasmid and strain construction, while *aceE* mutants were grown on TYA medium containing (per L) 10 g tryptone, 5 g NaCl, 1 g yeast extract, and 1 g sodium acetate trihydrate (Zhu et al., 2008). As needed, antibiotics were included in medium (final concentration): ampicillin (100 µg/mL), kanamycin (40 µg/mL), and chloramphenicol (20 µg/mL). For counter-selection against *sacB*, the medium was supplemented with 100 g/L sucrose, and NaCl was excluded.

The defined basal medium to which carbon/energy sources were added contained (per L): 8 g NH_4Cl, 1.2 g KH_2PO_4, 1.0 K_2HPO_4, 2.0 g K_2SO_4, 0.6 g $MgSO_4 \cdot 7H_2O$, 0.25 mg $ZnSO_4 \cdot 7H_2O$, 0.125 mg $CuCl_2 \cdot 2H_2O$, 1.25 mg $MnSO_4 \cdot H_2O$, 0.875 mg $CoCl_2 \cdot 6H_2O$, 0.06 mg H_3BO_3, 0.25 mg $Na_2MoO_4 \cdot 2H_2O$, 5.5 mg $FeSO_4 \cdot 7H_2O$, 20 mg $Na_2EDTA \cdot 2H_2O$, 20 mg citric acid, 20 mg thiamine·HCl. In shake flask cultures used 20.9 g 3-[*N*-morpholino]propanesulfonic acid (100 mM MOPS) while for batch processes used 25 mM MOPS. Thiamine was filtered sterilized, and other medium components were autoclaved in compatible mixtures, combined and then adjusted to a pH of 7.1 with 20% (w/v) NaOH.

Strains and genetic modifications. Strains used in this study are shown in Table 3.1. Gene knockouts in *E. coli* W were constructed by methods previously described (Datsenko and Wanner, 2000). Knockouts were selected on plates supplemented with kanamycin. Forward primers external to the target gene and reverse primers within the kanamycin resistance cassette

were used to confirm proper chromosomal integration (Table 3.2). The kan^R marker was removed by expression of FLP recombinase from pCP20 (Datsenko and Wanner, 2000). Gene knockouts and removal of the markers were verified by PCR. To construct MEC1320, the chloramphenicol-*sacB* (cam-*sacB*) cassette and 200 bp of homology flanking *aceE* was amplified from purified genomic DNA of MEC813 (Moxley and Eiteman, 2021) and integrated into the *aceE* locus of MEC1319 expressing the lambda red system from pKD46. Nucleotide sequences of homologous regions used to integrate DNA into the *aceE* locus were identical in *E. coli* C (ATCC 8739) and *E. coli* W (ATCC 9637).

To construct MEC1329 and MEC1330, error-prone PCR was used to generate an *aceE* fragment with random mutations and was subsequently integrated into the *aceE* locus of MEC1122 expressing the lambda red system from pKD46. The error-prone PCR fragment of *aceE* was generated using Stratagene GeneMorph II Random Mutagenesis Kit (Stratagene California, San Diego, CA, USA) using linearized (Spe1) pCM02 as template (Moxley and Eiteman, 2021). PCR was performed according to the manufacturer's specifications. The fragment was gel purified, and 100 ng used to transform MEC1122. Cells were recovered with TYA for 2 h at 30°C. The cells were centrifuged (5,000 × g for 1 min) and washed with 1 mL 0.9% NaCl, then 100 μl of the washed recovery was plated to defined medium agar supplemented with 2.5 g/L glucose and 100 g/L sucrose. Plates were incubated at 30°C for 2-3 days. Positive transformants were verified by PCR and subsequently screened for growth rate and pyruvate accumulation (data not shown). Two strains with decreased growth rates were chosen for sequencing to determine mutations.

Each *aceE* variant allele was PCR amplified from genomic DNA containing the respective allele and integrated into MEC1320 expressing the lambda red system from pKD46.

Counter-selection against *sacB* was used to select mutants that lost the cam-*sacB* cassette by plating transformants on medium containing sucrose (Thomason et al., 2014). Colonies were confirmed by colony PCR, and point-mutated *aceE* genes were amplified from the chromosome, gel purified, and sequenced to confirm mutations.

Plasmid construction. Plasmids used in this study are listed in Table 3.2. Plasmids were constructed using NEBuilder® HiFi Assembly (New England Biolabs, Ipswich, MA, USA). Phusion® High-Fidelity Polymerase (New England Biolabs, Ipswich, MA, USA) or PrimeSTAR® Max High-Fidelity Polymerase (Takara Bio, Mountain View, CA, USA) was used to amplify DNA for cloning and genome integration. Quick-DNA Miniprep and Zyppy™ Plasmid Miniprep Kits were used to purify genomic and plasmid DNA (Zymo Research, Irvine, CA, USA). DNA Clean and Concentrator, and Zymoclean™ Gel DNA Recovery Kits were used to purify PCR fragments (Zymo Research, Irvine, CA, USA). Restriction enzymes were purchased from New England Biolabs. Plasmids were confirmed by restriction digest and sequencing (ACGT, Inc., Wheeling, IL, USA).

To construct 44_ediss from 445_ediss gifted by Stefan Pflügl (Erian et al., 2018), primers were used to amplify a linear fragment containing the plasmid backbone, *budA*, and *budB*, then subsequently circularized to create the *budB-budA* operon. The new plasmid 44_ediss was confirmed by restriction digest and sequencing.

Shake flask experiments. A single colony from an LB plate was used to inoculate 3 mL TYA. After 6-10 h of growth, this culture was used to inoculate 3 mL of basal medium with 5 g/L D-(+)-glucose to an initial optical density at 600 nm (OD) of 0.05. After 8-12 h of growth, this

culture was used to inoculate three 500 mL baffled shake flasks containing 50 mL of basal medium with 5 g/L glucose to an OD of 0.02. All cultures were grown at 37°C on a rotary shaker at 225 rpm. Flasks were sampled for measurement of growth rate and/or extracellular metabolite concentrations. Some flasks were supplemented with 2.34 g/L $Na(CH_3COO)\cdot 3H_2O$ (1 g/L acetate) as described.

Batch and repeated batch processes. A single colony from an LB plate was used to inoculate 3 mL TYA. After 6-10 h, this culture was used to inoculate a 250 mL shake flask containing 50 mL of basal medium with 20 g/L glucose to an OD of 0.02. When the shake flask culture reached an OD of 1.5-2, the 50 mL were used to inoculate a 2.5 L bioreactor (Bioflo 2000, New Brunswick Scientific Co., New Brunswick, NJ, USA) containing 1.2 L basal medium with 40 g/L glucose. Duplicate batch processes were performed, and some cultures were supplemented with 18.72 g/L $Na(CH_3COO)\cdot 3H_2O$ (8 g/L acetate) as described. A repeated batch process started as a batch process described above except the medium was modified to increase NH_4Cl from 8 g/L to 10 g/L. Four times, approximately each time glucose was depleted, 56 mL of DI water with 44 g glucose, 40 mg kanamycin, 150 mg KH_2PO_4, 125 mg K_2HPO_4, 1.25 mg $FeSO_4\cdot 7H_2O$ and 75 mg $MgSO_4\cdot 7H_2O$ was added to the fermenter.

Batch studies were conducted with an initial agitation of 400 rpm and at 37°C. Air and/or oxygen-supplemented air was sparged at 1.25 L/min and agitation was adjusted up to 500 rpm to maintain a dissolved oxygen concentration above 40% of saturation. The pH was controlled at 7.0 using 30% (w/v) KOH or 20% (w/v) H_2SO_4. Antifoam 204 (Sigma) was used as necessary to control foaming.

Analytical methods. The optical density at 600 nm (OD) (UV-650 spectrophotometer, Beckman Instruments, San Jose, CA, USA) was used to monitor cell growth. Samples were routinely frozen at -20°C for further analysis, and thawed samples were centrifuged (4°C, 10000 × g for 10 min), and filtered (0.45 µm nylon, Acrodisc, Pall Corporation, Port Washington, NY). Liquid chromatography using a 7.8 × 300 mm Coregel 64H column (Concise Separations, San Jose, CA, USA) at 60°C with 4 mN H_2SO_4 as mobile phase was used to quantify pyruvate, glucose and organic products using RI detection (Eiteman and Chastain, 1997). Students T-test was used to compare data statistically, with 95% confidence interval the basis for significance.

3.4 Results

Variant strain screening for pyruvate and acetoin yield. Pyruvate occupies a key node in central metabolism. Any biochemical product derived from pyruvate in *E. coli* must compete with native pathways including pyruvate dehydrogenase, lactate dehydrogenase and pyruvate oxidase. Although deletions in genes coding for lactate dehydrogenase, pyruvate oxidase and PEP synthetase have minimal effect on aerobic cell growth and metabolism, a knockout in any of the three components of the pyruvate dehydrogenase complex (PDH) results in a growth requirement for acetate (Tomar et al., 2003). An alternative approach to reducing flux through PDH would be to reduce the intrinsic activity of the complex, for example, by amino acid substitutions affecting enzyme activity. Pyruvate accumulation at a yield of 0.66 g/g from glucose has previously been demonstrated in strains expressing variants of AceE, the E1 component of the PDH (Moxley and Eiteman, 2021). The goal of this study was to examine the use of AceE variants for a product derived from pyruvate, acetoin. Our hypothesis was that the

increased availability of pyruvate caused by the bottleneck created at PDH would increase the yield of pyruvate-derived acetoin.

E. coli W containing deletions in the *ldhA*, *poxB* and *ppsA* genes (MEC1319) was chosen as the host for acetoin production. Several *aceE* variant alleles from *E. coli* C strains (Moxley and Eiteman, 2021) were introduced into MEC1319 and screened in triplicate shake flasks for growth rate and pyruvate yield. We also examined MEC1322 which contains a deletion of the *aceE* gene, necessitating the supplementation of acetate into the medium. MEC1319 attained a growth rate of 0.87 ± 0.01 h^{-1}, and no pyruvate accumulated. Of the variants able to grow on glucose as the sole carbon source (Figure 3.2), MEC1332 (AceE[H106V] variant) attained the highest pyruvate yield of 0.49 ± 0.01 g/g while MEC1341 (AceE[H106M]) attained the lowest pyruvate yield of 0.32 ± 0.01 g/g. MEC1339 (AceE[N276S;R465C;V668A;Y696N]) and MEC1340 (AceE[V169A;P190Q;F532L] attained similar pyruvate yields of 0.44 ± 0.01 g/g and 0.42 ± 0.00 g/g, respectively. Pyruvate yield correlated inversely with maximum specific growth rate. MEC1332 attained the lowest growth rate of 0.43 ± 0.01 h^{-1}, almost 50% lower than MEC1319 expressing the native AceE. Each measured growth rate and yield was significantly different from other measured growth rates and yields ($p<0.05$).

MEC1342 (AceE[H106M;E401A]) and MEC1322 (Δ*aceE*) exhibited limited growth on glucose as the sole carbon source (data not shown). Thus, for these two strains only, the medium was supplemented with 1 g/L acetate to support biomass formation. After growth and acetate depletion, MEC1342 and MEC1322 converted glucose to pyruvate at yields of 0.39 ± 0.02 g/g and 0.45 ± 0.02 g/g, respectively.

In order to understand the impact of each AceE variant on acetoin yield, an acetoin production pathway was introduced into each strain via transformation of the 44_ediss plasmid.

The 44_ediss plasmid expresses acetolactate synthase, encoded by the *budB* gene, and acetolactate decarboxylase, encoded by the *budA* gene, each from *E. cloacae* ssp. *dissolvens* (Figure 3.1). Each transformed strain was examined for acetoin generation in triplicate flask cultures containing 5 g/L glucose or 5 g/L glucose plus 1 g/L acetate (Figure 3.3). Of the strains that grew on glucose as the sole carbon source, MEC1319/44_ediss displayed the lowest acetoin yield of 0.05 ± 0.00 g/g while MEC1332/44_ediss attained the greatest yield of 0.16 ± 0.00 g/g. MEC1341/44_ediss, MEC1340/44ediss, and MEC1339/44_ediss attained yields of 0.13 - 0.15 g/g. The difference in acetoin yields of the pairs MEC1339/MEC1341, MEC1341/MEC1340, and MEC1340/MEC1332 were not significantly difference ($p>0.05$). For these strains, high pyruvate yield in the absence of the acetoin pathway plasmid did not predict high acetoin yield when the heterologous pathway was introduced. The two strains with a severe restriction in PDH, which therefore required an acetate supplement, attained the highest acetoin yields. Specifically, MEC1322/44_ediss and MEC1342/44_ediss attained yields of 0.25 ± 0.01 g/g and 0.22 ± 0.01 g/g, respectively, and these yields were significantly different from each other and from yields achieved by other strains ($p<0.05$).

Controlled batch processes. During shake flask screening, acetoin titer was limited by low initial glucose concentration and potentially the absence of pH and dissolved oxygen control. Thus, selected strains were grown in batch culture in controlled bioreactors using 40 g/L glucose (Figure 3.4). The medium was supplemented with 8 g/L acetate for the growth of MEC1342/44_ediss, which had limited ability to grow on glucose as the sole carbon source. MEC1319/44_ediss generated acetoin at a yield of 0.07 g/g and achieved a final titer of 2.7 g/L (Figure 3.4a). MEC1340/44_ediss achieved a final acetoin titer of 8.5 g/L at a yield of 0.22 g/g

(Figure 3.4b) while MEC1332/44_ediss achieved a final acetoin titer of 11.2 g/L at a yield of 0.28 g/g (Figure 3.4c). For both these two variants, the culture accumulated about 6 g/L pyruvate by the time that glucose as depleted, and then the pyruvate was itself consumed with continued generation of acetoin. MEC1342/44_ediss, grown on acetate-supplemented medium, converted glucose to acetoin at a yield of 0.26 g/g and achieved a final acetoin titer of 10.5 g/L (Figure 3.4b). However, for this variant, after glucose and acetate were depleted, growth ceased, acetoin production slowed, and nearly 2 g/L pyruvate remained.

Acetolactate accumulated during growth on glucose, reaching a maximum concentration of about 1.5 g/L for MEC1332 and MEC1340 expressing 44_ediss and 2.5 g/L for MEC1342/44_ediss at the time of glucose depletion. Acetolactate had been fully metabolized by the end of each process.

Repeated batch process. Because MEC1332/44_ediss (containing AceE[H106V]) attained the greatest acetoin concentration under batch conditions, this strain was grown in a repeated-batch culture. In this case, 44 g glucose was added to the culture four times when glucose was depleted. MEC1332/44_ediss achieved an acetoin titer of 38.5 g/L (effectively 52.8 g/L with dilution) with an overall yield of 0.29 g/g and productivity of 0.9 g/L·h (Figure 3.5). Acetolactate and 2R,3R-butanediol were also detected during the process. Acetolactate reached a maximum concentration of less than 2 g/L and was fully metabolized by the end of the process. Butanediol was first detected at 17.4 h, and approximately 5.0 g/L had accumulated by the end of the process.

3.5 Discussion

The goal of this study was to assess the use of *aceE* variants to increase the production of acetoin, a pyruvate-derived biochemical. The Δ*aceE* strain and five *aceE* variant loci engineered into the chromosome of *E. coli* W were examined for acetoin production.

Of the five strains expressing different *aceE* variants, three (AceE[H106V], AceE[H106M], and AceE[H106M;E401A]) were previously generated using rational protein engineering (Moxley and Eiteman, 2021). Of the residues substituted in these variants, H106 is in the active site cleft and may contribute to orienting pyruvate in the active site, while E401 is positioned on a mobile loop gating the active site and contributes to loop stability (Arjunan et al., 2002; Kale et al., 2007). Two novel variants that allow pyruvate accumulation in *E. coli* were additionally generated using a random approach: MEC1339 (AceE[N276S;R465C;V668A;Y696N]) and MEC1340 (AceE[V169A;P190Q;F532L]).

Of the substitutions found in MEC1339, V668A and Y696N are located near the active site channel (Arjunan et al., 2002). An alpha helix proximal to the active site spans residues A663 – G679. Since V668 is positioned in the alpha helix and Y696 is oriented towards the N-terminal of the alpha helix, these mutations could be destabilizing the alpha helix and the active site channel structure. N276 is oriented near and facing the N-terminal tail of AceE, proximal to residues 261-263 which form part of the active site cleft (Arjunan et al., 2002). Therefore, N276S could impact the active site structure and/or the position of the N-terminal tail which interacts with AceF and is important for PDHc activity (Park et al., 2004). R465C is spatially located near a strand of residues 177-186, which contains the active site residue Y177 (Arjunan et al., 2002). R465C could be affecting activity through altering the position of this strand and thus shifting the position of Y177 in the active site.

Of the substitutions found in MEC1340, P190Q is the most radical substitution and is located closest to the active site. P190 is proximal to important active site residues V192 and M194 which provide stabilizing hydrogen bonds to the thiamine diphosphate cofactor. The disruption in bond angles as a result of the P190Q substitution likely destabilizes thiamine diphosphate binding to the active site (Arjunan et al., 2002). F532L is located in an alpha helix and proximal to active site residues D521 and E522, residues predicted to function in substrate channeling between the AceE and the lipoyl group of AceF. Similar to N267S and R465C from MEC1339, this substitution could impact activity by shifting the position of active site residues. V169A is located near the surface the AceE dimer and at the interface between the two AceE monomers, but might not impact activity or structure due to the apparent lack of interactions with nearby residues. Since these two variant strains were generated by random mutagenesis, some of these substitutions may have limited effect or their effect only occurs when the substitutions are made collectively.

Each *aceE* allele was integrated into an *E. coli* W strain containing knockouts in *poxB*, *ldhA*, and *ppsA*, then screened for growth rate and pyruvate yield. The resulting strains exhibited inversely correlated growth rates and pyruvate yields. Each variant allele likely confers unique carbon flux redistribution at the pyruvate node. This effect is also evident when the strains were screened for acetoin production in shake flasks. Strains containing variant *aceE* alleles attained ~1.6 – 4-fold higher acetoin yields than the strain expressing the wild-type *aceE*.

The variant strains harboring the 44_ediss plasmid differed in their ability to accumulate acetoin. All variants accumulated pyruvate and acetoin concurrently when grown in shake flask and controlled batch culture, and converted residual pyruvate to acetoin after glucose was depleted. The conversion of pyruvate to acetoin requires/generates no ATP nor NAD(P)H, and

the generation of CO_2 serves as the irreversible driving force for acetoin formation. Accumulation of pyruvate itself indicates carbon flux into the acetoin pathway limited acetoin production, and increasing product pathway efficiency may increase acetoin production rate and minimize pyruvate accumulation. Those strains studied which did not require acetate for growth were able to convert the accumulated pyruvate to acetoin after glucose depletion (Figures 4abc). However, MEC1342/44_ediss, having a severe *aceE* mutation that nearly eliminates growth on glucose as the sole carbon source, was unable to convert all the accumulated pyruvate to acetoin (Figure 4d). MEC1322/44_ediss, lacking *aceE*, generated about the same acetoin as MEC1342/44_ediss in shake flask culture (Figure 3). Thus, an optimal PDH flux for acetoin generation exists: if PDH has (large) wild-type activity, then a large fraction of glucose is used for native metabolism and acetoin yield is low, while if PDH is severely restricted, then some residual pyruvate remains unconverted, and the acetoin yield is also low. An intermediate PDH flux balances the need for growth and energy with the goal of acetoin formation.

Cells with severe *aceE* mutations growing on pyruvate were unable to provide sufficient energy to meet the maintenance requirements. Previously, AceE variant strains with *ldhA* and *poxB* knockouts were shown to consume accumulated pyruvate to support growth (Moxley and Eiteman, 2021), and an additional deletion of *ppsA* was required to block the metabolism of pyruvate. Thus, limiting pyruvate consumption through a restricted PDH did not support growth, suggesting the energy generated from acetyl-CoA formation and metabolism is insufficient for biomass formation. In the current study, AceE variant strains overexpressing the acetoin pathway in batch culture produced a similar growth phenotype: biomass formation ceased upon glucose depletion (Figure 4). As protein synthesis and turnover can account for 50% of total maintenance energy requirements (Nyström and Gustavsson, 1998; Lahtvee et al., 2014; Hanson

et al., 2021), the continued formation of acetoin in a medium of pyruvate as the sole carbon source (after glucose depletion) appears to be contingent on some PDH flux to generate a threshold level of energy. Energy generated from pyruvate metabolism in a Δ*ldhA* Δ*poxB* Δ*ppsA* strain must come from PDH itself and from the metabolism of acetyl-CoA. One route for ATP formation is via the Pta-AckA pathway through acetate formation (Enjalbert et al., 2017; Wolfe, 2005), though intracellular acetyl-CoA levels are likely too low to generate detectable quantities of acetate from this pathway. Cells might also metabolize pyruvate/acetyl-CoA through the glyoxylate shunt, which is induced when glucose is absent (Kumari et al., 2000; Walsh and Koshland et al., 1984). Whereas acetate formation would permit ATP generation, the TCA cycle or the glyoxylate shunt would allow cells to generate precursor molecules as well as NADH. These pathways providing a limited acetyl-CoA supply to generate energy enable the complete conversion of pyruvate to acetoin. When acetyl-CoA metabolism is essentially blocked, however, as is the case with MEC1342/44_ediss, the conversion of pyruvate to acetoin cannot be sustained in the absence of glucose.

During controlled batch processes, less than 2 g/L acetolactate accumulated during exponential growth, and this intermediate was metabolized by the end of the process. A likely explanation for this observation is that *in vivo* ALS activity is greater than that of ALDC. Of these two enzymes, only kinetic parameters for ALDC from *E. cloacae* ssp. *dissolvens* are available: the K_M is 12.2 mM, and k_{cat} is 0.96 s^{-1} (Ji et al., 2018) while known ALS enzymes have a turnover number 100 times greater (Atsumi and Liao, 2009). Even without kinetic parameters for the specific ALS used, the low affinity turnover rate of ALDC, taken together with the observed accumulation of acetolactate, support the hypothesis that ALDC is the rate limiting step for acetoin formation. About 5 g/L 2R,3R-butanediol was also detected in the

prolonged fed-batch process. Although a heterologous butanediol dehydrogenase was not expressed, the presence of this biochemical is likely due to promiscuous activity of endogenous dehydrogenases as previously reported in *E. coli* (Nielsen et al., 2010; Nakashima et al., 2014).

Competition between central metabolism and product pathways for metabolites directly impacts the metabolic flux toward a product of interest. Central metabolic enzymes typically have high turnover and catalytic efficiencies compared with enzymes of secondary metabolism (Bar-Even et al., 2011). Thus, an introduced pathway must invariably compete directly with central metabolism. Common strategies to increase flux through product pathways include gene deletion and the overexpression of pathway genes. In this study, implementation of these two strategies alone in batch culture resulted in 2.7 g/L acetoin at a yield of 0.07 g/g (MEC1319/44_ediss, Figure 4a), much lower than the maximum theoretical yield of acetoin from glucose of 0.489 g/g. Wild-type PDH has a K_M of 260 µM and a k_{cat} of 38 s^{-1} (Kale et al., 2007). The kinetic parameters of ALS from *E. cloacae* ssp. *dissolvens* have not been characterized, though ALS from *Bacillus subtilis* has a K_M of 13,600 µM and a k_{cat} of 121 s^{-1} (Atsumi and Liao, 2009). The intracellular pyruvate concentration when *E. coli* is growing maximally is about 5,000 µM (Rahman et al., 2006, Vemuri et al., 2006). Using Michaelis-Menten kinetics and these parameters as benchmarks, the wild-type PDH is operating at near its maximum reaction rate (i.e., about 36 s^{-1}), while ALS is at 25% of its maximum (33 s^{-1}). However, increased ALS expression would tend to lower intracellular pyruvate concentration, which would reduce the reaction rate of ALS more than for PDH because of the much greater K_M of ALS, making ALS even less competitive. In contrast, a variant strain with reduced PDH activity would lower the reaction rate for the conversion of pyruvate to acetyl-CoA, and would also tend to increase intracellular pyruvate concentration, both benefiting acetoin formation.

Although these calculations do not consider the complex phenomena which influence enzyme kinetics *in vivo,* including expression level, protein turnover and the presence of inhibitors, this analysis serves to illustrate the benefit of reduced PDH flux via the modification of the native enzyme.

An important result is that a severe restriction in PDH flux does not correlate to high acetoin yield and productivity when the heterologous pathway is introduced into an *aceE* variant strain. Of the four strains compared in batch culture, MEC1332/44_ediss (AceE[H106V]) achieved the greatest acetoin productivity and yield (Figure 4c) even though MEC1342/44_ediss (AceE[H106M;E401A]) directed more carbon to pyruvate and acetoin (Figure 4d). MEC1332/44_ediss also maintained this performance in repeated batch processes, which permitted prolonged acetoin production by the periodic addition of glucose. Thus, the optimal restriction in PDH flux appears to be contextual, and likely depends on the particular kinetic parameters of the introduced pathway, as well as their expression level and the energy demands associated with plasmid and protein maintenance. However, this trend was not observed in results from the initial screening in shake flasks (Figures 2 and 3). The decreased performance of MEC1342/44_ediss (AceE[H106M;E401A]) under controlled batch conditions is evident when glucose is depleted and the pyruvate concentration is relatively high, a circumstance that would not occur during screening in shake flasks with relatively low glucose concentrations (5 g/L). The difference in strain performance between shake flasks and controlled reactors highlights the importance of assessing strains in controlled reactors as results from initial screening experiments are not always consistent when a process is scaled-up.

Targeted modulation of PDH to increase the yield of acetoin has, to the best of our knowledge, not been explored. Previously, acetoin generation with a pyruvate-producing strain

of *E. coli*, containing deletions in *ldhA*, *poxB*, *ppsA*, and *aceEF* among others, has been studied using the rationale that the increased availability of pyruvate will lead to increased acetoin formation (Nielsen et al. 2010). However, the strain only produced 0.87 g/L acetoin using complex medium (LB) with 10 g/L glucose, a result similar to our current results for MEC1319/44_ediss, which led to 2.7 g/L acetoin from 40 g/L glucose as the sole carbon source. Restricting flux through PDH benefits pyruvate and acetoin formation. However, simply eliminating PDH activity and providing for growth with acetate supplementation is not an optimal strategy for producing pyruvate-derived compounds.

Expression of an enzyme variant with modified kinetic parameters is just one method to modulate the flux at a key branch point in central metabolism, and this approach complements the modification of the promoter for the gene(s) coding for the same enzyme. The use of inducible or characterized, constitutive promoters are well suited for monocistronic genes or operons lacking regulatory networks. For example, the native *aceE* promoter was replaced with a weaker promoter to decrease the expression of *aceE*, resulting in improved L-valine production in *Corynebacterium glutamicum* (Buchholz et al., 2013). In *C. glutamicum*, *aceE* is monocistronic and not significantly regulated (Schreiner et al., 2005). In *E. coli*, *aceE* is part of an operon where the three components of the PDH (*aceE*, *aceF*, and *lpdA*) are transcribed with *pdhR*, whose gene product acts as a pyruvate-sensitive global repressor for the *pdhR-aceEF-lpdA* operon as well as other genes involved in cell replication, motility, and respiration (Ogasawara et al., 2007; Göhler et al., 2011; Anzai et al., 2020). Moreover, though the *pdhR* promoter dominates *aceEF* expression, promoter sequences upstream of *aceEF*, independent from PdhR regulation, can also drive *aceEF* expression (Spencer and Guest, 1985; Quail and Guest, 1995; Olvera et al. 2009). Thus, expression from P*pdhrR* and P*aceE* must both be reduced to modulate

PDH activity in *E. coli* effectively (Ziegler et al., 2022). Complex transcriptional regulation and redundancy of promoters can pose a challenge when engineering weak promoters to decrease carbon flux through a branchpoint. As an alternative to decreasing the expression of a gene transcribed within a complex operon, the use of enzyme variants with decreased activity represents a simple strategy to accomplish a similar goal of reducing flux.

The titer of two pyruvate-derived products, acetoin and 2R,3R-butanediol, reached 42.5 g/L with a yield of 0.34 g/g at a productivity of 1.0 g/L·h in a medium with glucose as the sole carbon source, corresponding to an effective concentration of 59 g/L considering the dilution due to the glucose feed. Among the strains examined in the context of acetoin formation, the *aceE*$^{[H106V]}$ allele allowed the optimal carbon distribution at the pyruvate node for acetoin production, offering the ideal balance for cells between metabolizing pyruvate through the PDH to allow growth and partitioning a portion of the pyruvate for acetoin production. A potential advantage of using PDH variants is that they can maximize the effectiveness of a kinetically slow, introduced pathway by directly partitioning the precursor metabolite between growth and the introduced pathway, allowing for a fine tuning of metabolism aligned with cellular demands. This approach of modifying native enzyme *activity* could readily be combined with existing strategies such as promoter engineering, optimization in introduced pathway genes or other chromosomal modifications.

ACKNOWLEDGMENTS

The authors acknowledge financial support of the U.S. National Science Foundation (CBET-1802533). The authors also acknowledge the generous donation of the 445_ediss plasmid from Stefan Pflügl at Technische Universität Wien.

3.6 REFERENCES

Anzai, T., Imamura, S., Ishihama, A., Shimada, T., 2020. Expanded roles of pyruvate-sensing PdhR in transcription regulation of the *Escherichia coli* K-12 genome: fatty acid catabolism and cell motility. Microb Genom 6. https://doi.org/10.1099/mgen.0.000442

Arjunan, P., Nemeria, N., Brunskill, A., Chandrasekhar, K., Sax, M., Yan, Y., Jordan, F., Guest, J.R., Furey, W., 2002. Structure of the Pyruvate Dehydrogenase Multienzyme Complex E1 Component from *Escherichia coli* at 1.85 Å Resolution. Biochemistry 41, 5213–5221. https://doi.org/10.1021/bi0118557

Atsumi, S., Li, Z., Liao, J.C., 2009. Acetolactate synthase from *Bacillus subtilis* serves as a 2-ketoisovalerate decarboxylase for isobutanol biosynthesis in *Escherichia coli*. Appl Environ Microbiol 75, 6306–6311. https://doi.org/10.1128/AEM.01160-09

Atsumi, S., Liao, J.C., 2008. Directed evolution of *Methanococcus jannaschii* citramalate synthase for biosynthesis of 1-propanol and 1-butanol by *Escherichia coli*. Appl Environ Microbiol 74, 7802–7808.

Bar-Even, A., Noor, E., Savir, Y., Liebermeister, W., Davidi, D., Tawfik, D.S., Milo, R., 2011. The moderately efficient enzyme: Evolutionary and physicochemical trends shaping enzyme parameters. Biochemistry 50, 4402–4410. https://doi.org/10.1021/BI2002289/SUPPL_FILE/BI2002289_SI_004.XLS

Buchholz, J., Schwentner, A., Brunnenkan, B., Gabris, C., Grimm, S., Gerstmeir, R., Takors, R., Eikmanns, B.J., Blombach, B., 2013. Platform Engineering of *Corynebacterium glutamicum* with Reduced Pyruvate Dehydrogenase Complex Activity for Improved Production of L-Lysine, L-Valine, and 2-Ketoisovalerate. Appl Environ Microbiol 79, 5566–75. https://doi.org/10.1128/AEM.01741-13

Causey, T.B., Zhou, S., Shanmugam, K.T., Ingram, L.O., 2003. Engineering the metabolism of *Escherichia coli* W3110 for the conversion of sugar to redox-neutral and oxidized products: Homoacetate production. Proc Natl Acad Sci U S A 100, 825–832. https://doi.org/10.1073/pnas.0337684100

Datsenko, K.A., Wanner, B.L., 2000. One-step inactivation of chromosomal genes in *Escherichia coli* K-12 using PCR products. Proc Natl Acad Sci U S A 97, 6640–6645. https://doi.org/10.1073/pnas.120163297

Dittrich, C.R., Vadali, R. v, Bennett, G.N., San, K., 2005. Redistribution of metabolic fluxes in the central aerobic metabolic pathway of *E. coli* mutant strains with deletion of the *ackA-pta* and *poxB* pathways for the synthesis of isoamyl acetate. Biotechnol Prog 21, 627–631.

Eiteman, M.A., Chastain, M.J., 1997. Optimization of the ion-exchange analysis of organic acids from fermentation. Anal Chim Acta 338, 69–75. https://doi.org/10.1016/S0003-2670(96)00426-6

Enjalbert, B., Millard, P., Dinclaux, M., Portais, J.-C., Létisse, F., 2017. Acetate fluxes in *Escherichia coli* are determined by the thermodynamic control of the Pta-AckA pathway. Sci Rep 7, 1–11.

Erian, A.M., Gibisch, M., Pflügl, S., 2018. Engineered *E. coli* W enables efficient 2,3-butanediol production from glucose and sugar beet molasses using defined minimal medium as economic basis. Microbial Cell Factories 2018 17:1 17, 1–17. https://doi.org/10.1186/S12934-018-1038-0

Flores, N., Xiao, J., Berry, A., Bolivar, F., Valle, F., 1996. Pathway engineering for the production of aromatic compounds in *Escherichia coli*. Nat Biotechnol 14, 620–623. https://doi.org/10.1038/nbt0596-620

Göhler, A.-K.K., Kökpinar, Ö., Schmidt-Heck, W., Geffers, R., Guthke, R., Rinas, U., Schuster, S., Jahreis, K., Kaleta, C., 2011. More than just a metabolic regulator - elucidation and validation of new targets of PdhR in *Escherichia coli*. BMC Syst Biol 5, 1–12. https://doi.org/10.1186/1752-0509-5-197/TABLES/4

Gounaris, A.D., Turkenkopf, I., Civerchia, L.L., Greenlie, J., 1975. Pyruvate decarboxylase III: Specificity restrictions for thiamine pyrophosphate in the protein association step, sub-unit structure. Biochimica et Biophysica Acta (BBA)-Protein Structure 405, 492–499.

Hanson, A.D., McCarty, D.R., Henry, C.S., Xian, X., Joshi, J., Patterson, J.A., García-García, J.D., Fleischmann, S.D., Tivendale, N.D., Harvey Millar, A., 2021. The number of catalytic cycles in an enzyme's lifetime and why it matters to metabolic engineering. Proc Natl Acad Sci U S A 118, e2023348118. https://doi.org/10.1073/PNAS.2023348118/SUPPL_FILE/PNAS.2023348118.SD07.XLSX

Ji, F., Feng, Y., Li, M., Yang, Y., Wang, T., Wang, J., Bao, Y., Xue, S., 2018. Studies on structure-function relationships of acetolactate decarboxylase from *Enterobacter cloacae*. RSC Adv 8, 39066–39073.

Ji, X.J., Huang, H., Ouyang, P.K., 2011. Microbial 2,3-butanediol production: A state-of-the-art review. Biotechnol Adv 29, 351–364. https://doi.org/10.1016/j.biotechadv.2011.01.007

Ji, X.-J., Xia, Z.-F., Fu, N.-H., Nie, Z.-K., Shen, M.-Q., Tian, Q.-Q., Huang, H., 2013. Cofactor engineering through heterologous expression of an NADH oxidase and its impact on metabolic flux redistribution in *Klebsiella pneumoniae*. Biotechnol Biofuels 6, 1–9.

Kale, S., Arjunan, P., Furey, W., Jordan, F., 2007. A dynamic loop at the active center of the *Escherichia coli* pyruvate dehydrogenase complex E1 component modulates substrate

utilization and chemical communication with the E2 component. J Biol Chem 282, 28106–16. https://doi.org/10.1074/jbc.M704326200

Kandasamy, V., Liu, J., Dantoft, S.H., Solem, C., Jensen, P.R., 2016. Synthesis of (3*R*)-acetoin and 2, 3-butanediol isomers by metabolically engineered *Lactococcus lactis*. Sci Rep 6, 1–9.

Koffas, M.A.G., Jung, G.Y., Stephanopoulos, G., 2003. Engineering metabolism and product formation in *Corynebacterium glutamicum* by coordinated gene overexpression. Metab Eng 5, 32–41. https://doi.org/10.1016/S1096-7176(03)00002-8

Kumari, S., Beatty, C.M., Browning, D.F., Busby, S.J.W., Simel, E.J., Hovel-Miner, G., Wolfe, A.J., 2000. Regulation of acetyl coenzyme A synthetase in *Escherichia coli*. J Bacteriol 182, 4173–4179.

Lahtvee, P.-J., Seiman, A., Arike, L., Adamberg, K., Vilu, R., 2014. Protein turnover forms one of the highest maintenance costs in *Lactococcus lactis*. Microbiology 160, 1501–1512.

Lan, E.I., Liao, J.C., 2013. Microbial synthesis of n-butanol, isobutanol, and other higher alcohols from diverse resources. Bioresour Technol 135, 339–349.

Langley, D., Guest, J.R., 1978. Biochemical genetics of the alpha-keto acid dehydrogenase complexes of *Escherichia coli* K12: genetic characterization and regulatory properties of deletion mutants. J Gen Microbiol 106, 103–117. https://doi.org/10.1099/00221287-106-1-103

Løken, J.P., Størmer, F.C., 1970. Acetolactate decarboxylase from *Aerobacter aerogenes*: purification and properties. Eur J Biochem 14, 133–137.

Mao, Y., Fu, J., Tao, R., Huang, C., Wang, Z., Tang, Y.-J., Chen, T., Zhao, X., 2017. Systematic metabolic engineering of *Corynebacterium glutamicum* for the industrial-level production of optically pure D-(−)-acetoin. Green Chemistry 19, 5691–5702.

Marcheschi, R.J., Li, H., Zhang, K., Noey, E.L., Kim, S., Chaubey, A., Houk, K.N., Liao, J.C., 2012. A synthetic recursive "+ 1" pathway for carbon chain elongation. ACS Chem Biol 7, 689–697.

Moxley, W.C., Eiteman, M.A., 2021. Pyruvate Production by *Escherichia coli* by Use of Pyruvate Dehydrogenase Variants. Appl Environ Microbiol 87, e00487-21. https://doi.org/10.1128/AEM.00487-21

Nakashima, N., Akita, H., Hoshino, T., 2014. Establishment of a novel gene expression method, BICES (biomass-inducible chromosome-based expression system), and its application to the production of 2,3-butanediol and acetoin. Metab Eng 25, 204–214. https://doi.org/10.1016/j.ymben.2014.07.011

Nielsen, D.R., Yoon, S.H., Yuan, C.J., Prather, K.L.J., 2010. Metabolic engineering of acetoin and meso-2,3-butanediol biosynthesis in *E. coli*. Biotechnol J 5, 274–284. https://doi.org/10.1002/BIOT.200900279

Nyström, T., Gustavsson, N., 1998. Maintenance energy requirement: what is required for stasis survival of *Escherichia coli*? Biochimica et Biophysica Acta (BBA)-Bioenergetics 1365, 225–231.

Ogasawara, H., Ishida, Y., Yamada, K., Yamamoto, K., Ishihama, A., 2007. PdhR (pyruvate dehydrogenase complex regulator) controls the respiratory electron transport system in *Escherichia coli*. J Bacteriol 189, 5534–41. https://doi.org/10.1128/JB.00229-07

Oliver, J.W.K., Machado, I.M.P., Yoneda, H., Atsumi, S., 2013. Cyanobacterial conversion of carbon dioxide to 2, 3-butanediol. Proc Natl Acad Sci U S A 110, 1249–1254.

Olvera, L., Mendoza-Vargas, A., Flores, N., Olvera, M., Sigala, J.C., Gosset, G., Morett, E., Bolívar, F., 2009. Transcription Analysis of Central Metabolism Genes in *Escherichia coli*. Possible Roles of σ38 in Their Expression, as a Response to Carbon Limitation. PLoS One 4, e7466. https://doi.org/10.1371/JOURNAL.PONE.0007466

Park YH, Wei W, Zhou L, Nemeria N, Jordan F. 2004. Amino-terminal residues 1− 45 of the *Escherichia coli* pyruvate dehydrogenase complex E1 subunit interact with the E2 subunit and are required for activity of the complex but not for reductive acetylation of the E2 subunit. Biochemistry 43(44):14037-46.

Quail, M.A., Guest, J.R., 1995. Purification, characterization and mode of action of PdhR, the transcriptional repressor of the *pdhR–aceEF–lpd* operon of *Escherichia coli*. Mol Microbiol 15, 519–529. https://doi.org/10.1111/J.1365-2958.1995.TB02265.X

Rahman, M., Hasan, M.R., Oba, T., Shimizu, K., 2006. Effect of *rpoS* gene knockout on the metabolism of *Escherichia coli* during exponential growth phase and early stationary phase based on gene expressions, enzyme activities and intracellular metabolite concentrations. Biotechnol Bioeng 94, 585–595. https://doi.org/10.1002/bit.20858

Reed, L.J., Willms, C.R., 1966. Purification and resolution of the pyruvate dehydrogenase complex (*Escherichia coli*). Methods Enzymol 9, 247–265. https://doi.org/10.1016/0076-6879(66)09057-8

Schloss, J. v, van Dyk, D.E., Vasta, J.F., Kutny, R.M., 1985. Purification and properties of *Salmonella typhimurium* acetolactate synthase isozyme II from *Escherichia coli* HB101/pDU9. Biochemistry 24, 4952–4959.

Schreiner, M.E., Fiur, D., Holátko, J., Pátek, M., Eikmanns, B.J., 2005. E1 Enzyme of the Pyruvate Dehydrogenase Complex in *Corynebacterium glutamicum*: Molecular Analysis of the Gene and Phylogenetic Aspects. J Bacteriol 187, 6005–6018. https://doi.org/10.1128/JB.187.17.6005-6018.2005

Siebert, D., Altenbuchner, J., Blombach, B., 2021. A timed off-switch for dynamic control of gene expression in *Corynebacterium glutamicum*. Front Bioeng Biotechnol 649.

Spencer, M.E., Guest, J.R., 1985. Transcription analysis of the *sucAB, aceEF* and *lpd* genes of *Escherichia coli*. Mol Gen Genet 200, 145–154. https://doi.org/10.1007/BF00383328

Sun, J.-A., Zhang, L.-Y., Rao, B., Shen, Y.-L., Wei, D.-Z., 2012. Enhanced acetoin production by *Serratia marcescens* H32 with expression of a water-forming NADH oxidase. Bioresour Technol 119, 94–98.

Tarmy, E.M., Kaplan, N.O., 1968. Chemical characterization of D-lactate dehydrogenase from *Escherichia coli* B. J Biol Chem 243, 2579–2586.

Thomason, L.C., Sawitzke, J.A., Li, X., Costantino, N., Court, D.L., 2014. Recombineering: Genetic engineering in bacteria using homologous recombination. Curr Protoc Mol Biol 106, 1–16. https://doi.org/10.1002/0471142727.mb0116s106

Tomar, A., Eiteman, M.A., Altman, E., 2003. The effect of acetate pathway mutations on the production of pyruvate in *Escherichia coli*. Appl Microbiol Biotechnol 62, 76–82. https://doi.org/10.1007/s00253-003-1234-6

Tovilla-Coutiño, D.B., Momany, C., Eiteman, M.A., 2020. Engineered citrate synthase alters Acetate Accumulation in *Escherichia coli*. Metab Eng 61, 171–180. https://doi.org/10.1016/J.YMBEN.2020.06.006

Utter, M.F., Keech, D.B., 1963. Pyruvate carboxylase. J. biol. Chem 238, 2603–2608.

Vemuri, G.N., Altman, E., Sangurdekar, D.P., Khodursky, A.B., Eiteman, M.A., 2006. Overflow Metabolism in *Escherichia coli* during Steady-State Growth: Transcriptional Regulation and Effect of the Redox Ratio. Appl Environ Microbiol 72, 3653–3661. https://doi.org/10.1128/AEM.72.5.3653-3661.2006

Walsh, K., Koshland, D.E., 1984. Determination of flux through the branch point of two metabolic cycles. The tricarboxylic acid cycle and the glyoxylate shunt. Journal of Biological Chemistry 259, 9646–9654.

Williams, F.R., Hager, L.P., 1966. Crystalline flavin pyruvate oxidase from *Escherichia coli*: I. Isolation and properties of the flavoprotein. Arch Biochem Biophys 116, 168–176.

Wolfe, A.J., 2005. The acetate switch. Microbiology and molecular biology reviews 69, 12–50.

Xiao, Z., Lu, J.R., 2014. Strategies for enhancing fermentative production of acetoin: A review. Biotechnol Adv 32, 492–503. https://doi.org/10.1016/j.biotechadv.2014.01.002

Yakandawala, N., Romeo, T., Friesen, A.D., Madhyastha, S., 2008. Metabolic engineering of *Escherichia coli* to enhance phenylalanine production. Appl Microbiol Biotechnol 78, 283–291.

Zhang, K., Li, H., Cho, K.M., Liao, J.C., 2010. Expanding metabolism for total biosynthesis of the nonnatural amino acid L-homoalanine. Proc Natl Acad Sci U S A 107, 6234–6239.

Zhang, X., Zhang, R., Bao, T., Rao, Z., Yang, T., Xu, M., Xu, Z., Li, H., Yang, S., 2014. The rebalanced pathway significantly enhances acetoin production by disruption of acetoin reductase gene and moderate-expression of a new water-forming NADH oxidase in *Bacillus subtilis*. Metab Eng 23, 34–41.

Zhu, Y., Eiteman, M.A., Altman, R., Altman, E., 2008. High Glycolytic Flux Improves Pyruvate Production by a Metabolically Engineered *Escherichia coli* Strain. Appl Environ Microbiol 74, 6649–6655. https://doi.org/10.1128/AEM.01610-08

Ziegler, M., Hägele, L., Gäbele, T., Takors, R., 2021. CRISPRi enables fast growth followed by stable aerobic pyruvate formation in *Escherichia coli* without auxotrophy. Eng Life Sci 22, 70–84. https://doi.org/10.1002/ELSC.202100021

Table 3.1 - Strains used in this study.

Strain	Relevant characteristics	Reference
ATCC 8739	*Escherichia coli* C	Wild-type
ATCC 9637	*Escherichia coli* W	Wild-type
MEC813	ATCC 8739 Δ*ldhA* Δ*poxB* Δ*aceE*::cam-*sacB*	Moxley and Eiteman, 2021
MEC1122	ATCC 8739 Δ*ldhA* Δ*poxB* Δ*ppsA* Δ*aceE*::cam-*sacB*	This study
MEC1319	ATCC 9637 Δ*ldhA* Δ*poxB* Δ*ppsA*	This study
MEC1320	MEC1319 Δ*aceE*::cam-*sacB*	This study
MEC1321	MEC1319 Δ*aceE*::Kan	This study
MEC1322	MEC1319 Δ*aceE*	This study
MEC1329	MEC1122 Δ*aceE*::*aceE*$^{[N276S;R465C;V668A;Y696N]}$	This study
MEC1330	MEC1122 Δ*aceE*::*aceE*$^{[V169A;P190Q;F532L]}$	This study
MEC1332	MEC1319 Δ*aceE*::*aceE*$^{[H106V]}$	This study
MEC1339	MEC1319 Δ*aceE*::*aceE*$^{[N276S;R465C;V668A;Y696N]}$	This study
MEC1340	MEC1319 Δ*aceE*::*aceE*$^{[V169A;P190Q;F532L]}$	This study
MEC1341	MEC1319 Δ*aceE*::*aceE*$^{[H106M]}$	This study
MEC1342	MEC1319 Δ*aceE*::*aceE*$^{[H106M;E401A]}$	This study

Table 3.2 - Plasmids used in this study.

Name	Relevant characteristics	Description	Source
pKD4	Amp^R, Kan^R; R6K ori	Source of Kan^R cassette	Datsenko et al. 2000
pKD46	Amp^R; pSC101 ori (ts); *araBAD* promoter for λ Red genes	λ Red helper plasmid	Datsenko et al. 2000
pCP20	Amp^R, Cam^R; pSC101 ori (ts)	Expression of FLP recombinase	Datsenko et al. 2000
pCM02	Amp^R; pUC ori	*aceE* template for EP-PCR	Moxley and Eiteman, 2021
445_ediss	Kan^R; pUC ori	Expression of *budB*, *budA*, and *budC*	Erian et al., 2018
44_ediss	Kan^R; pUC ori	Expression of *budB* and *budA*	This study

Table 3.2 - Primers used in this study.

Name	Description	Sequence 5'-3'
MEP166	ldhA_F	TTAAGCATTCAATACGGGTATTGTG
MEP167	ldhA_R	GTCATTACTTACACATCCCGCCATC
MEP168	aceE_F	TGAGCGTTCTCTGCGTCGTCTGGA G
MEP169	aceE_R	ATCGCCAACAGAGACTTTGATCTC
MEP288	poxB_F	CCGGTTGTCGCTGCCTGC
MEP289	poxB_R	TTCAAACAGATAGTTATGCGCGGCC
MEP291	ppsA_R	CGTTTAGGTGAACGATCATGCGC
MEP418	ace-seq-1	GAAATATCTGGAACACCGTGG
MEP419	ace-seq-2	CCAAAGGCAAAGCGACAG
MEP420	ace-seq-3	CTTACTATAAAGAAGACGAGAAAGGTC
MEP503	KD4-HA-poxB-F	GATGAACTAAACTTGTTACCGTTATCACATTCAGGAGATGGAGAACCATGGTGTAGGCT GGAGCTGCTTC
MEP504	KD4-HA-poxB-R	CCTTATTATGACGGGAAATGCCACCCTTTTTACCTTAGCCAGTTCGTTTTCATATGAATA TCCTCCTTA
MEP579	pKD4-HA-Cpps-F	AGAAATGTGTTTCTCAAACCGTTCATTTATCACAAAAGGATTGTTCGATGGTGTAGGCT GGAGCTGCTTC
MEP671	KD4_RB_ldhA_F	TATTTTTAGTAGCTTAAATGTGATTCAACATCACTGGAGAAAGTCTTATGGTGTAGGCTG GAGCTGCTTC
MEP795	pKD4-REB-aceE-F	ACAGGTTCCAGAAAACTCAACGTTATTAGATAGATAAGGAATAACCCATGGTGTAGGCT GGAGCTGCTTC
MEP796	pKD4-REB-aceE-R	GATTTCGATAGCCATTATTCTTTTACCTCTTACGCCAGACGCGGGTTAACCATATGAATA TCCTCCTTAG
MEP848	aceE-EP-F	ATGTCAGAACGTTTCCCAAATGACGTGGATCCGATCGAAACTCGCGACTGGCTCCAGGC G
MEP849	cmsB-HA-aceE EP-F	AGTATCTGATCGACCAACTGCTTGCTGAAGCCCGCAAAGGCGGTGTAAACTGTGACGGA AGATCACTTCG
MEP850	cmsB-HA-aceE EP-R	GCCCAGCGCCGCAACCACGACATAAGAAGCATCAACTTCGAAGTGGTGACGCTGTCCAT ATGCACAGATG
MEP851	aceE-EP-R	TTACGCCAGACGCGGGTTAACTTTATCTGCATCGATGTTGAATTTGGCGATTGCGTCAGC
MEP920	ediss budC F	CTGGCCCGGCGAGGTATGAAGTCTCATCGTTGTAGTCGGCGATAG

Name	Description	Sequence 5'-3'
MEP921	ediss budC R	TTCGTATCTCGCCGGGCCAGATTCCGACTACATGACCGGCCAGTC
MEP1010	KD4-R-W-ldhA	CTCCCCTGGAATGCAGGGGAGCGGCAAGATTAAACCAGTTCGTTCGGGCACATATGAATATCCTCCTTAG
MEP1011	ppsA-F-W	CGCACAGAAGCGTAGGACGTAATG
MEP1012	KD4-R-W-ppsA	CGACTGAACGCCGCCGGGGATTTATTTTATTTCTTCAGTTCAGCCAGCATATGAATATCCTCCTTAG

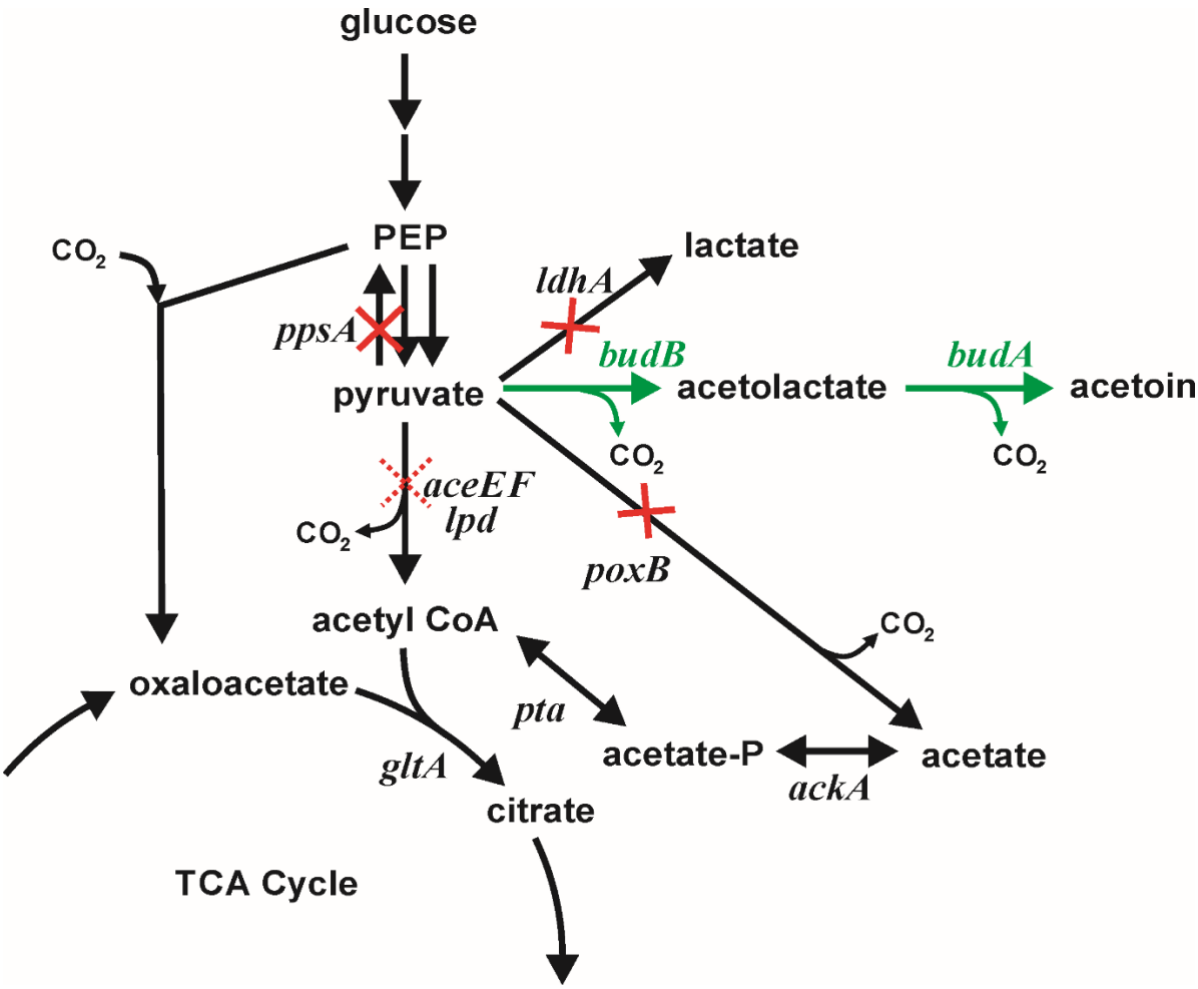

Figure 3.1 - Key biochemical pathways for the conversion of glucose to acetoin in *E. coli*. Gene knockouts performed in this study are indicated by solid red "×". Flux through the PDH was partly curtailed (dotted red "×") by the introduction of *aceE* variant alleles coding amino acid substitutions in the E1 component of the complex. Heterologous *budB* and *budA* genes from *Enterobacter cloacae* ssp. *dissolvens* were expressed for the conversion of pyruvate to acetoin (green).

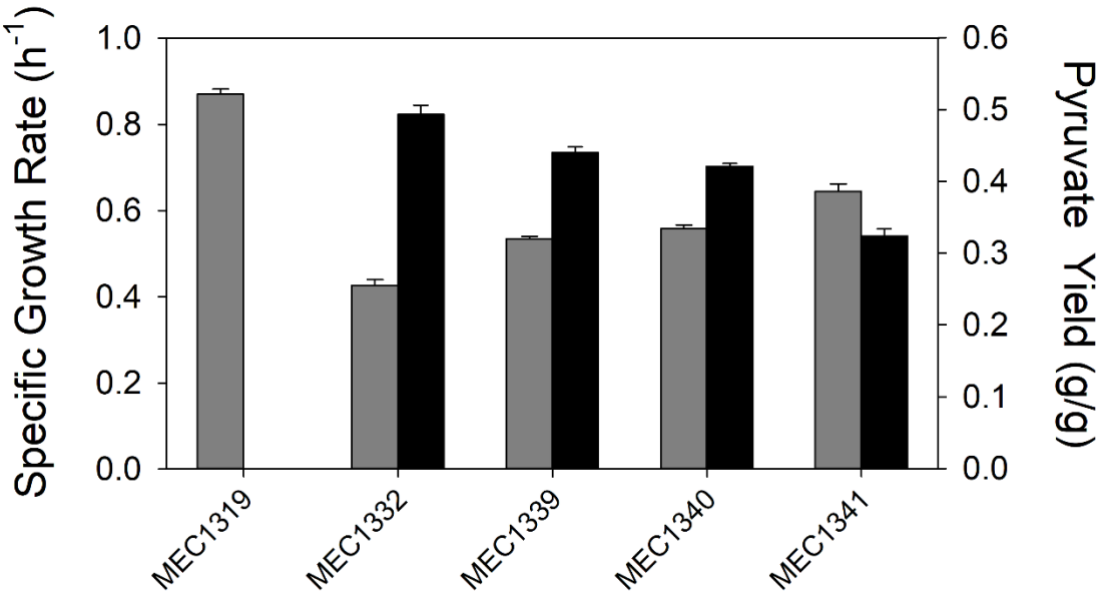

Figure 3.2 - Comparison of *E. coli* W Δ*ldhA* Δ*poxB* Δ*ppsA* AceE variants grown in shake flasks with 5 g/L glucose: specific growth rate (h^{-1}, gray bars) and pyruvate yield (g/g, black bars). Error bars indicate standard deviation from three replicates.

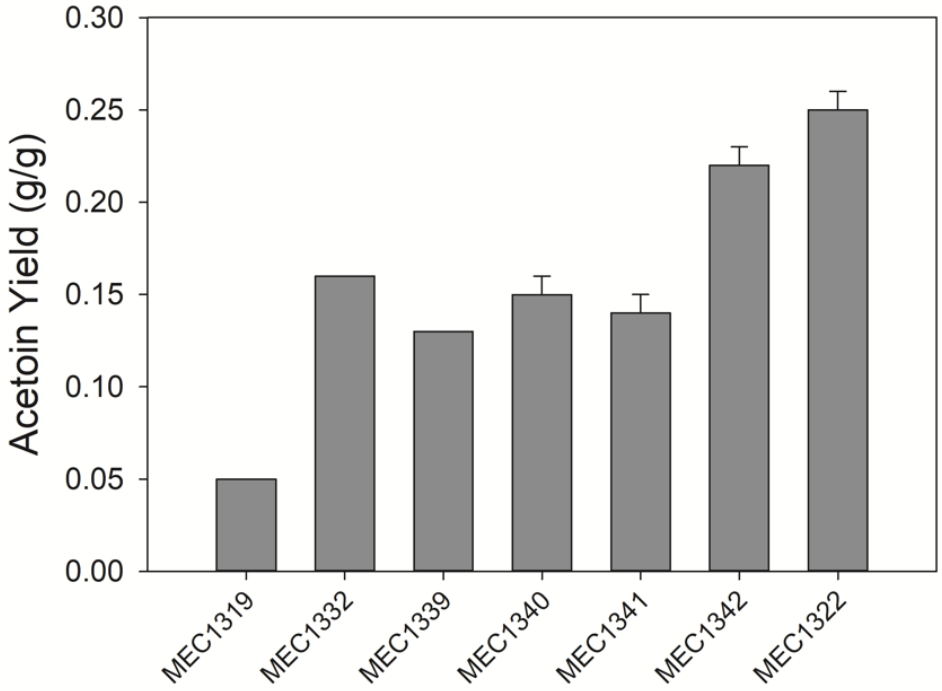

Figure 3.3 - Comparison of *E. coli* W Δ*ldhA* Δ*poxB* Δ*ppsA* AceE variants harboring plasmid 44_ediss grown in shake flasks with 5 g/L glucose: acetoin yield (g/g, gray bars). Error bars indicate standard deviation from three replicates. MEC1322/44_ediss and MEC1342/44_ediss were supplemented with 1 g/L acetate to support growth.

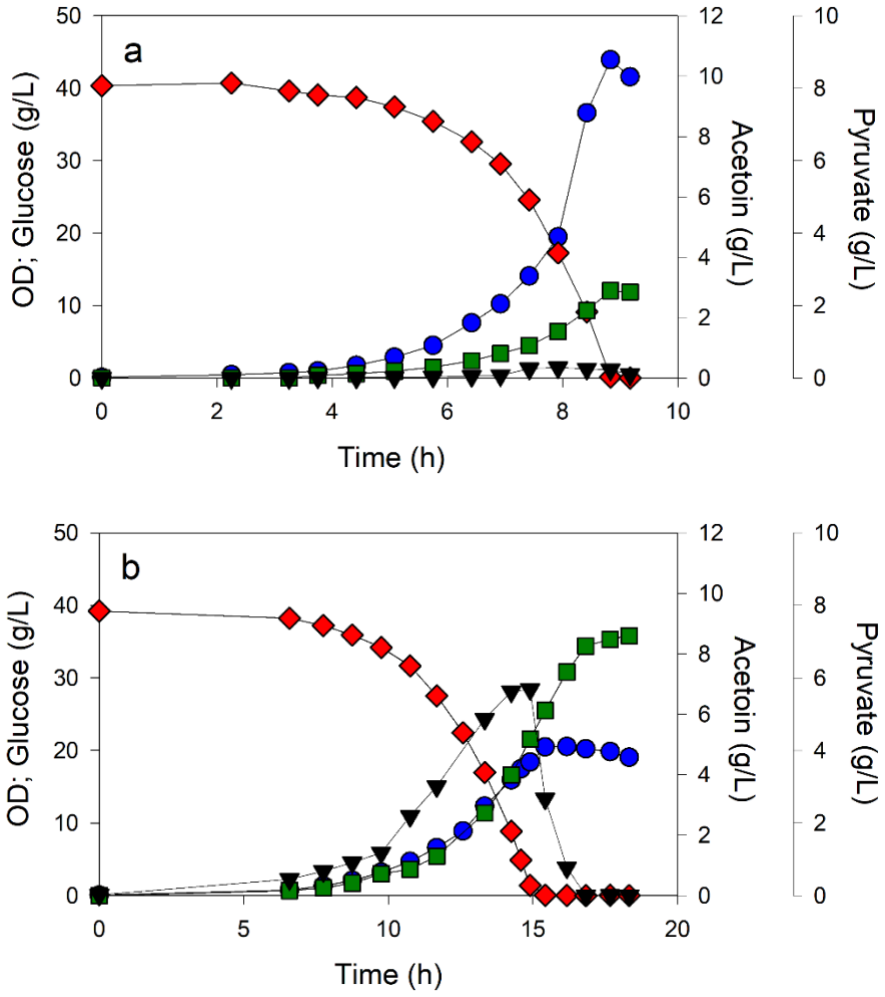
a
OD; Glucose (g/L)
Acetoin (g/L)
Pyruvate (g/L)
Time (h)
b
OD; Glucose (g/L)
Acetoin (g/L)
Pyruvate (g/L)
Time (h)

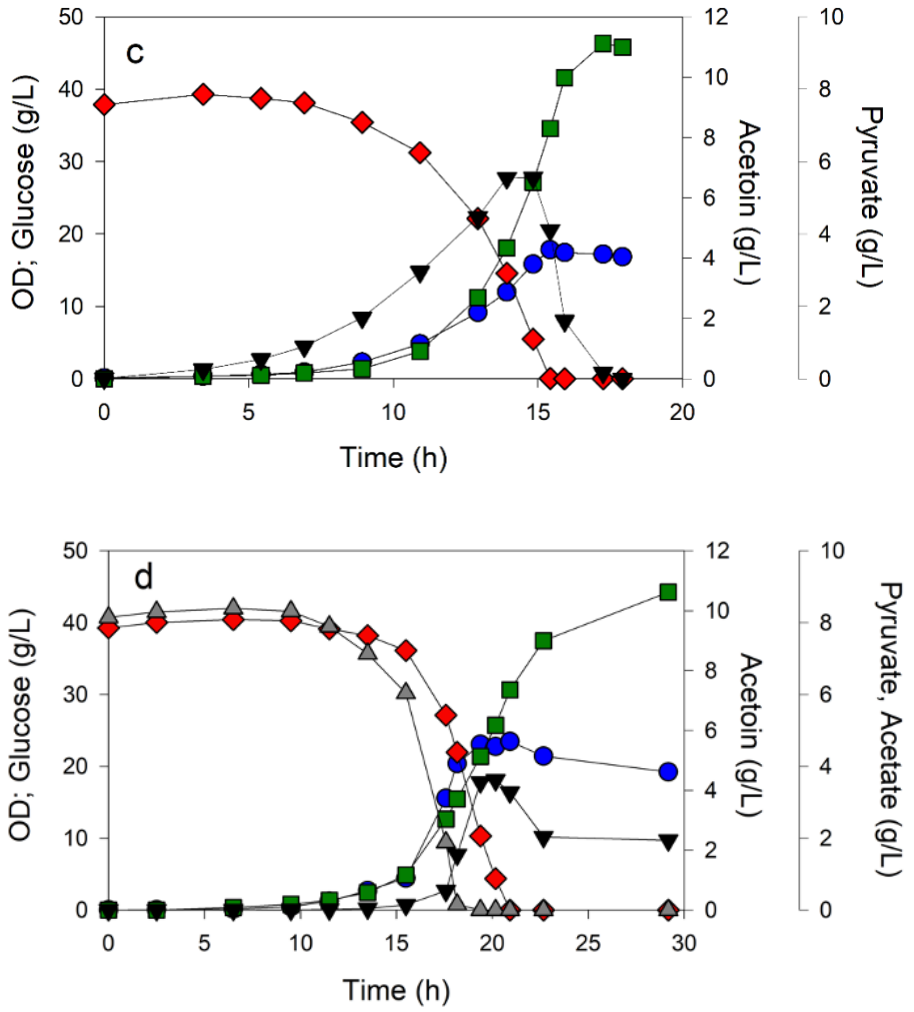

Figure 3.4 - Controlled 1.25 liter batch growth of *E. coli* W Δ*ldhA* Δ*poxB* Δ*ppsA* AceE variants harboring plasmid 44_ediss with 40 g/L glucose. a) MEC1319; b) MEC1340; c) MEC1332; d) MEC1342. Glucose (◆), pyruvate (▼), OD (●), acetate (▲), acetoin (■).

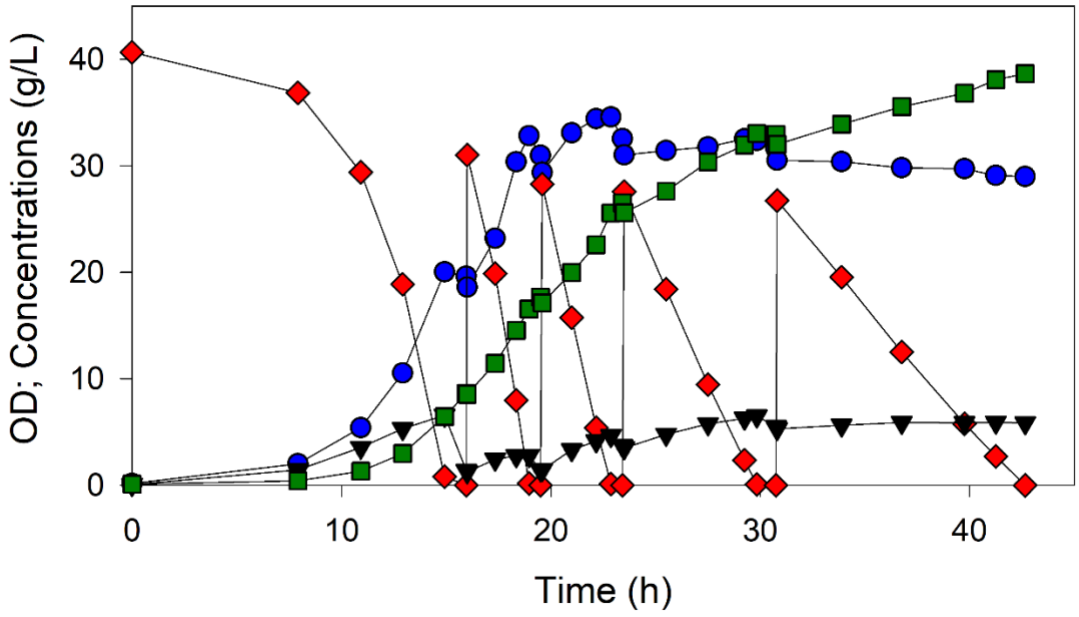

Figure 3.5 - Controlled 1.25 liter repeated-batch growth of MEC1332 (W Δ*ldhA* Δ*poxB* Δ*ppsA* Δ*aceE*::*aceE*$^{[H106V]}$) harboring plasmid 44_ediss initially with 40 g/L glucose. A 56 mL solution containing 44 g glucose and 40 mg kanamycin was added (four times) when glucose was depleted. Glucose (◆), pyruvate (▼), OD (●), acetoin (■).

CHAPTER 4

PYRUVATE PRODUCTION FROM SUCROSE BY ESCHERICHIA COLI

Moxley, W.C. and Eiteman, M.A. To be submitted to *Engineering in Life Sciences*.

4.1 ABSTRACT

Sucrose is an abundant, inexpensive, renewable carbohydrate and attractive feedstock for the biotechnological production of chemicals. *Escherichia coli* W, one of the few *E. coli* strains able to metabolize sucrose as the sole carbon source, has been used to produce a variety of industrially relevant chemicals from sucrose. The potential for *E. coli* W to produce pyruvate from sucrose was investigated in this study. The repressor for the *csc* regulon was deleted in strains of *E. coli* W able to accumulate pyruvate from glucose and were screened for pyruvate yield from sucrose. Pyruvate accumulated at yields ranging from 0.23 – 0.57 g pyruvate/g sucrose and were accompanied by the accumulation of various levels of fructose and/or glucose. Selected strains were examined in 1.25 L controlled batch processes with 40 g/L sucrose to obtain time-course resolution data for pyruvate production and the accumulation of monosaccharides. The assimilation of accumulated pyruvate was observed, which demonstrates a difference in the metabolic capabilities of glucose- and sucrose-grown *E. coli* cultures. An engineered strain expressing AceE[H106M;E401A] generated pyruvate at a maximum volumetric productivity of 2.3 ± 0.1 g pyruvate/L·h and yield of 0.71 ± 0.02 g pyruvate/g sucrose. The results demonstrate pyruvate production from sucrose is feasible with comparable volumetric productivity and yield to glucose-based processes.

4.2 INTRODUCTION

The bioproduction of fuels and chemicals relies on the availability of inexpensive and renewable feedstocks. Glucose has predominantly been used as a carbon source for many microbial products such as ethanol, succinic acid, and lactic acid. Sucrose is an attractive alternative to glucose as it requires less processing, can be directly recovered from renewable

sources such as sugar cane or sugar beets, and is cheaper than glucose in some parts of the world (Kunamneni and Singh, 2005; van der Poel et al., 1998; Yim et al., 2011). While glucose metabolism in many bacteria such as *Escherichia coli* is well studied, sucrose metabolism is poorly understood. Only a few wild-type *E. coli* strains have been isolated that can metabolize sucrose, including EC3132, B-62, and W (Bockmann et al., 1992; Sabri et al., 2013; Tsunekawa et al., 1992). Over the past two decades, *E. coli* has been engineered to produce many biochemicals from sucrose, including poly-3-hydroxybutyrate, 2,3-butanediol, 1,4-butanediol, succinate, D-lactate, and L-threonine (Arifin et al., 2011; Erian et al., 2018; Lee et al., 2010; Shukla et al., 2004; Wang et al., 2011; Yim et al., 2011).

E. coli W is the best studied sucrose metabolizing strain (Archer et al., 2011; Arifin et al., 2014; Sabri et al., 2013; Steen et al., 2014). It contains the *csc* regulon encoding four proteins: a transcriptional repressor (CscR), sucrose permease (CscB), invertase (CscA), and fructokinase (CscK). These *csc* genes allow *E. coli* W to metabolize sucrose efficiently to support high growth rates when the sucrose concentration is above ~ 10 g/L, although a deletion of the repressor *cscR* improves growth at sucrose concentrations below 10 g/L (Bockmann et al., 1992; Sabri et al., 2013). Additionally, *E. coli* W growing on sucrose generates small amounts of acetate, facilitating its growth to high cell densities on defined medium and making it an attractive strain for industrial applications (Arifin et al., 2014; Lee and Chang, 1993).

Pyruvate is a key metabolic intermediate in glycolysis and a commodity chemical that serves as an intermediate for the production of 2,3-butanediol, valine, alanine, and isoprenoids (Blombach et al., 2007; Erian et al., 2018; Rinaldi et al., 2022; Rolf et al., 2020; Smith et al., 2006; Zhu et al., 2008). Pyruvate will accumulate in *E. coli* to nearly an 80% yield from glucose using strains having a deletion or reduced activity in the pyruvate dehydrogenase complex

(Tomar et al., 2003; Zelić et al., 2003; Zhu et al., 2008; Ziegler et al., 2021). To the best of our knowledge, pyruvate accumulation has never been studied using sucrose as a carbon source. To this end, the goal of this study is to engineer *E. coli* W to accumulate pyruvate from sucrose. Deletions of *poxB* (pyruvate oxidase), *ldhA* (lactate dehydrogenase), *ppsA* (phosphoenolpyruvate synthase), and *cscR* (*csc* repressor protein) were incorporated into *E. coli* W. Additionally, the flux through PDH was reduced by use of *aceE* variants (Moxley and Eiteman, 2021). Strains were evaluated for pyruvate production in batch and fed-batch processes using sucrose as the sole carbon source.

4.3 MATERIAL AND METHODS

Media. Cultures were routinely grown on Lysogeny Broth during plasmid and strain construction, while *aceE* mutants were grown on TYA medium containing (per L) 10 g tryptone, 5 g NaCl, 1 g yeast extract, and 1 g sodium acetate trihydrate (Zhu et al., 2008). As needed, antibiotics were included in medium (final concentration): ampicillin (100 µg/mL), kanamycin (40 µg/mL), and chloramphenicol (20 µg/mL).

The defined basal medium to which carbon/energy sources were added contained (per L): 8 g NH_4Cl, 1.2 g KH_2PO_4, 1.0 K_2HPO_4, 2.0 g K_2SO_4, 0.6 g $MgSO_4 \cdot 7H_2O$, 0.25 mg $ZnSO_4 \cdot 7H_2O$, 0.125 mg $CuCl_2 \cdot 2H_2O$, 1.25 mg $MnSO_4 \cdot H_2O$, 0.875 mg $CoCl_2 \cdot 6H_2O$, 0.06 mg H_3BO_3, 0.25 mg $Na_2MoO_4 \cdot 2H_2O$, 5.5 mg $FeSO_4 \cdot 7H_2O$, 20 mg $Na_2EDTA \cdot 2H_2O$, 20 mg citric acid, 20 mg thiamine·HCl. In shake flask cultures, 20.9 g/L 3-[*N*-morpholino]propanesulfonic acid (100 mM MOPS) was used while batch processes used 25 mM MOPS. Thiamine was filter sterilized, and other medium components were autoclaved in compatible mixtures, combined and then adjusted to a pH of 7.1 with 20% (w/v) KOH.

Strains and genetic modifications. Strains used in this study are shown in Table 4.1. Gene knockouts in *E. coli* W were constructed by methods previously described (Datsenko and Wanner, 2000). Primers used to amplify the kan^R cassette from pKD4 targeting *cscR* were previously described (Sabri et al., 2013). Knockouts were selected on plates supplemented with kanamycin. Forward (5'-GATACAGCGGCAGCACAATGATCC-3') and reverse (5'-CGAACATTACGGATTACAGCTCG-3') primers external to the target gene were used to confirm proper chromosomal integration. The kan^R marker was removed by expression of FLP recombinase from pCP20 (Datsenko and Wanner, 2000). Gene knockouts and removal of the markers were verified by PCR.

Each *aceE* variant allele was PCR amplified from genomic DNA containing the respective allele and integrated into MEC1320 expressing the lambda red system from pKD46. Counter-selection against *sacB* was used to select mutants that lost the cam-*sacB* cassette by plating transformants on medium containing sucrose (Thomason et al., 2014). Colonies were confirmed by colony PCR, and point-mutated *aceE* genes were amplified from the chromosome, gel purified, and sequenced to confirm mutations.

Shake flask experiments. A single colony from an LB plate was used to inoculate 3 mL TYA. After 6-10 h of growth, this culture was used to inoculate 3 mL of basal medium with 5 g/L sucrose to an initial optical density at 600 nm (OD) of 0.05. After 8-12 h of growth, this culture was used to inoculate three 250 mL baffled shake flasks containing 25 mL of basal medium with 20 g/L sucrose to an OD of 0.02. Some seed cultures and experimental flasks were supplemented with acetate as described (using $Na(CH_3COO)\cdot 3H_2O$). All cultures were grown at 37°C on a

rotary shaker at 225 rpm. Flasks were sampled for extracellular metabolite concentrations when the OD reached 2 - 5, about 6-10 h of growth.

Batch processes. A single colony from an LB plate was used to inoculate 3 mL TYA. After 6-10 h, this culture was used to inoculate a 250 mL shake flask containing 50 mL of basal medium with 20 g/L sucrose to an OD of 0.02, with some cultures supplemented with 9.36 g/L $Na(CH_3COO)\cdot 3H_2O$ (4 g/L acetate) as described. When the shake flask culture reached an OD of 1.5-2, the 50 mL were used to inoculate a 2.5 L bioreactor (Bioflo 2000, New Brunswick Scientific Co., New Brunswick, NJ, USA) containing 1.2 L basal medium with 40 g/L sucrose. Duplicate batch processes were performed, unless otherwise stated. Some cultures were supplemented with acetate as described.

Batch bioreactor studies were conducted with an initial agitation of 400 rpm and at 37°C. Air and/or oxygen-supplemented air was sparged at 1.25 L/min with agitation adjusted to 500 rpm to maintain a dissolved oxygen concentration above 40% of saturation. The pH was controlled at 7.0 using 30% (w/v) KOH or 20% (w/v) H_2SO_4. Antifoam 204 (Sigma) was used as necessary to control foaming.

Analytical methods. The optical density at 600 nm (OD, UV-650 spectrophotometer, Beckman Instruments, San Jose, CA, USA) was used to monitor cell growth. Samples were routinely frozen at -20°C for further analysis, and thawed samples were centrifuged (4°C, 10000 × g for 10 min), and filtered (0.45 µm nylon, Acrodisc, Pall Corporation, Port Washington, NY). Liquid chromatography using RI detection was used to quantify pyruvate, sucrose, fructose, glucose and

other organic products (Eiteman and Chastain, 1997). Sulfuric acid (5.5 mN) was used as eluent with a column temperature of 30°C.

4.4 RESULTS

Variant strain screening for pyruvate yield. Previous studies have shown that *E. coli ldhA poxB ppsA* containing variant *aceE* alleles accumulate pyruvate when grown on glucose as the sole carbon source (Moxley et al., 2022 submitted, Moxley & Eiteman, 2021). The *aceE* gene encodes the E1 component of the PDH complex, which is the rate limiting step of pyruvate oxidation to acetyl CoA in aerobically grown *Escherichia coli* (Kale et al., 2007). Based on this principle, *E. coli* W, which natively contains the *csc* regulon expressing non-phosphotransferase system (PTS) sucrose catabolism proteins, was engineered to produce pyruvate from sucrose.

To assess pyruvate formation from sucrose, several *E. coli* W *ldhA poxB ppsA cscR* strains containing variant *aceE* alleles were screened for pyruvate yield in triplicate shake flasks using 20 g/L sucrose as the sole carbon source (Figure 4.1). MEC1357, containing the wild-type *aceE*, did not accumulate pyruvate. Of the variants able to grow on sucrose as the sole carbon source, MEC1361 (AceE[V169A;P190Q;F532L]) obtained the highest pyruvate yield at 0.50 ± 0.01 g/g and MEC1362 (AceE[H106M]) obtained the lowest pyruvate yield of 0.23 ± 0.02 g/g. MEC1360 (AceE[N276S;R465C;V668A;Y696N]) and MEC1359 (AceE[H106V]) obtained pyruvate yields of 0.33 ± 0.04 g/g and 0.42 ± 0.01 g/g, respectively.

MEC1358, containing an *aceE* deletion, and MEC1363 (AceE[H106M;E401A]) were unable to grow on sucrose as the sole carbon source, necessitating the supplementation of 0.75 g/L acetate to support biomass formation. MEC1358 achieved a slightly higher pyruvate yield (0.57 ± 0.06 g/g) compared to MEC1363 (0.50 ± 0.00 g/g). Because some sucrose remained in

the culture, and fructose and/or glucose was detected in all samples (data not shown), yield was calculated based on mass of pyruvate formed divided by mass of monosaccharide units consumed.

The wild-type MEC1357 accumulated a small quantity of fructose (only) at a yield of ~ 0.02 g/g. MEC1358, MEC1359, MEC1360, and MEC1363 accumulated approximately equal molar quantities of glucose and fructose at yields of 0.08 – 0.10 g/g (each). MEC1361 and MEC1362 accumulated approximately equal molar quantities of glucose and fructose at yields of 0.04 g/g and 0.20 g/g, respectively. Because the calculated monosaccharide "yields" represent a single time point in growth, they do not represent the full extent of accumulation. Therefore, additional time course studies were undertaken to understand the accumulation of monosaccharides, as well as the accumulation of pyruvate under controlled conditions.

Controlled batch processes. Maximal rates of sucrose uptake and glycolytic flux have been previously observed when the sucrose concentration is higher than ~10 g/L (Arifin et al., 2014). Thus, selected strains were studied in controlled batch culture using 40 g/L sucrose (Figure 4.2). MEC1357 (n=1) achieved a growth rate of 0.79 h^{-1} and accumulated 0.60 g/L pyruvate in 14 h (Figure 4.2a). Glucose and fructose accumulated in approximately equimolar amounts, reaching maximum concentrations of 7.5 - 8.3 g/L at 14 h, before being metabolized completely by 16 h. MEC1360 (n=2) achieved a growth rate of 0.44 ± 0.00 h^{-1} and accumulated 11.6 ± 0.1 g/L pyruvate in 14 h before re-assimilating pyruvate (Figure 4.2b). Glucose and fructose again accumulated to equimolar amounts (average maximal concentration of 4.8 g/L) before being metabolized simultaneously by 17 h. MEC1361 (n=1) achieved a growth rate of 0.43 h^{-1} and

accumulated 15.1 g/L pyruvate in 16 h before pyruvate was slowly re-assimilated (Figure 4.2c). In this case, glucose and fructose accumulated to 0.3 g/L and 0.5 g/L, respectively.

MEC1363 (n=2) has a severe mutation in AceE necessitating medium supplementation with 8 g/L acetate to support biomass formation. Acetate was depleted in 13 h, at which time pyruvate concentration was 2 g/L, and the concentrations of fructose and glucose were both less than 1 g/L. During the 7 h after acetate depletion, pyruvate accumulated to 21.8 ± 0.6 g/L with a productivity of 2.3 ± 0.1 g/L·h and yield of 0.71 ± 0.02 g/g. In this case, pyruvate was not re-assimilated and only fructose but not glucose accumulated. The maximum fructose concentration was 3.6 ± 1.4 g/L at 17 h, and fructose was metabolized slowly as sucrose became depleted.

4.5 DISCUSSION

The goal of this research was to examine pyruvate production from sucrose using *E. coli* W. Seven strains with differences in the *aceE* allele were first screened in shake flask studies: a wild-type *aceE*, a Δ*aceE* strain, and 5 strains containing mutations which have previously been shown to lead to pyruvate accumulation from glucose (Moxley and Eiteman, in review). All strains contained deletions of the *ldhA, poxB, ppsA*, and *cscR* genes. To ensure sucrose uptake rates in shake flasks were representative of batch cultures, where relatively high sugar concentrations are often used, the initial sucrose concentration was 20 g/L. Each variant *aceE* allele and the Δ*aceE* strain indeed accumulated pyruvate, suggesting carbon flux distribution at the pyruvate node is similar when grown on either glucose or sucrose (Figure 4.1). Surprisingly, the variant *aceE* strains also accumulated fructose and glucose, leading to more detailed batch studies in controlled fermenters at the 1.25 liter scale and consideration of how sucrose and monosaccharides are metabolized.

PTS-mediated glucose uptake and subsequent catabolism through glycolysis is well studied and has evolved to support high glucose uptake rates and glycolytic fluxes. Similarly, the fructose PTS system facilitates the import of fructose and belongs to the same PTS superfamily as the glucose PTS system (Jeckelmann and Erni, 2019; Postma et al., 1993). One characteristic of these uptake processes is that pyruvate formation is coupled with sugar import through the phosphorylation of EI, for which phosphoenolpyruvate (PEP) serves as the phosphate donor generating P~EI and pyruvate. During growth on glucose and other PTS-associated sugars, the majority of pyruvate is generated by EI phosphorylation (Emmerling et al., 2002; Sauer and Eikmanns, 2005). In contrast, the sucrose uptake, encoded by the *csc* regulon genes, is not PTS-mediated and relies on a sucrose-H^+ symporter (CscB) (Bockmann et al., 1992). Sucrose is subsequently hydrolyzed into glucose and fructose intracellularly by invertase (CscA).

Since sucrose import by CscB is not PTS-mediated, sucrose uptake rate is mediated by the concentration of sucrose in the medium which results in culture growth rates directly related to sucrose concentration (Arifin et al., 2014). Additionally, *csc* gene expression is negatively regulated by CscR, which drastically decreases growth rates at sucrose concentrations less than 2 g/L (Sabri et al., 2013). To maximize sucrose uptake rates, *cscR* was deleted in all strains in this study. In batch cultures with initially 40 g/L sucrose, each selected *aceE* variant and wild-type strain exhibited decelerated specific sucrose uptake when the sucrose concentration decreased to less than 10 g/L (Figure 4.2). This observation is consistent with previous studies and demonstrates the benefit of using relatively high sucrose concentrations even when the *csc* genes are fully derepressed (Arifin et al., 2011; Sabri et al., 2013). This potential disadvantage in using sucrose as a carbon source could be overcome by a fed-batch or repeated-batch process which maintains a sucrose concentration above 10 g/L (Erian et al., 2018).

In most batch cultures glucose and fructose accumulated in the supernatant, reaching maximum concentrations in late exponential phase before being co-metabolized. Others have reported the accumulation of these monosaccharides from bacteria metabolizing sucrose through the *csc* pathway (Löwe et al., 2017; Sabri et al., 2013). For example, a maximum of about ~1.25 g/L of glucose and fructose accumulated when *E. coli* W was grown on 20 g/L sucrose (Sabri et al., 2013). Fructose and glucose also accumulated during sucrose utilization in *Pseudomonas putida* KT2440 expressing an invertase (*cscA*) and sucrose transporter (*cscB*) (Löwe et al. 2017). That study noted that expression of invertase, in the absence of the sucrose transporter, conferred sucrose utilization through the extracellular cleavage of sucrose (Löwe et al. 2017). Extracellular invertase activity was confirmed and suggests that CscA, a cytosolic enzyme, can "leak" out across the cell membrane (Löwe et al., 2017). Similarly, Sahin-Tóth et al. investigated a plasmid that conferred sucrose utilization to *E. coli* K-12, a strain incapable of utilizing sucrose as a carbon source and found that the overexpression of invertase alone was sufficient for sucrose utilization (Sahin-Tóth et al., 1999). Invertase activity was detected in the periplasmic space and the cell-free supernatant, indicating that high expression of CscA caused leakage of invertase into the periplasmic space and supernatant and resulted in extracellular sucrose cleavage that supplied monosaccharides for cell growth (Sahin-Tóth et al., 1999). Thus, accumulation of glucose and fructose in strains examined in this study could be caused by membrane-, periplasm-, or supernatant-associated invertase activity. To test whether invertase was present in the extracellular and membrane environment, strains which accumulated glucose and fructose could be cultured and sampled during exponential phase of growth and subsequently measured for invertase activity in the cell-free supernatant and membrane fractions of the sample, as described previously (Sahin-Tóth et al., 1999).

An interesting observation is the apparent suppression of glucose/fructose accumulation when MEC1363 was grown on a mixture of sucrose and acetate (Figure 4.2d). Because MEC1363 required acetate for growth, it was the only strain studied in batch culture that was supplemented with acetate. To confirm that acetate consumption caused this phenotype, a strain that does not require acetate for growth, such as MEC1357 containing the WT *aceE* allele, could be grown on a mixture of sucrose and acetate. MEC1357 grown on sucrose accumulated significant amounts of monosaccharides, thus a difference would be expected if the addition of acetate suppresses this phenotype (Fig 2a). If the extracellular accumulation of monosaccharides from sucrose is caused by CscA leaking into the periplasmic space and supernatant, it may be related to the intracellular concentration of CscA and, therefore, the expression levels of *cscA*. This result would be consistent with other reports of CscA leakage when highly expressed (Löwe et al., 2017; Sahin-Tóth et al., 1999). To test if acetate influences the abundance of CscA, *cscA* expression levels could be analyzed in cultures with and without supplemented acetate.

During batch culture of MEC1363, only fructose accumulated after acetate depletion (Figure 4.2d), a result that was different from that of other strains. If this phenotype is a result of acetate consumption, batch growth of MEC1357 on a mixture of sucrose and acetate would likely result in a similar phenotype. One possible explanation is that sucrose is hydrolyzed extracellularly and glucose is co-consumed with sucrose, resulting in the accumulation of only fructose. To test this hypothesis, the rates of glucose and fructose consumption could be compared in batch culture grown on sucrose with and without supplementation of acetate. To ensure the concentration of each monosaccharide is sufficient to measure consumption rates after acetate depletion, the culture could be supplemented with ~5 g/L of each monosaccharide at a specific time point. If, in this experiment, glucose is preferentially consumed before fructose, the

consumption of glucose may be facilitated by the PTS system (Görke and Stülke, 2008). Genes encoding the glucose PTS system are downregulated during growth on sucrose, which is consistent with results from batch experiments without acetate supplementation during which glucose and fructose were co-metabolized (Figure 4.2a-c; Arifin et al., 2014). Altered expression of the glucose PTS system could be tested by measuring expression levels of *ptsG*, encoding a glucose-specific PTS component, in strains grown on sucrose with and without acetate supplementation (Meadow et al., 1990).

One distinct difference between *aceE* variant strains grown on sucrose or glucose is the consumption of accumulated pyruvate when grown on sucrose but not on glucose. Previous research has demonstrated that strains lacking genes responsible for pyruvate consumption (*ldhA*, *poxB*, and *ppsA*) do not metabolize pyruvate when grown on glucose (Moxley and Eiteman, 2021). When grown on sucrose, accumulated pyruvate is re-assimilated, seemingly dependent on the relative flux through the PDH. That is, pyruvate consumption was not observed in MEC1363 with severe AceE substitutions even after acetate was metabolized (Figure 4.2d), but pyruvate re-assimilation was observed in MEC1360 and MEC1361 with moderate substitutions in AceE (Figure 4.4bc). When pyruvate is re-assimilated in Δ*poxB* Δ*ppsA* Δ*ldhA* strains, it is oxidized to acetyl-CoA and enters the TCA cycle via condensation with oxaloacetate to form citrate via citrate synthase [GltA, EC 2.3.3.16]. Thus, reassimilation of pyruvate through acetyl-CoA depends on the availability of oxaloacetate. Citrate synthase has a K_M of 0.03 mM for oxaloacetate and 0.12 mM for acetyl-CoA which are similar to the intracellular concentrations of each metabolite (0.13 mM and 0.03 mM, respectively) when wild-type *E. coli* is growing on glucose (Peng et al., 2004; Pereira et al., 1994). Interestingly, the oxaloacetate pool is thought to be elevated during growth on sucrose compared to growth on glucose (Arifin et al., 2014). Thus,

the difference in pyruvate re-assimilation between strains growing on glucose compared to growth on sucrose could be attributed to intracellular oxaloacetate levels. A greater oxaloacetate concentration would facilitate the consumption of acetyl-CoA via citrate synthase, drawing pyruvate at a sufficient level to provide maintenance energy for the cell. Thus, consumption of accumulated pyruvate in glucose-grown cultures would be limited by a lower oxaloacetate concentration. Even though carbon from pyruvate would cycle back to oxaloacetate, the transition to stationary phase induces gluconeogenic pathways, such as *pck* [PEP carboxykinase; EC:4.1.1.49], that divert oxaloacetate to PEP for gluconeogenesis which would tend to decrease the oxaloacetate concentration below 0.03 mM (Goldie, 1984). To test this, the oxaloacetate levels could be diminished by the induction of a competing enzyme near the onset of sugar depletion and pyruvate assimilation in MEC1360 (Figure 4.2b). For example, oxaloacetate decarboxylase [ODx, EC 4.1.1.112], encoded by *odx* in *C. glutamicum*, catalyzes the decarboxylation of oxaloacetate to CO_2 and pyruvate, and could consume the pool of oxaloacetate (Klaffl and Eikmanns, 2010). Decreased pyruvate assimilation after ODx expression would support the hypothesis that elevated intracellular oxaloacetate during growth on sucrose is a factor in pyruvate assimilation.

The present study demonstrates pyruvate production from sucrose using *E. coli* W with yields comparable to those obtained when using glucose. Important parameters for pyruvate production in *E coli* W using sucrose were ensuring sucrose concentrations above 10 g/L and greatly diminishing the flux through PDH. To achieve higher titers and yields, a fed-batch process using MEC1363 can be developed where sucrose and/or acetate are fed such that the sucrose concentration is maintained above 10 g/L and the medium optimized to support high cell densities. This work expands the substrate range for pyruvate production using sucrose, an

inexpensive and readily available fermentation feedstock. Further studies on the relationship between acetate and monosaccharide accumulation or consumption in addition to the assimilation of accumulated pyruvate could contribute to our understanding of sucrose metabolism in *E. coli* W, an area of *E. coli* metabolism that is not well studied.

Acknowledgments

The authors acknowledge financial support of the U.S. National Science Foundation (CBET-1802533).

4.6 REFERENCES

Archer, C.T., Kim, J.F., Jeong, H., Park, J.H., Vickers, C.E., Lee, S.Y., Nielsen, L.K., 2011. The genome sequence of *E. coli* W (ATCC 9637): Comparative genome analysis and an improved genome-scale reconstruction of *E. coli*. BMC Genomics 12, 1–20. https://doi.org/10.1186/1471-2164-12-9

Arifin, Y., Archer, C., Lim, S.A., Quek, L.E., Sugiarto, H., Marcellin, E., Vickers, C.E., Krömer, J.O., Nielsen, L.K., 2014. *Escherichia coli* W shows fast, highly oxidative sucrose metabolism and low acetate formation. Appl Microbiol Biotechnol 98, 9033–9044. https://doi.org/10.1007/S00253-014-5956-4

Arifin, Y., Sabri, S., Sugiarto, H., Krömer, J.O., Vickers, C.E., Nielsen, L.K., 2011. Deletion of *cscR* in *Escherichia coli* W improves growth and poly-3-hydroxybutyrate (PHB) production from sucrose in fed batch culture. J Biotechnol 156, 275–278. https://doi.org/10.1016/J.JBIOTEC.2011.07.003

Blombach, B., Schreiner, M.E., Holátko, J., Bartek, T., Oldiges, M., Eikmanns, B.J., 2007. L-Valine production with pyruvate dehydrogenase complex-deficient *Corynebacterium glutamicum*. Appl Environ Microbiol 73, 2079–2084. https://doi.org/10.1128/AEM.02826-06

Bockmann, J., Heuel, H., Lengeler, J.W., 1992. Characterization of a chromosomally encoded, non-PTS metabolic pathway for sucrose utilization in *Escherichia coli* EC3132. Mol Gen Genet 235, 22–32. https://doi.org/10.1007/BF00286177

Datsenko, K.A., Wanner, B.L., 2000. One-step inactivation of chromosomal genes in *Escherichia coli* K-12 using PCR products. Proc Natl Acad Sci U S A 97, 6640–6645. https://doi.org/10.1073/pnas.120163297

Emmerling, M., Dauner, M., Ponti, A., Fiaux, J., Hochuli, M., Szyperski, T., Wüthrich, K., Bailey, J.E., Sauer, U., 2002. Metabolic flux responses to pyruvate kinase knockout in *Escherichia coli*. J Bacteriol 184, 152–164. https://doi.org/10.1128/JB.184.1.152-164.2002

Erian, A.M., Gibisch, M., Pflügl, S., 2018. Engineered *E. coli* W enables efficient 2,3-butanediol production from glucose and sugar beet molasses using defined minimal medium as economic basis. Microb Cell Fact 17, 1–17. https://doi.org/10.1186/S12934-018-1038-0

Goldie, H., 1984. Regulation of transcription of the *Escherichia coli* phosphoenolpyruvate carboxykinase locus: studies with *pck-lacZ* operon fusions. J Bacteriol 159, 832–836.

Görke, B., Stülke, J., 2008. Carbon catabolite repression in bacteria: many ways to make the most out of nutrients. Nat Rev Microbiol 6, 613–624. https://doi.org/10.1038/nrmicro1932

Jeckelmann, J.M., Erni, B., 2019. Carbohydrate Transport by Group Translocation: The Bacterial Phosphoenolpyruvate: Sugar Phosphotransferase System, in: Subcellular Biochemistry. pp. 223–274. https://doi.org/10.1007/978-3-030-18768-2_8

Klaffl, S., Eikmanns, B.J., 2010. Genetic and functional analysis of the soluble oxaloacetate decarboxylase from *Corynebacterium glutamicum*. J Bacteriol 192, 2604–2612. https://doi.org/10.1128/JB.01678-09

Kunamneni, A., Singh, S., 2005. Response surface optimization of enzymatic hydrolysis of maize starch for higher glucose production. Biochem Eng J 27, 179–190. https://doi.org/10.1016/j.bej.2005.08.027

Lee, J.W., Choi, S., Park, J.H., Vickers, C.E., Nielsen, L.K., Lee, S.Y., 2010. Development of sucrose-utilizing *Escherichia coli* K-12 strain by cloning β-fructofuranosidases and its application for L-threonine production. Appl Microbiol Biotechnol 88, 905–913. https://doi.org/10.1007/s00253-010-2825-7

Lee, S.Y., Chang, H.N., 1993. High cell density cultivation of *Escherichia coli* W using sucrose as a carbon source. Biotechnology Letters 1993 15:9 15, 971–974. https://doi.org/10.1007/BF00131766

Löwe, H., Schmauder, L., Hobmeier, K., Kremling, A., Pflüger-Grau, K., 2017. Metabolic engineering to expand the substrate spectrum of *Pseudomonas putida* toward sucrose. Microbiologyopen 6, e00473. https://doi.org/10.1002/mbo3.473

Meadow, N.D., Fox, D.K., Roseman, S., 1990. The bacterial phosphoenolpyruvate: Glycose phosphotransferase system. Annu Rev Biochem 59, 497–542. https://doi.org/10.1146/annurev.bi.59.070190.002433

Moxley, W.C., Eiteman, M.A., 2021. Pyruvate Production by *Escherichia coli* by Use of Pyruvate Dehydrogenase Variants. Appl Environ Microbiol 87, e00487-21. https://doi.org/10.1128/AEM.00487-21

Peng, L., Arauzo-Bravo, M.J., Shimizu, K., 2004. Metabolic flux analysis for a *ppc* mutant *Escherichia coli* based on 13C-labelling experiments together with enzyme activity assays and intracellular metabolite measurements. FEMS Microbiol Lett 235, 17–23. https://doi.org/10.1016/j.femsle.2004.04.003

Pereira, D.S., Donald, L.J., Hosfield, D.J., Duckworth, H.W., 1994. Active site mutants of *Escherichia coli* citrate synthase. Effects of mutations on catalytic and allosteric properties. Journal of Biological Chemistry 269, 412–417.

Postma, P.W., Lengeler, J.W., Jacobson, G.R., 1993. Phosphoenolpyruvate:carbohydrate phosphotransferase systems of bacteria. Microbiol Rev 57, 543–594. https://doi.org/10.1128/mr.57.3.543-594.1993

Rinaldi, M.A., Ferraz, C.A., Scrutton, N.S., 2022. Alternative metabolic pathways and strategies to high-titre terpenoid production in *Escherichia coli*. Nat Prod Rep 39, 90–118. https://doi.org/10.1039/D1NP00025J

Rolf, J., Julsing, M.K., Rosenthal, K., Lütz, S., 2020. A Gram-Scale Limonene Production Process with Engineered *Escherichia coli*. Molecules 25, 1881. https://doi.org/10.3390/MOLECULES25081881

Sabri, S., Nielsen, L.K., Vickers, C.E., 2013. Molecular control of sucrose utilization in *Escherichia coli* W, an efficient sucrose-utilizing strain. Appl Environ Microbiol 79, 478–487. https://doi.org/10.1128/AEM.02544-12

Sahin-Tóth, M., Lengyel, Z., Tsunekawa, H., 1999. Cloning, sequencing, and expression of *cscA* invertase from *Escherichia coli* B-62. Can J Microbiol 45, 418–422.

Sauer, U., Eikmanns, B.J., 2005. The PEP—pyruvate—oxaloacetate node as the switch point for carbon flux distribution in bacteria: We dedicate this paper to Rudolf K. Thauer, Director of the Max-Planck-Institute for Terrestrial Microbiology in Marburg, Germany, on the occasion of his 65th birthday. FEMS Microbiol Rev 29, 765–794. https://doi.org/10.1016/J.FEMSRE.2004.11.002

Shukla, V.B., Zhou, S., Yomano, L.P., Shanmugam, K.T., Preston, J.F., Ingram, L.O., 2004. Production of d(−)-lactate from sucrose and molasses. Biotechnology Letters 2004 26:9 26, 689–693. https://doi.org/10.1023/B:BILE.0000024088.36803.4E

Smith, G.M., Lee, S.A., Reilly, K.C., Eiteman, M.A., Altman, E., 2006. Fed-batch two-phase production of alanine by a metabolically engineered *Escherichia coli*. Biotechnol Lett 28, 1695–1700. https://doi.org/10.1007/S10529-006-9142-3

Steen, J.A., Bohlke, N., Vickers, C.E., Nielsen, L.K., 2014. The Trehalose Phosphotransferase System (PTS) in *E. coli* W Can Transport Low Levels of Sucrose that Are Sufficient to Facilitate Induction of the *csc* Sucrose Catabolism Operon. PLoS One 9, e88688. https://doi.org/10.1371/journal.pone.0088688

Tomar, A., Eiteman, M.A., Altman, E., 2003. The effect of acetate pathway mutations on the production of pyruvate in *Escherichia coli*. Appl Microbiol Biotechnol 62, 76–82. https://doi.org/10.1007/s00253-003-1234-6

Tsunekawa, H., Azuma, S., Okabe, M., Okamoto, R., Aiba, S., 1992. Acquisition of a sucrose utilization system in *Escherichia coli* K-12 derivatives and its application to industry. Appl Environ Microbiol 58, 2081–2088. https://doi.org/10.1128/AEM.58.6.2081-2088.1992

van der Poel, P., Schiweck, H., Schwartz, T., 1998. Sugar Technology, Beet and Cane Sugar Manufacture. https://doi.org/10.36961/st

Wang, J., Zhu, J., Bennett, G.N., San, K.Y., 2011. Succinate production from sucrose by metabolic engineered *Escherichia coli* strains under aerobic conditions. Biotechnol Prog 27, 1242–1247. https://doi.org/10.1002/BTPR.661

Yim, H., Haselbeck, R., Niu, W., Pujol-Baxley, C., Burgard, A., Boldt, J., Khandurina, J., Trawick, J.D., Osterhout, R.E., Stephen, R., Estadilla, J., Teisan, S., Schreyer, H.B., Andrae, S., Yang, T.H., Lee, S.Y., Burk, M.J., van Dien, S., 2011. Metabolic engineering of *Escherichia coli* for direct production of 1,4-butanediol. Nat Chem Biol 7, 445–452. https://doi.org/10.1038/nchembio.580

Zelić, B., Gerharz, T., Bott, M., Vasić-Rački, Đ., Wandrey, C., Takors, R., 2003. Fed-Batch Process for Pyruvate Production by Recombinant *Escherichia coli* YYC202 Strain. Eng Life Sci 3, 299–305. https://doi.org/10.1002/ELSC.200301756

Zhu, Y., Eiteman, M.A., Altman, R., Altman, E., 2008. High Glycolytic Flux Improves Pyruvate Production by a Metabolically Engineered *Escherichia coli* Strain. Appl Environ Microbiol 74, 6649–6655. https://doi.org/10.1128/AEM.01610-08

Ziegler, M., Hägele, L., Gäbele, T., Takors, R., 2021. CRISPRi enables fast growth followed by stable aerobic pyruvate formation in *Escherichia coli* without auxotrophy. Eng Life Sci 22, 70–84. https://doi.org/10.1002/ELSC.202100021

Table 4.1 - Strains used in this study.

Strain	Relevant characteristics	Reference
ATCC 9637	*Escherichia coli* W	Wild-type
MEC1319	ATCC 9637 Δ*ldhA* Δ*poxB* Δ*ppsA*	Moxley et al., submitted
MEC1322	ATCC 9637 Δ*ldhA* Δ*poxB* Δ*ppsA* Δ*aceE*	Moxley et al., submitted
MEC1332	ATCC 9637 Δ*ldhA* Δ*poxB* Δ*ppsA* Δ*aceE*::*aceE*$^{[H106V]}$	Moxley et al., submitted
MEC1339	ATCC 9637 Δ*ldhA* Δ*poxB* Δ*ppsA* Δ*aceE*::*aceE*$^{[N276S;R465C;V668A;Y696N]}$	Moxley et al., submitted
MEC1340	ATCC 9637 Δ*ldhA* Δ*poxB* Δ*ppsA* Δ*aceE*::*aceE*$^{[V169A;P190Q;F532L]}$	Moxley et al., submitted
MEC1341	ATCC 9637 Δ*ldhA* Δ*poxB* Δ*ppsA* Δ*aceE*::*aceE*$^{[H106M]}$	Moxley et al., submitted
MEC1342	ATCC 9637 Δ*ldhA* Δ*poxB* Δ*ppsA* Δ*aceE*::*aceE*$^{[H106M;E401A]}$	Moxley et al., submitted
MEC1357	MEC1319 Δ*cscR*::Kan	This study
MEC1358	MEC1322 Δ*cscR*::Kan	This study
MEC1359	MEC1332 Δ*cscR*::Kan	This study
MEC1360	MEC1339 Δ*cscR*::Kan	This study
MEC1361	MEC1340 Δ*cscR*::Kan	This study
MEC1362	MEC1341 Δ*cscR*::Kan	This study
MEC1363	MEC1342 Δ*cscR*::Kan	This study

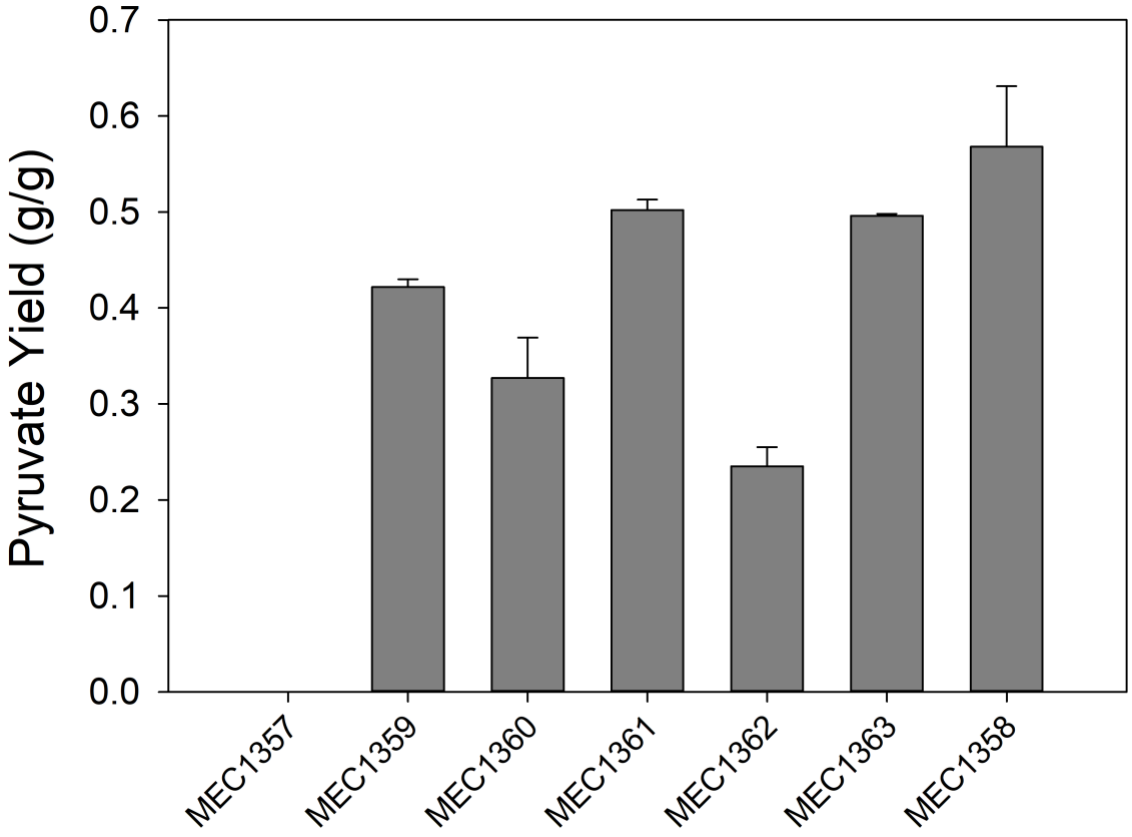

Figure 4.1 - Comparison of pyruvate yield (g/g) in *E. coli* W Δ*ldhA* Δ*poxB* Δ*ppsA* Δ*cscR* AceE variants grown in shake flasks with 40 g/L sucrose. Error bars indicate standard deviation from three replicates.

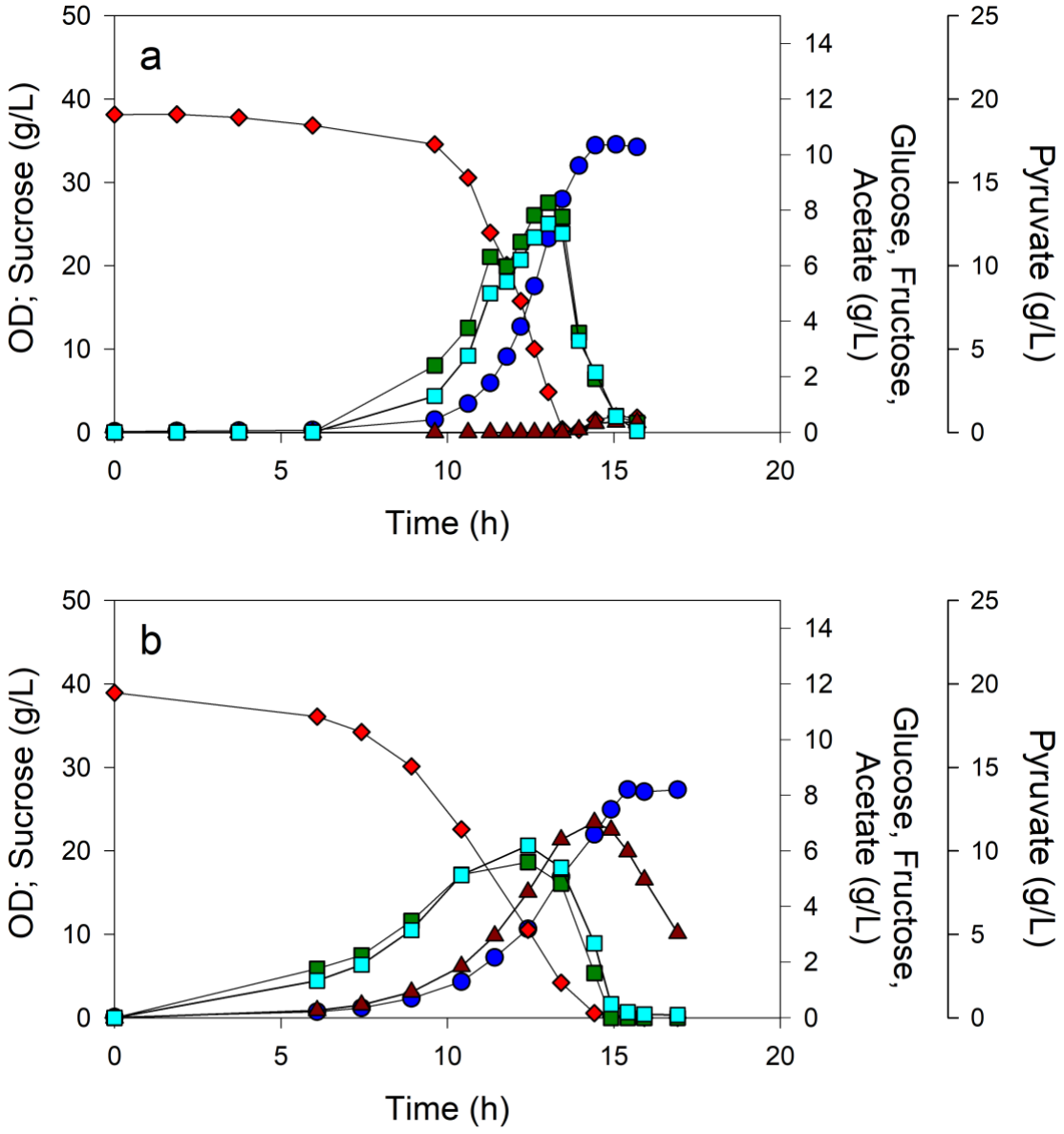
a
b
OD; Sucrose (g/L)
Glucose, Fructose, Acetate (g/L)
Pyruvate (g/L)
Time (h)
0
5
10
15
20
0
10
20
30
40
50
0
2
4
6
8
10
12
14
0
5
10
15
20
25

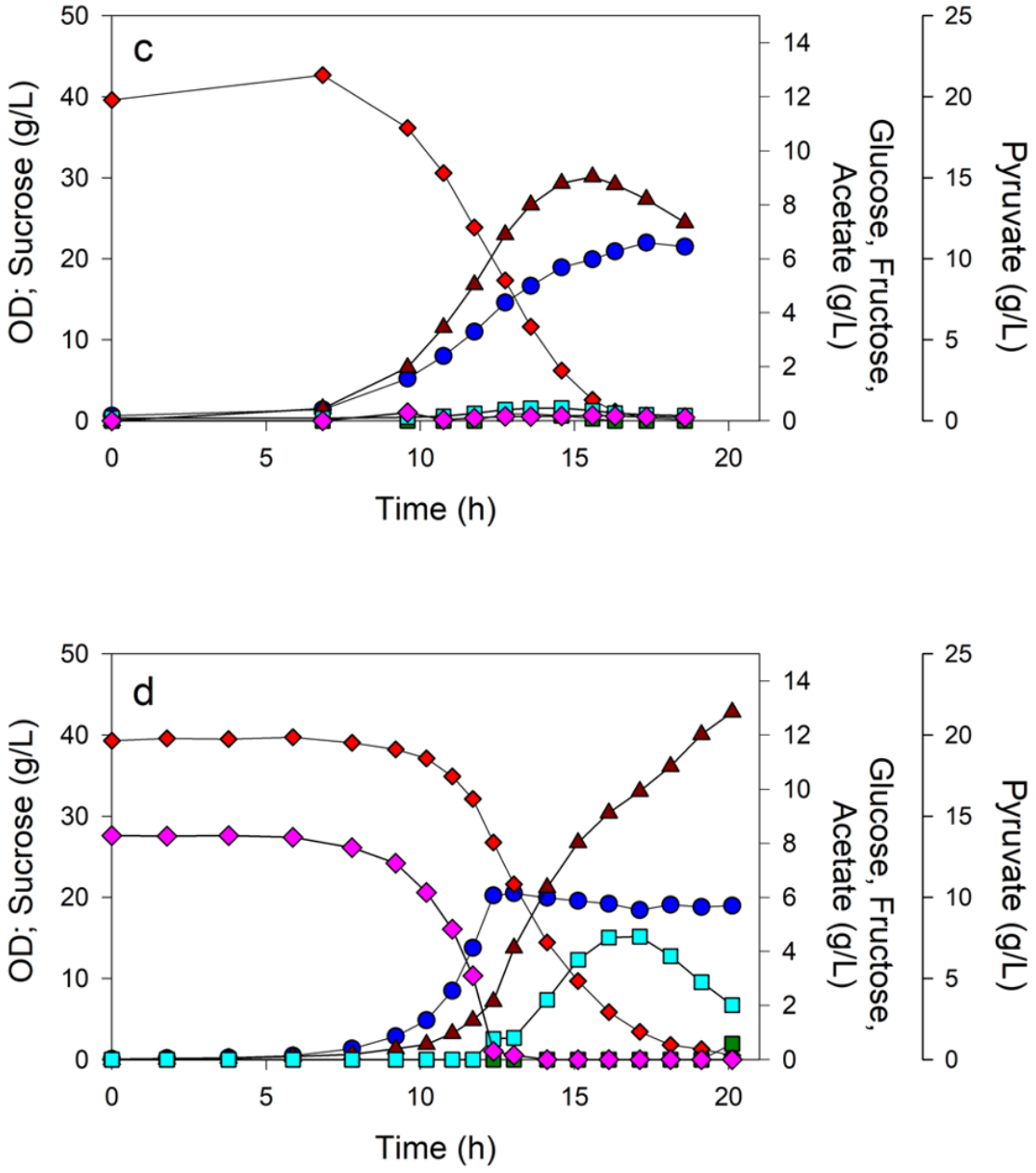

Figure 4.2 - Controlled 1.25 liter batch growth of *E. coli* W Δ*ldhA* Δ*poxB* Δ*ppsA* Δ*cscR* AceE variants harboring with 40 g/L sucrose. a) MEC1357; b) MEC1360; c) MEC1361; d) MEC1363. Sucrose (◆), pyruvate (▲), OD (●), acetate (◆), glucose (■), fructose (■).

CHAPTER 5

CONCLUSIONS AND FUTURE DIRECTIONS

5.1 CONCLUSIONS

The fundamental goal of this research was to develop an additional metabolic engineering tool to enhance the production of pyruvate-derived chemicals. The core hypothesis was that modifying a key enzyme at the pyruvate branchpoint, AceE of the PDHc, can allow for decrease metabolic flux toward biomass formation and increase the availability of pyruvate for a competing production pathway. Thus, AceE variants that confer decreased growth rates and/or accumulate pyruvate likely have altered kinetic parameters that decrease the specific activity of PDHc and represent an additional tool for modifying metabolic flux at the pyruvate node.

Chapter 1 provides proof-of-concept that modifying AceE is a feasible means to modulate pyruvate flux. Through rational protein engineering, 16 different *aceE* alleles were constructed that transcribe variants of AceE with one or two substitutions in or near the active site. The variants conferred different growth rates and pyruvate yields when incorporated into a strain with deletions in pyruvate-consuming byproduct pathways (*poxB* and *ldhA*). Three of the variant strains displayed different and inversely proportional growth rates and pyruvate yields, indicating that the conversion of pyruvate to acetyl-CoA was decreased at various magnitudes and unique to each specific variant allele. Studies of pyruvate-producing strains grown in 1 L controlled bioreactors suggested that an additional deletion in *ppsA* is necessary for ensuring PDHc is the sole pyruvate-consuming pathway. The bottleneck effect conferred by AceE

variants was further evident in chemostat studies comparing the AceE[H106V] variant strain and the WT AceE strain at the same growth rate. AceE[H106V] imposed a 65% increase in glucose uptake rate and 2.6-fold increase in *aceE*$^{[H106V]}$ expression to confer the same growth rate as a strain containing the WT *aceE* allele. The work demonstrates that pyruvate flux can be portioned away from central metabolism using protein engineering to decrease metabolic flux through a key pathway and presumably decrease the activity of an enzyme, an uncommon strategy in metabolic engineering.

The research detailed in Chapter 2 provided two additional *aceE* variants, through random mutagenesis, that are unique to those generated by rational protein design. The suit of five *aceE* variants was applied to the production of acetoin as a model pyruvate-derived product. The shift of carbon flux from central metabolism to acetoin production was evident by *aceE* variant strains attaining ~1.6 – 4-fold higher acetoin yields than the WT *aceE* strain when screened in shake flasks. A strict reduction in PDHc flux did not correlate with high performance when producing a pyruvate-derived product in controlled batch process, which demonstrates the benefit of *aceE* variants that confer a balance in metabolic flux between growth and product formation. Additionally, an *aceE* variant that allows carbon flux toward central metabolism can sustain prolonged product formation, demonstrated by the high performance of the *aceE*$^{[H106V]}$ variant strain in a prolonged, repeated-batch process. In the case of acetoin production, the *aceE*$^{[H106V]}$ variant maximized product yield and titer from a kinetically slow competing pathway although a different pathway may benefit from the use of a different *aceE* variant. An advantage of having a suite of *aceE* variants is the ability to test a production pathway in strains that partition metabolic flux to differing degrees, allowing one to match the production pathway to the *aceE* variant that provides the best yields, productivities, and titers.

In Chapter 4, expanding the substrate range for pyruvate production was explored by engineering *E. coli* to produce pyruvate from sucrose. *E. coli* W, a strain which naturally utilizes sucrose, was able to convert sucrose to pyruvate when the native *aceE* was deleted or replaced with a variant *aceE.* The work demonstrates the applicability of *aceE* variants when using a non-PTS sugar conferring a metabolism that is distinctly different than glucose metabolism. Results obtained when strains were supplemented with acetate may indicate a previously unidentified effect acetate imparts on sucrose metabolism. Additional experiments following up on these findings may lead to an improved understanding of sucrose metabolism in *E. coli* W, an area of metabolism that is not well characterized. Nevertheless, the best preforming strain produced pyruvate at rates and yields comparable to those obtained when grown on glucose, suggesting sucrose is a viable alternative to glucose for pyruvate production.

5.2 FUTURE DIRECTIONS

AceE variants, as used in the work reported here, permit static control over the partition of carbon flux between biomass and product formation. The impact AceE variants have on growth rate helps understand how each variant affects metabolism but may limit their applicability to certain industrial processes. For example, a two-stage bioprocess is characterized by fast biomass formation followed by a growth-limited production phase, which results in increased theoretical maximal production rates compared to growth-associated processes where biomass and product formation are balanced throughout the process (Figure 5.1; Burg et al., 2016). Typically, the concentration of a specific nutrient, such as phosphate or nitrogen, is limited in the medium to allow a specific maximum biomass concentration. The depletion of the limited nutrient marks the shift from biomass formation to product formation. Batch culture of

MEC992 (*E. coli* Δ*poxB* Δ*ldhA* Δ*aceE* Δ*ppsA*), which is auxotrophic for acetate, is an example of a two-stage process (Figure 2.4a). In this example, acetate serves as the limiting nutrient and once depleted, growth ceases and pyruvate accumulates. An absolute or drastic reduction in PDHc flux, corresponding to a deletion of *aceE* or *aceF*, can impact the metabolic fitness and productive lifetime of cells through eliminating acetyl-CoA formation and flux through the oxidative TCA cycle during the growth-limited production phase. In contrast, a fully active PDHc may limit productivities of pyruvate-derived products if the competing enzyme does not have comparable kinetic parameters. Thus, AceE variants may improve productivities of pyruvate-derived products in two-stage processes by reducing competition between PDHc and a competing pathway while contributing to the productive lifetime of cells and allowing some carbon flux to acetyl-CoA.

The slow growth phenotype conferred by AceE variants is the main hurdle limiting their applicability to a two-stage process. One possible way to increase the growth rate of a strain with limited PDH activity is to supply acetate to alleviate the reduced acetyl-CoA formation rate (Moxley and Eiteman, 2021). Though this strategy is simple and effective, it may be undesirable due to the added cost of an additional carbon source. Another possible approach exists using dynamic metabolic control strategies, where gene expression can be differentially controlled throughout a process by internal or external signals (Liu et al., 2018). Thus, a pathway or gene that supports a high growth rate in an AceE variant strain could be differentially regulated such that it is active in the biomass formation phase and “turned off” at the transition to the production phase.

5.3 REFERENCES

Burg, J.M., Cooper, C.B., Ye, Z., Reed, B.R., Moreb, E.A., Lynch, M.D., 2016. Large-scale bioprocess competitiveness: the potential of dynamic metabolic control in two-stage fermentations. Curr Opin Chem Eng 14, 121–136.

Liu, D., Mannan, A.A., Han, Y., Oyarzún, D.A., Zhang, F., 2018. Dynamic metabolic control: towards precision engineering of metabolism. J Ind Microbiol Biotechnol 45, 535–543.

Moxley, W.C., Eiteman, M.A., 2021. Pyruvate Production by *Escherichia coli* by Use of Pyruvate Dehydrogenase Variants. Appl Environ Microbiol 87, e00487-21. https://doi.org/10.1128/AEM.00487-21

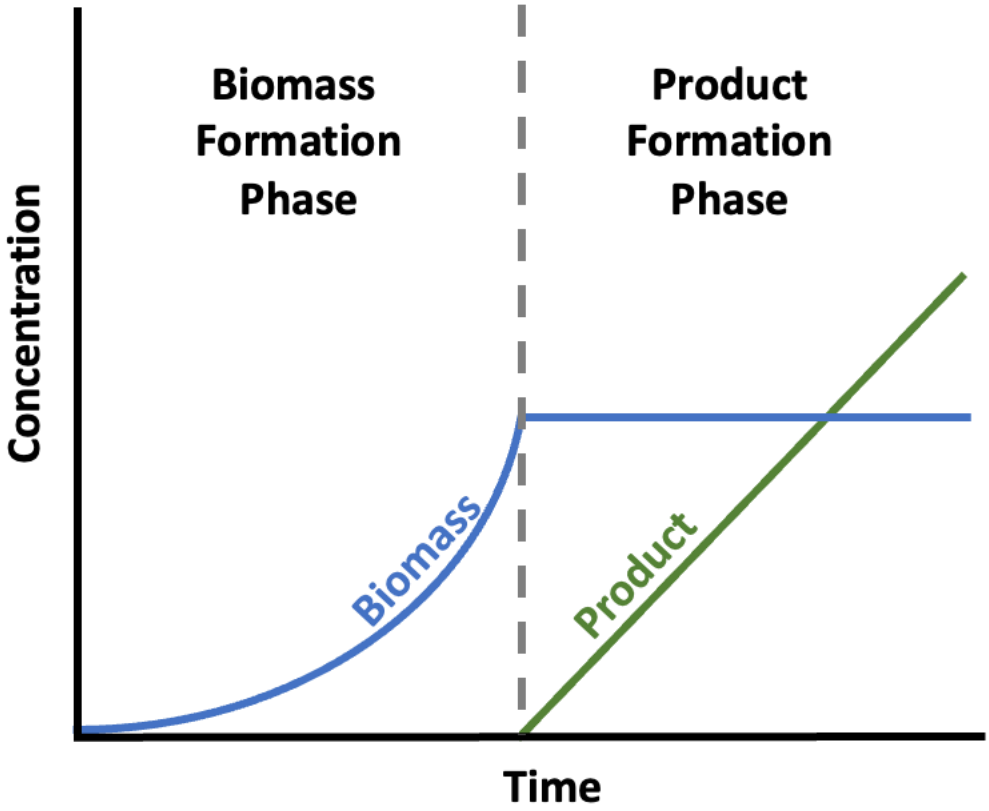

Figure 5.1 – A representation of a two-stage bioprocess. The transition from the biomass formation phase to the product formation phase is indicated by a dashed line.

APPENDIX

PYRUVATE PRODUCTION BY ESCHERICHIA COLI BY USE OF PYRUVATE DEHYDROGENASE VARIANTS

CHAPTER 2 SUPPORTING INFORMATION

Moxley, W.C. and Eiteman, M.A. 2021 *Applied and Environmental Microbiology* 87:e00487-21.

Table S2.1. Chemostat results. Cultures were grown in 0.5 liters of a nitrogen-limited defined medium with nominally 15 g/L glucose as the sole carbon source. After 3-4 residence times to achieve a steady-state, the feed and effluent were measured for the concentrations of organic compounds and the ammonium ion.

		Feed		Effluent				
Strain	D (h^{-1})	Glucose (g/L)	N (mg/L)	Glucose (g/L)	N (mg/L)	Biomass (dry g/L)	Acetate (g/L)	Pyruvate (g/L)
MEC905	0.144	14.9	213	3.09	0.0	1.43	0.00	7.73
MEC905	0.202	15.0	187	4.79	0.1	1.52	0.00	6.29
MEC905	0.266	14.7	247	5.84	0.0	1.50	0.00	5.18
MEC961	0.155	14.2	236	4.84	0.0	1.97	0.91	0.07
MEC961	0.208	14.2	236	6.39	0.1	1.94	0.82	0.05
MEC961	0.283	14.2	236	7.70	0.3	1.95	0.72	0.08

Table S2.2 RT-qPCR results from chemostat experiments. One-step quantitative reverse transcriptase PCR was performed on samples taken for each dilution rate at steady-state.

	D	Average C_T		ΔC_T	$\Delta\Delta C_T$	*aceE*
Strain	(h^{-1})	*aceE*	*rpoD*	*aceE-rpoD*		Fold Change
MEC905	0.144	26.95 ± 0.09	25.21 ± 0.06	1.74 ± 0.11	-1.07 ± 0.11	2.10 (1.94 - 2.27)
MEC905	0.202	26.15 ± 0.03	24.70 ± 0.05	1.45 ± 0.06	-1.36 ± 0.06	2.56 (2.45 - 2.67)
MEC905	0.266	26.46 ± 0.11	25.10 ± 0.06	1.37 ± 0.13	-1.66 ± 0.13	3.17 (2.90 - 3.45)
MEC961	0.155	28.66 ± 0.14	25.85 ± 0.07	2.81 ± 0.15	0.00 ± 0.15	1.00 (0.85 - 1.15)
MEC961	0.208	27.75 ± 0.10	24.70 ± 0.05	3.06 ± 0.12	0.00 ± 0.12	1.00 (0.88 - 1.12)
MEC961	0.283	27.23 ± 0.03	24.20 ± 0.08	3.03 ± 0.08	0.00 ± 0.08	1.00 (0.92 - 1.08)